Archimer
https://archimer.ifremer.fr

Assessing and predicting the changes for inorganic mercury and methylmercury concentrations in surface waters of a tidal estuary (Adour Estuary, SW France)

Stoichev Teodor [1, *], Thibaut De Chanvalon Aubin [2], Veloso Sandrine [2], Deborde Jonathan [2, 3], Tessier Emmanuel [2], Lanceleur Laurent [2], Amouroux David [2, *]

[1] Interdisciplinary Center of Marine and Environmental Research (CIIMAR/CIMAR), University of Porto, Terminal de Cruzeiros de Leixoes, Av. General Norton de Matos s/n, 4450-208 Matosinhos, Portugal
[2] Universite de Pau et des Pays de l'Adour, E2S UPPA, CNRS, IPREM, Institut des Sciences Analytiques et de Physico-chimie pour l'Environnement et les matériaux, Pau, France
[3] Ifremer, LITTORAL, Laboratoire Environnement Ressources des Pertuis Charentais, F-17390 La Tremblade, France

* Corresponding authors : Teodor Stoichev, email address : tstoichevbg@yahoo.com ; David Amouroux, email address : david.amouroux@univ-pau.fr

Abstract :

Total and dissolved concentrations of inorganic mercury (IHg) and methylmercury (MeHg) in water (Adour Estuary) were determined during three sampling campaigns and related to biogeochemical variables (nutrients, organic matter). Factors (sampling time, sample type) were included in analysis of covariance with effect separation. The urban estuary suffered historically from anthropogenic sources, however, decreased emissions have reduced Hg concentrations. Total IHg (0.51–3.42 ng L−1) and MeHg (25–81 pg L−1) concentrations are additively described by suspended particulate matter and particulate organic carbon. Higher total concentrations, carried by organic-rich particles, were found near specific discharge points (0.79–8.02 ng L−1 and 34–235 pg L−1 for IHg and MeHg, respectively). The associated high dissolved MeHg concentrations could not be explained only by biogeochemical variables. Better efficiency of the models is found for total than for dissolved concentrations. Models should be checked with other contaminants or with estuaries, suffering from downstream contamination.

Graphical abstract
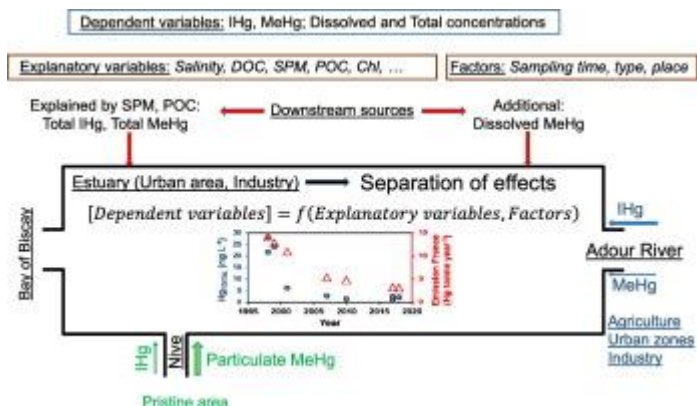
Highlights

► Hg species studied in water of estuary with upstream and downstream input ► 10-Fold decrease of Hg concentrations in 20 years due to lower Hg emission ► ANCOVA additive models evaluated input of Hg species via organic-rich particles ► Total Hg species in water additively depicted by particulate organic carbon and SPM ► Dissolved methylmercury and, especially inorganic Hg sorbed on suspended particles

Keywords : Effect separation, Contaminant transport, Pollution sources, Analysis of covariance, Mercury speciation, Water

1. Introduction

The estuarine concentrations of mercury species have been studied more often in sediment and biological samples and less often in water, in spite of the importance of water compartment for the transport of contaminants (Navarro et al., 2012; Stoichev et al., 2018). The reasons are possibly related with difficulties in sample storage and analytical determinations of low levels of Hg species in water samples. The total concentrations of contaminants in estuarine waters depend on upstream river concentrations, lateral input and mixing between river and ocean water but also on in situ processes, such as sedimentation / resuspension phenomena. Total concentrations of Hg species are better predictor for their transport while dissolved concentrations, especially those of methylmercury, should represent more bioavailable forms. Riverine export is a very important source of both inorganic mercury (IHg) and methylmercury (MeHg) to coastal ocean, and, due to very high productivity, is able to affect MeHg

53 concentrations in coastal species contributing to majority of human MeHg exposure (Liu et al.,

54 2021). Furthermore, upon transition from rivers to coastal zone, sedimentation of fine and

55 organic rich particles stimulates bacterial reduction of oceanic sulfate that may increase the

56 net methylation of IHg (Azaroff et al., 2019; Stoichev et al., 2019). Mercury speciation studies

57 in water from estuaries (Leermakers et al., 2001; Balcom et al., 2008; Wang et al., 2009;

58 Bratkic et al., 2013; Gosnell et al., 2016), bays and lagoons (Horvat et al., 1999; Bloom et al.,

59 2004; Stoichev et al., 2016) is focused mainly on contaminated zones worldwide.

60 　　　　The Adour Estuary (SW France) is medium size dynamic mesotidal estuary. Its

61 urban/industrial downstream part is deteriorated due to numerous anthropogenic impacts

62 (SDAGE-PDM, 2014; Cavalheiro et al., 2017). Both surface sediments (Stoichev et al., 2004)

63 and water (Stoichev et al., 2006) from the Adour estuary were found to be moderately

64 contaminated with Hg species with numerous sources situated in the downstream urban area.

65 The concentrations of Hg species in local wastewaters in Adour Estuary (Point, 2004) varied

66 two to five orders of magnitude (dissolved and particulate, respectively), which should be

67 investigated, especially in light of possible bioaccumulation. Higher anthropogenic impact on

68 European eels in Adour estuary occurred downstream compared to upstream sites (Arleny et

69 al., 2007). However, unlike other coastal systems (Aly et al., 2013; Stoichev et al., 2018), the

70 Adour estuary hydrodynamics efficiently exports pollutants (Sharif et al., 2014; Stoichev et al.,

71 2004; Azaroff et al., 2019) that would make it able to recover rapidly if pollution would stop.

72 Largest water quality improvement occurs in regions, experiencing recent control on Hg

73 emission (Driscoll et al., 2013) and, therefore, Adour Estuary (France) would be a possible

74 example of coastal system in rapid recovery.

75 　　　　Multiple regression (MR) was used to separate biogeochemical processes of addition

76 and removal of contaminants in water during estuarine mixing for case of single and strong

77 upstream contamination source (Stoichev et al., 2016). However, in Adour Estuary, there are

78 downstream contamination sources, complicating the separation of biogeochemical variables.

79 As a strategy, categorical variables (factors) were included, taking into account sample type

80 and sampling time. Water from different upstream and estuarine locations in Adour Estuary,

3

81 as well as from urban tributaries, was collected during three sampling campaigns. The

82 development of generalized additive models (GAM) allowed finding the combinations of factors

83 and important continuous variables involved in IHg and MeHg variations. However, GAM

84 consume degrees of freedom, lack simple analytical representation and were used here only

85 as preliminary insight on the variables to be included in analysis of covariance (ANCOVA)

86 models to study the variability of IHg and MeHg in different type of water samples and their

87 eventual sources in the downstream part. The resulting simple spatial / temporal equations

88 would depict the IHg and MeHg concentrations as additive functions of specific biogeochemical

89 variables. Such approach, using both categorical and continuous variables, was already

90 applied to model estuarine biogeochemistry of organic contaminants (Stoichev et al., 2021).

91 Additionally, marked difference in land use between Adour and Nive (a downstream tributary)

92 will allow some estimation on its possible effect on IHg and MeHg concentrations. The

93 concentrations from this study and measured up to 20 years ago in estuarine (Stoichev et al.,

94 2006; Sharif et al., 2014) and upstream water (Point, 2004) of Adour will be compared and

95 discussed in light of decreased emissions.

96

2. Methods

98 *2.1. Study area*

99 The Adour River (South-West France, Gulf of Biscay) is 310 km long and has 6189 km^2

100 drainage area (Stoichev et al., 2006). Different soils have developed near Adour River: Luvisol,

101 Cambisol, Podzol, Albeluvisol, but also calcaric soils (Calcisol, rendzic Leptosol and calcaric

102 Fluvisol) (ESBN, 2005). Important tributary in the estuarine area of Adour is Nive with 850 km^2

103 drainage area (Fabre, 1998) and more homogeneous soil types – Cambisol and acid-organic

104 Umbrisol (ESBN, 2005). The main difference between Adour and Nive is related to land use.

105 The Nive usually drains forested areas, small size farming and small urban zones. Industry,

106 intense agriculture and bigger urban centers (Pau, Tarbes, Mont-de-Marsan, Dax, Lourdes)

107 are situated along the Adour River watershed, inducing more important contamination with

4

108 nitrates, pesticides and organic compounds of Adour compared to Nive (SDAGE-PDM, 2014).

109 The average river discharge of Adour is about 350 $m^3 s^{-1}$ and it is the third largest freshwater

110 inflow to Bay of Biscay (Borja et al., 2019) while for Nive it is 25 $m^3 s^{-1}$ (Point et al., 2003).

111 The Adour Estuary has narrow estuarine channel (about 500 m width, down to 200 m

112 at the mouth) with almost no intertidal area, resulting in a short residence time (hours to days)

113 of water and particles (Point et al., 2007). Tidal amplitude is between 2 and 5 m with influence

114 observed up to 70 km upstream. Significant urban and industrial activities are located on the

115 estuarine shores including sewage treatment, wood industry, waste incineration, electronics,

116 metallurgy, harbor and aquaculture. Despite the importance of the upstream sources, non-

117 negligible downstream fluxes compared to upstream (IHg: 4%, MeHg: 9%) are transported at

118 low river discharge from wastewaters (Point, 2004).

119

120 *2.2. Sampling*

121 Bulk water samples (up to 30 cm depth) were collected at decreasing tide within the tidal limit

122 of the estuary on three occasions: May 2017 (representing flood period), September 2017 (dry

123 conditions) and January 2018 (low temperatures) and kept in cool box until laboratory. The

124 tide coefficients were between 78 (May) and 109 (Jan). The upstream samples (1, 2, 3, 4, Fig.

125 1) are considered as upstream references, representative of the Hg species delivery from

126 rivers. The downstream estuarine samples (A, B, C, D), collected with a ship from the middle

127 of the main channel, are situated in the urban area. Samples with high anthropogenic impact

128 are collected in the estuary near outlets of water treatment plants (WTPs) "St Frédéric" (6) and

129 "Pont de l'Aveugle" (8). Samples from urban tributaries before entering the estuary were

130 Aritxague (7) and "Moulin d'Esbouc" (9, influenced by WTP "St Bernard"). Some

131 biogeochemical characteristics (pH, O_2, water temperature (T), conductivity) were measured

132 on site with multiparametric probe HANNA Instrumentsc® HI-9829 or calculated afterward

133 (salinity (Sal)).

134

135 *2.3. Experimental*

2.3.1. Cleaning procedures for Hg speciation

All materials were cleaned using ultra-trace protocol (Bravo et al. 2018). Water (1L) was collected in polypropylene and stored in Teflon® bottles. All bottles and vials for sampling and analysis were first cleaned using detergents (RBS™) and rinsed thoroughly. It is then successively decontaminated in two baths of 10% (v/v) nitric acid (HNO$_3$) and a bath of 10% (v/v) hydrochloric acid (HCl) with rinsing steps (deionized water) between each bath. In each bath, the material undergoes a sonication step for a minimum of 2 h. Similar procedure was applied for decontamination of plastic caps but in 1% acids for shorter time (15 min each bath). After rinsing with deionized water, all material was dried under a laminar flow hood and stored in plastic bags until use on site.

2.3.2. Sample pre-treatment for Hg speciation

One part of the sample was transferred into 250 mL Teflon® bottle then acidified with acetic acid (0.5 - 1% depending on the particle load) for the analysis of Hg species. These samples correspond to the analysis of the total unfiltered fraction. The samples for determination of dissolved fraction (marked with subscript D) were filtered under vacuum (0.45 μm PVDF filters, Durapore). The filtrates were transferred and acidified similarly to total fraction with 0.5% acetic acid. Samples are stored in the dark at 4°C until extraction and analysis.

2.3.3. Chemical analysis

Mercury species concentrations were measured by capillary gas chromatography coupled to ICP-MS (GC Trace Ultra, XSerie II ICP-MS Thermo Scientific) after spiking with enriched 4stable isotopes of ^{199}IHg and ^{201}MeHg for species-specific isotope dilution analysis (Navarro et al., 2012; Bouchet et al., 2013; Sharif et al., 2014; Azad et al., 2019). Isotope tracer's solutions were prepared for each analytical session and their concentration was regularly determined by reverse isotope dilution. The Hg species were derivatized with sodium tetrapropylborate at pH 3.9 and extracted into 2,2,4-trimethylpentane. It should be noted that

163 the filter-passing fraction contains both dissolved and most colloidal Hg species but will be

164 referred to here as "dissolved" fraction for wording simplicity.

165   Quality assurance and quality control (QA/QC) was based on laboratory and field blanks,

166 replicate analysis (Cavalheiro et al. 2016) and on repeated participations in international inter-

167 laboratory comparisons (e.g. GEOTRACES inter-calibration cruises for Hg species in

168 seawater). The repeatability was determined as average from all samples (unfiltered and

169 filtered, n=72) of the relative standard deviations (RSD) for the triplicate analysis and was 1.5%

170 for IHg and 3.4% for MeHg. The limits of detection (LOD) were calculated using the results

171 from the field blank samples and were similar for total and for dissolved Hg species. The limits

172 of detection (LODs) for IHg_{DISS} and IHg were calculated as three times the standard deviation

173 (SD) of the concentrations found in the blank samples. Since the $MeHg_{DISS}$ and MeHg were

174 not detected in the blanks, the LODs in this case were estimated from 3×SD of the background

175 noise equivalent concentrations. For both total and dissolved species, the LODs were 0.03-

176 0.07 ng L^{-1} and 3 pg L^{-1} for IHg and MeHg, respectively. The results for IHg_{DISS} and IHg were

177 corrected with the average blank value.

178   The concentrations of total nitrogen (TN, mg L^{-1}) and dissolved organic carbon (DOC,

179 mg L^{-1}) were determined in the filter-passing fraction (through 0.7 µm pre-combusted GF/F

180 filters) by chemiluminescence and high temperature catalytic oxidation method, respectively,

181 using a Shimadzu TOC-L CSH/CSN analyzer (Lee and Kim, 2018; García-Martín et al., 2021).

182 Nutrient concentrations (µM) (phosphates (PO_4), nitrates (NO_3), nitrites (NO_2), ammonia (NH_4)

183 and silicates (SiO_4)) were determined in the dissolved fraction (0.45 µm AC filters) by

184 colorimetric procedures using a Shimadzu UV-1800 spectrophotometer (Koroleff, 1969; Mullin

185 and Riley, 1955; Murphey and Riley, 1962; Strickland and Parsons, 1972). The concentrations

186 of suspended particulate matter (SPM, mg L^{-1}), chlorophyll a (Chl, µg L^{-1}), and phaeopigments

187 (Pha, µg L^{-1}) were determined in particulate fraction as previously described (Abril et al., 2002;

188 Aminot and Kérouel, 2004; Lorenzen, 1967, Savoye et al., 2012). Particulate organic carbon

189 (POC, % on particle weight basis or POC_V, mg L^{-1}, on sample volume basis) was measured

7

190 after removal of carbonates by infrared spectroscopy via high temperature combustion on a

191 Shimadzu TOC-L/SSM-5000A analyzer (Azaroff et al., 2019). δ13C and δ15N of particulate

192 organic forms were measured using an elemental analyzer (Flash 2000, ThermoFisher

193 Scientific) coupled with an isotope ratio mass spectrometer (IRMS, Isoprime, GV Instruments)

194 (Savoye et al., 2003, 2012).

195

196 *2.4. Statistical analysis*

197 *2.4.1. Preprocessing*

198 The database is included in supplementary materials (xlsx file). Dissolved and total

199 concentrations of IHg, MeHg as well as the percentage of MeHg relative to total Hg (%MeHg)

200 were dependent variables (Y_i). Biogeochemical characteristics were used as continuous

201 explanatory variables (X_i). Active chlorophyll (actChl), ratio between Chl and POC ($R_{Chl/POC}$)

202 and partition coefficient of organic carbon (K_{OC}) were also used as X_i:

203 $$ActChl = [Chl]/([Chl] + [Pha]) \tag{1}$$

204 $$R_{Chl/POC} = [Chl]/(10[SPM][POC]) \tag{2}$$

205 $$K_{OC} = 10^4[POC]/[DOC] \tag{3}$$

206 Other explanatory variables were categorical (factors). Factor "type" has four levels: effluents

207 from Sewage Treatment Plant (STP), urban tributaries (Urban/STP), upstream and estuarine

208 waters. In order to study the effect of Nive on the dependent variables, factor "place" was also

209 included in the models. It has also four levels: "Adour", "Nive", "Trib" (samples from urban

210 tributaries before entering the estuary) and "Trib/Adour" (samples near the outlet of urban

211 tributaries with possible effect of the Adour estuarine water). Third factor in the models was

212 "time" with levels May, September and January.

213 Continuous explanatory variables (average, geometric mean, range) are shown in

214 Tables SI-1, SI-2 and SI-3 from supplementary materials for different levels of factors "time",

215 "type" and "place", respectively. Levels for place "Trib" and "Trib/Adour" are combined into one

216 level "Trib_Trib/Adour" (Table SI-3), representing all urban stream samples. There is additional

217 column regarding Adour upstream samples in order to compare with Nive. Significant

8

218 difference ($p < 0.10$) for variables at different factor levels is studied with Wilcoxon rank sum

219 test.

220 Local background levels (LBLs, Table SI-1) were calculated using "estuary" and

221 "upstream" data as 90th percentiles contained within average ± 3σ intervals (where σ is the

222 standard deviation), or as averages from data contained within average ± 4σ intervals, for 3σ

223 and 4σ methods, respectively (Gredilla et al., 2015). Ranges between 4σ and 3σ values are

224 considered as LBL. The proportion (P) of samples with X_i equal to LBL, higher than LBL and

225 lower than LBL are also presented (Table SI-2, SI-3) with the respective binomial errors.

226 Statistical data treatment was carried out using R software (R core team, 2017). The

227 dependent variables (Y_i) were represented as functions of q explanatory variables X_i. As

228 required for linear models, both Y_i and X_i were normalized using graphical visualization of

229 density function and Box-Cox transformations to give transformed variables Y_T and $X_{T,i}$:

230 $Y_T = \ln Y$ Y: IHg, MeHg, IHg_D, $MeHg_D$, %MeHg   (4a)

231 $Y_T = \sqrt{Y}$ Y: $\%MeHg_D$ (4b)

232 $X_T = \ln X$ X: NO_2, SiO_4, DOC, Chl, Pha, K_{OC} (5a)

233 $X_T = \sqrt{X}$ X: $R_{Chl/POC}$ (5b)

234 $X_T = 1/\sqrt{X}$ X: Sal, O_2, PO_4, NO_3, NH_4,   (5c)

235 $X_T = 1/X$ X: TN, POC   (5d)

236 $X_T = X$ X: pH, T, SPM, ActChl, δ13C, δ15N   (5e)

237 High correlations for transformed explanatory variables $X_{i,T}$ ($p < 10^{-5}$) were observed between

238 O_2 and T, TN and NO_3, NH_4 and NO_2. Therefore, to avoid collinearity, part of X_i (O_2, NH_4, TN)

239 were not considered.

240 The dependent variables (average, geometric mean, range) and dissolved fractions

241 (F_D, %) are shown in Tables SI-4, SI-5 and SI-6 for different levels of factors "time", "type" and

242 "place", respectively. Significant difference ($p < 0.10$) between groups studied with t test on

243 transformed dependent variables (Eqs. 4a, 4b) and with Wilcox test on F_D. Like with X_i, LBLs

244 (Table SI-4) and the proportion of samples with Y_i equal, higher and lower than LBL (Tables

245 SI-5, SI-6) were calculated.

9

246

247 *2.4.2. Analysis of variance*

248 The effect of factor levels was determined by ANOVA with time/type and time/place initially

249 included. Models were simplified by leaving only significant factors (p<0.1). Factor levels with

250 similar effects on $Y_{i,T}$ were combined. Thus, for each Y_i, specific levels determined factors

251 time1, type1, place1. The obtained dependences and adjusted R^2 (adjR^2) are shown in Table

252 SI-7. The effect of different factors was often additive and, in case some interaction exists, its

253 mean square is at least an order of magnitude smaller than the mean squares for additive

254 effects of both factors (Table SI-7 footnote).

255

256 *2.4.3. Generalized additive models*

257 Generalized additive models (GAM) were developed as a function of $X_{i,T}$ and of parametric

258 terms – factors: "time1", "type1" or "place1" (part 2.4.1). The factors were included in the

259 intercept $a_0(…)$ in the forms: a_0(time1), a_0(type1), a_0(place1), a_0(time1, type1) and a_0(time1,

260 place1).

261 $$Y_T = a_0(…) + s(X_{T,i}) \tag{6}$$

262 X_i: pH, Sal, T, PO_4, NO_3, NO_2, SiO_4, DOC, Chl, Pha, SPM, POC, δ13C, δ15N, $R_{Chl/POC}$, ActChl, K_{OC}

263 $$Y_T = a_0(…) + s(Sal_T) + s(X_{T,i}) \tag{7}$$

264 X_i: pH, PO_4, NO_3, NO_2, SiO_4, DOC, Chl, Pha, SPM, POC, δ13C, δ15N, $R_{Chl/POC}$, ActChl, K_{OC}

265 $$Y_T = a_0(…) + s(SPM_T) + s(X_{T,i}) \tag{8}$$

266 X_i: PO_4, NO_3, NO_2, SiO_4, DOC, Chl, Pha, SPM, POC, δ13C, δ15N, $R_{Chl/POC}$, ActChl, K_{OC}

267 Initially, all $X_{i,T}$ enter in GAM as smoothed functions (s). However, if their estimated degrees of

268 freedom (edf) equal 1, they become parametric linear terms. If necessary, the number of factor

269 levels in "time1", "type1" and "place1" is additionally decreased (Table SI-8, 117 models). The

270 slope c_1 (should be near 1) and intercept c_0 (should be near 0) of the linear dependence

271 between model (Y_{MOD}) and experimental (Y_{EXP}) values and the root mean square deviation of

272 transformed variable ($RMSD_T$) for sample size n were calculated:

10

$$RMSD_T = \sqrt{\frac{\Sigma(Y_{EXP,T,i} - Y_{MOD,T,i})^2}{n}} \qquad (9)$$

Only models that showed significant effects ($p<0.1$) and with $c_1>0.25$ were considered further

and compared using analysis of deviance.

2.4.4. Linear models with continuous explanatory variables

In the linear models (LM), the relationship is expressed by L_1 or L_2, the index representing the

highest interaction order, described in the starting model:

$$L_2(X_{T,1}, X_{T,2}, \ldots, X_{T,i}, \ldots, X_{T,q}) = \sum_{i=1}^{q} a_i X_{T,i} + \sum_{i \neq j} a_{i,j} X_{T,i} X_{T,j} \qquad (10)$$

$$L_1(X_{T,1}, X_{T,2}, \ldots, X_{T,i}, \ldots, X_{T,q}) = \sum_{i=1}^{q} a_i X_{T,i} \qquad (10)$$

The coefficients a_i and a_{ij} represent the simple terms for variable X_i and the double interactions,

respectively. The specific indexing of the explanatory variables X_i is explained in Tables SI-8,

SI-9 and SI-10. Higher order effects (quadratic and cubic for Sal and SPM; only quadratic for

the rest of the variables) were checked for variables having significant simple effect. The

number of coefficients in the starting models never exceed 13 in order to avoid

overparametrization (Crawley, 2007). Minimal adequate models were obtained by gradual

deletion of non-significant terms (Stoichev et al., 2019). The stability of coefficients is studied

by bootstrap with row resampling (online resources, Minimal Adequate ANCOVA) and

equations with unstable coefficients are eliminated. Only equations with $c_1>0.5$ are included

for further consideration.

One starting approach could be multiple regression (MR) with simple effects without

interactions:

$$Y_T = L_1(pH_T, Sal_T, T_T, PO_{4,T}, NO3_T, NO_{2,T}, SiO_{4,T}, DOC_T, SPM_T, POC_T, \delta13C_T, \delta15N_T) \qquad (11)$$

All equations with $RMSD_T$, c_1 and c_0 are presented in Table SI-9 (six models). Significant

variables $X_{i,T}$ from MR equations were used for analysis of covariance (ANCOVA) by including

factor-dependent intercepts: a_0(time), a_0(type), a_0(place), a_0(time, type), a_0(time, place). For

each one of the five combinations of factors only simple effects or higher order effects of

299 significant X_i were included but without interactions. Minimal adequate ANCOVA having more
300 than two X_i were deleted.

301 Another starting approach is based on the same X_i as in the generalized additive model
302 (GAM) equations (Table SI-8) to develop ANCOVA. The factors were also the same but with
303 the original levels of "time", "type" and "place" (Fig. 1). All starting equations with two X_i have
304 higher order effects of significant X_i and interaction terms. After stepwise simplification, only
305 models with additive effects of X_i were included (Table SI-10, 60 models). Equations with factor
306 "place" were not considered if separated levels "Trib" or "Trib/Adour" appeared because they
307 were not important for the dependent variables Y_i. Schematic representation of the used
308 models is shown in Fig. 2.

309 After preliminary evaluation of the dependences of Hg species concentrations from
310 factors and biogeochemical variables, additional models for the MeHg, MeHg$_D$ and IHg$_D$ were
311 also developed from starting expressions:

312 $$\ln[MeHg] = a_0(type) + L_2(IHg_T, POC_T) + (IHg_T)^2 + (POC_T)^2 \tag{12a}$$

313 $$\ln[MeHg_D] = a_0(type) + L_2(IHg_{D,T}, X_{T,i}) + (IHg_{D,T})^2 + (X_{T,i})^2 + (X_{T,i})^3 \tag{12b}$$

314 $$\ln[IHg_D] = a_0(type) + L_2(IHg_T, POC_T) + (IHg_T)^2 + (POC_T)^2 \tag{12c}$$

315 The variables X_i are Sal or SPM for Eq. 12b. The same criteria for model simplification and
316 selection as previously described were used (supplementary materials, Minimal Adequate
317 ANCOVA). The values of RMSD$_T$ for ANCOVA models (Table SI-10), selected for further
318 consideration, are marked in bold.

319

3. Results

321 *3.1. Factor-separated biogeochemical variables and concentrations of Hg species*

322 Between-time differences of biogeochemical variables (Table SI-1) show that samples in May
323 are characterized with higher DOC, low SPM, lower nutrient content and δ13C, having
324 particulate organic matter rich in Chl due to phytoplankton development compared to Sept and
325 Jan. Samples in Jan have more NO$_3$ and less Chl, δ15N and ActChl. Selected biogeochemical

variables, grouped according to factor "type" (Table SI-2), demonstrating significant between-type differences, are shown in Fig. 3. The Adour Estuary is loading a low content of organic-rich suspended particles. Compared to upstream samples, estuarine ones have higher DOC and lower POC concentrations. Both Urban/STP and STP samples have more nutrients (NO_2, NH_4) and organic matter (DOC, POC) compared to upstream and estuarine samples. Therefore, important local downstream sources were observed, but they are rapidly diluted in the estuarine water. Samples from type "STP" (compared to Urban/STP) are particularly rich in all nutrients (except SiO_4), SPM and POC. Additionally, the organic matter in STP is more particle-associated and with low $R_{Chl/POC}$. Water from STP may have suffered slight oxygen depletion and is rich in CO_2 (lower pH) from partly oxidized organic matter. For most of the variables within Urban/STP (7, 8, 9, Fig. 1) between-site differences were not observed. However, POC was higher in site 7 (8.88±1.08%) compared to sites 8 and 9 combined (6.45±0.56%). Concentrations (µM) of NO_3 and NO_2 were higher in site 8 (NO_3: 228.5±161.3; NO_2: 3.58±0.36) compared to sites 7 and 9 combined (NO_3: 92.1±27.8; NO_2: 2.72±0.45). The effect of land use was studied by comparison between upstream water from Adour (agriculture area) and Nive (pristine area) Rivers, showing that Nive has less nutrients (NO_3, NO_2, PO_4) and its organic matter is more particle-associated (Table SI-3).

Between-time differences for Hg species concentrations (Table SI-4, Fig. 4) showed the lowest concentrations of IHg and IHg_D in May, probably due to lower SPM concentrations and higher in Sept, especially for Urban/STP stations. Although not significant, the highest concentrations of MeHg and $MeHg_D$ were observed in Sept. Significant variations of %MeHg and %$MeHg_D$ (particularly high in May) were noticed. Higher average dissolved fraction F_D for IHg was observed in Jan (43%) compared to May (30%) and Sept (23%), while, for MeHg, F_D was very stable over time (between 66 and 73%).

Between-type differences (Fig 4, Table SI-5) showed that "STP" have higher total IHg concentrations, all above the background levels, compared to the rest of the samples, while IHg_D concentrations do not fluctuate as much across type levels. Both MeHg and $MeHg_D$ showed significantly higher concentrations, all above the background levels, in STP compared

13

354 to the rest of the sample type. Samples from STP have smaller average F_D of MeHg (46%)

355 compared to the rest of sample types (68–73%). Within Urban/STP no significant differences

356 between samples were observed except for $MeHg_D$, with lower concentration in site 8 (26±4

357 pg L^{-1}) compared to sites 7 and 9 combined (41±11 pg L^{-1}). No significant difference was

358 observed for total and dissolved IHg between upstream samples from Adour and Nive Rivers

359 (Fig. 4). On the contrary, lower total MeHg and similar $MeHg_D$ concentrations were observed

360 in Adour compared to Nive (Fig. 4, Table SI-6), which led to significant difference in average

361 F_D for MeHg (81% and 65% in Adour and Nive Rivers, respectively).

362   The dependence between concentrations of Hg species and some biogeochemical

363 variables for each sampling campaign (Fig. SI-1) shows that IHg is mainly carried by SPM

364 while particulate organic matter and IHg determines the concentrations of MeHg. Salinity has

365 no clear effect on Hg species concentrations in water from Adour Estuary.

366

3.2. Minimal adequate models to depict Hg species concentrations

368 The development of generalized additive models (GAM) allowed finding the combinations of

369 factors and important transformed explanatory variables ($X_{i,T}$) to explain dependent variables

370 (Y_i). However, GAM consume more degrees of freedom, lack simple analytical representation

371 and here were used only as preliminary insight on the variables to be included in some starting

372 ANCOVA models. Simple analytical expressions for Y_i were selected from supplementary

373 materials (minimal adequate ANCOVA). Equations 13–15 concern IHg and MeHg total

374 concentrations:

375 $$\ln[IHg] = a_0\left(time_{Sept(+)}; type_{Upstream(-)}\right) + |a_{11}|[SPM] - |a_{12}|/[POC] \tag{13}$$

376 $$\ln[MeHg] = a_0\left(type_{Urban/STP(-)}\right) + |a_{11}|[SPM] - |a_{12}|/[POC] \tag{14}$$

377 $$\ln[MeHg] = a_0\left(type_{Urban/STP(-)}\right) - |a_{12}|/[POC] + |a_{18}|\ln[IHg] \tag{15}$$

378 $$\ln[\%MeHg] = a_0\left(time_{Sept(-)}; type_{STPUrban/STP(-)}\right) - |a_{11}|[SPM] - |a_{12}|/[POC] + |a_{12,12}|/[POC]^2$$

379 $$\tag{16}$$

380 The slope c_1 of the dependence between model and experimental values (Eqs. 13-15) is

381 between 0.81–0.89, except for %MeHg (Eq. 16, 0.69). The standard error of c_1 is in the range

382 6.2–9.0% and adjR^2 is between 0.756 and 0.836. These models describe behavior of Y_i with

383 range ratio of at least an order of magnitude.

384 For dissolved species, only models for MeHg$_D$ (Eqs. 17, 18) match the selection criteria:

385 $$\ln[MeHg_D] = a_0(type_{STP\,(+)}) + |a_2|/\sqrt{Sal} - |a_{2,2}|/Sal + |a_3|\,T \tag{17}$$

386 $$\ln[MeHg_D] = a_0(type_{STP\,(+)}) - |a_{11}|[SPM] + |a_{11,11}|[SPM]^2 - |a_{11,11,11}|[SPM]^3 + |a_{19}|\ln[IHg_D] \tag{18}$$

387 The slope c_1 is 0.67 with standard error 11.3% (Eq. 17) and 0.87 with standard error 7.1% (Eq.

388 18). As with the bulk samples, the models for Y_i in dissolved phase describe range ratios of an

389 order of magnitude. However, the quality characteristics of models for dissolved concentrations

390 are worse than those for total concentrations when only biogeochemical variables are used

391 (Eq. 17). For the same reason, no equations were selected for IHg$_D$.

392   In all equations, Y_i are functions of at least one factor. The total and dissolved

393 concentrations of MeHg depend only on type and the concentrations of IHg – both on type and

394 time. In all minimal adequate models, the interactions between continuous explanatory

395 variables were checked, but the effects were always additive. The most important

396 biogeochemical variables, affecting total concentrations of IHg, MeHg and %MeHg were SPM

397 and POC (Eqs. 13, 14, 16) which are statistically separated in Fig. 5. Such additive effects are

398 separated by leaving one of the variables to vary while the others are fixed. Fixed values of

399 dependent variables were determined as group-based averages according to factor levels in

400 the minimal adequate models. Similarly, the effects of Sal and T (Eq. 17) on MeHg$_D$ were

401 separated in Fig. SI-2 (supplementary materials). In Fig. 5 and Fig. SI-2, the concentrations of

402 Hg species are represented as simple functions of frequently measured biogeochemical

403 variables. Nonetheless, in order to evaluate the effect of IHg precursors in the net methylation

404 processes, the effects of IHg (and IHg$_D$) on total and dissolved MeHg concentrations,

405 respectively, were separated from the effects of other biogeochemical variables X_i in Fig. 6.

406

4. Discussion

407

408 *4.1. Recovery and long-term changes of Adour Estuary contamination by Hg compounds*

15

409 Advanced technologies in WTPs and discontinuing use of Hg-containing products are

410 expected to improve environmental water quality in Adour concerning Hg. Previous data on

411 dissolved and particulate IHg, MeHg concentrations in Adour upstream (SPM 8 mg L^{-1}) and

412 Nive (SPM 2 mg L^{-1}) Rivers from 2001-2002 are available (Point, 2004) and compared with

413 total concentrations in May 2017 (with similar SPM values, Table SI-6 footnote). Despite

414 slightly higher SPM values, four to seven times lower concentrations were measured in these

415 rivers in May 2017 (e.g., in Adour upstream, 0.837 ng L^{-1} and 35 pg L^{-1} for IHg and MeHg,

416 respectively) compared to 2001-2002 (3.50 ng L^{-1} and 231 pg L^{-1} for IHg and MeHg,

417 respectively). Likewise, concentrations of Hg_{TOT} (sum of total IHg and MeHg) and MeHg in

418 sample type "estuary" from this study (Table 1) are compared with previous data from Adour

419 estuarine surface water with similar salinity range (0.1–16.9) as presented here (Stoichev et

420 al., 2006; Sharif et al., 2014), and exhibit an important recovery of the estuary regarding Hg

421 contamination. Concentrations of Hg_{TOT} for the period 1998–2018 were not related to salinity

422 but to anthropogenic Hg emissions (E) to the environment such as in the air for France

423 (https://www.citepa.org/fr/2021-hg/) during respective sampling year (Table 1). The variables E

424 and Hg_{TOT} co-vary with time ($\ln[Hg_{TOT}]$ and E are strongly correlated, p<0.0005), both having

425 the greatest reduction during the first decade of the studied 20-year period. Such high

426 correlation between Hg_{TOT} and emissions to the air (E) requires further explanation. Decrease

427 of anthropogenic Hg emission to the atmosphere has been observed not only in France but

428 also in all Europe (Driscoll et al., 2013). Therefore, important trans-border contamination is not

429 expected, meaning changes of deposited Hg in France should be dependent on changes of E

430 (https://www.emep.int/). Additionally, the emissions of metals within industrial effluents in France

431 decreased between 2004 and 2018 (SDES-OFB, 2020), similarly to the other emissions to the

432 environment. According to European Environment Agency, industrial releases of metals

433 (including Hg) to water for the 27 member states was reduced by about 50% between 2010

434 and 2017 (https://www.eea.europa.eu/ims). Therefore, the variations of emitted Hg to the air

435 could be an indirect measure of changes of Hg, affecting aquatic environment, either from

436 deposited Hg on soil or via direct point sources. The extrapolation of Hg_{TOT} concentrations in

16

437 Adour estuarine waters (Table 1) to "zero" anthropogenic Hg emissions lead to a natural

438 background concentration of 0.71±0.21 ng L^{-1}. This value is only two to three times lower than

439 current local background concentration of IHg (Table SI-4) thus, the Hg contamination in the

440 Adour Estuary is getting closer to the modelled level for "pristine" aquatic environment. It is an

441 example of a coastal system in recovery that rapidly responds to changes of anthropogenic

442 Hg emissions due to its specific hydrodynamics. In contrast, the Aveiro Lagoon, although also

443 in recovery, would require more than 300 years to reduce by 50% the historical Hg pollution,

444 localized in upstream area of the lagoon with more limited exchange with the ocean and

445 receiving small freshwater flow (Pato et al., 2008; Stoichev et al, 2018).

446

447 *4.2. Depicting IHg and MeHg concentrations in urban estuary by biogeochemical variables*

448 Such low IHg concentrations would change the behavior of MeHg in the last 20 years.

449 Previously, MeHg concentrations in Adour Estuary depended on biogeochemical variables but

450 not on IHg concentrations (Stoichev et al., 2006). However, the transformed concentrations of

451 MeHg in the current study are highly correlated with those of IHg in both dissolved (p<0.001)

452 and bulk samples (p<0.0001) indicating that, at ng L^{-1} levels of IHg, MeHg depends not only

453 on biogeochemical variables, such as POC (Fig. SI-1, Table SI-11), but is probably limited by

454 IHg availability.

455 Separation of effects of SPM and POC for the total concentrations showed the transport

456 of IHg and MeHg are similarly governed by mixing particles with different Hg content (Fig. 5).

457 As observed in Bach Dang tropical estuary (Navarro et al., 2012), IHg is carried by particulate

458 matter in Adour Estuary. Subsequently, IHg is involved in the production of MeHg as described

459 by Eq. 15, which is equivalent to Eq. 14 (Fig. 6). Fine organic-rich particles carry preferably

460 MeHg (compared to IHg) irrespectively of the sampling campaign. Thus, the %MeHg

461 decreases with SPM and increases with POC. Similarly, particulate MeHg in Nalon Estuary is

462 correlated with POC (Pavoni et al., 2021).

463 In dissolved phase, separation of effect of Sal and T showed that MeHg$_D$ concentrations

464 slightly depend on salinity, showing possible remobilization at intermediate salinity (Fig. SI-2).

17

465 The concentrations of MeHg$_D$ increased with T, explaining clearly higher %MeHg$_D$ in warm

466 seasons while no such effect was observed for %MeHg in the bulk phase (Table SI-4). The

467 effect of SPM on MeHg$_D$ is separated from the influence of IHg$_D$ as precursor for MeHg$_D$

468 production (Fig. 6). It demonstrates that, at high SPM, lower MeHg$_D$ concentrations are

469 expected, probably as a result from MeHg$_D$ sorption on particulate matter.

470   It was not possible to develop equations explaining variations of IHg$_D$ neither by

471 biogeochemical variables nor by including IHg concentration as explanatory variable (Eq. 12

472 c). Models describing IHg$_D$ as function of SPM and non-linear function of IHg were developed

473 (supplementary materials Equations). The best results were in the form:

474 $$[IHg_D] = [IHg] - d_1[SPM](1 - \exp(-d_2[IHg])) \qquad\qquad 0 \leq [IHg_D] \leq [IHg] \qquad (19)$$

475 The slope c_1 for the dependence between model and experimental values of IHg$_D$ is

476 0.733±0.114. Thus, Eq. 19 is the only simple model for IHg$_D$ that produces relatively good

477 results. The coefficient d_1=0.131±0.018 represents maximum particulate concentration (µg g^{-1}

478 ^{1}) of IHg while d_2=0.631±0.197 is related to how steeply particulate concentration is increasing

479 with increasing IHg total concentration before reaching saturation plateau. The non-linear

480 effects (Fig. SI-3 a, b) show that high SPM concentrations strongly limit the release of IHg in

481 the dissolved form. Thus, despite higher concentration of IHg in STP samples, there is

482 depletion of IHg$_D$ due to much higher SPM concentration. Similar procedure developed for

483 MeHg$_D$ as function of SPM and total MeHg concentrations demonstrated linear effects (Fig.

484 SI-3 c, d). Although MeHg$_D$ also decreases with SPM, IHg$_D$ is retained on particles in much

485 higher extent. Similarly, sorption of IHg$_D$ on high concentrations of SPM was observed in Aveiro

486 Lagoon while no such effect was noticed for MeHg$_D$ (Stoichev et al. 2016; 2018). Possibly, as

487 in the Seine Estuary, high SPM concentrations induced flocculation of colloidal and sorption of

488 truly dissolved IHg (Laurier et al., 2003). Preliminary results have shown that this process

489 occurs at low salinity and low river discharge in the Adour Estuary and influences trace metals

490 partitioning (Point, 2004).

18

491   Higher total concentrations were found near specific discharge points (0.79–8.02 ng L^{-1} and 34–235 pg L^{-1}) compared to those in upstream and estuarine samples (0.51–3.42 ng L^{-1}

492

493   and 25–81 pg L^{-1} for IHg and MeHg, respectively). However, clear Hg contamination (MeHg,

494    $MeHg_D$, IHg) was found only at the STP station (concentration higher than LBL, $P_+=100\%$,

495   Table SI-5, Fig. 4), where high concentrations of organic-rich particles and nutrients were

496   observed. The distinction between STP and the other sample types is even more noticeable

497   for MeHg than for IHg. High total concentrations of IHg and MeHg in STP could be explained

498   by more organic matter and SPM (Fig. 5) but they are only two to three times higher than the

499   background values (Table SI-4) and have no great impact on estuarine water. Similarly, local

500   wastewaters can be sources of musks and alkylphenols to Adour Estuary but have limited

501   effect due to contaminants reactivity and a large dilution of these anthropogenic tributaries

502   (Cavalheiro et al., 2017). The effect separation of Sal/T and SPM/IHg_D also shows

503   concentrations of $MeHg_D$ in STP that are higher than expected, despite higher concentrations

504   of SPM (Fig. 6, Fig. SI-2). The removal of IHg in WTPs is higher than that of MeHg (Stoichev

505   et al. 2009). Therefore, effluent from STP (6, Fig. 1) might be slight source of MeHg to the

506   Adour Estuary, probably as a result of more labile organic matter in STP station.

507   Higher MeHg concentrations with lower F_D were found in Nive than in Adour upstream

508   (Fig. 4, Table SI-6). Despite much lower flowrate, Nive River transports about 9 % of MeHg to

509   the estuary during dry periods (Point, 2004). Sediments from Nive River have less IHg and

510   more MeHg than from Adour (Stoichev et al., 2004) suggesting higher MeHg accumulation or

511   net methylation potentials, and explained by specific organic matter and total sulphur content

512   in sediments. Thus, well defined maximum of MeHg concentration in Adour/Nive sediments

513   have been observed at 0.3% total S and 2.5–3.0% organic C irrespectively of the sampling

514   campaigns (Stoichev et al., 2004), while the concentrations of iHg were maximal at higher

515   concentrations of both total S (0.4–0.7%) and organic C (3.5%). Lower DOC concentrations

516   and particles richer in POC in Nive may be involved in higher particulate MeHg concentrations

517   compared to Adour. Favorable microenvironment for methylation might occur near organic-

518   rich particles (Ortiz et al., 2015). Alternatively, complexation of IHg with higher concentration

19

519 of dissolved organic matter in Adour River (Table SI-3) would produce less reactive complexes

520 (Stoichev et al., 2002) and decrease the availability for methylation.

521

5. Conclusions

523 The statistical effect separation by analysis of covariance was found useful to study IHg and

524 MeHg biogeochemistry in estuary with possible downstream contamination sources. Reduced

525 emissions of Hg rapidly decreased the contamination of estuarine water with Hg. Low Hg

526 concentrations nowadays are modifying the extent of MeHg, becoming limited by IHg. Thus,

527 both IHg and MeHg total concentrations are determined by organic-rich particles in a similar

528 way, but the effect of organic matter is stronger for MeHg. Dissolved/colloidal concentrations,

529 especially of IHg, decreased at high levels of SPM, possibly by sorption/flocculation. Total IHg

530 and MeHg, found near specific discharge points, are carried by organic-rich particles and have

531 negligible effect on estuarine water quality due to significant dilution. However, concentrations

532 of dissolved MeHg near specific points are higher than predicted values, obtained by the

533 statistical models, accounting for biogeochemical variables. The method efficiency is

534 dependent upon availability of enough biogeochemical explanatory variables, and it is usually

535 better for total than for dissolved concentrations. It is probable that more than two continuous

536 variables are simultaneously required to explain dissolved concentrations. The utility of relating

537 simple biogeochemical variables with IHg and MeHg concentrations should be checked for

538 other estuaries affected by downstream contamination with Hg or with other contaminants.

539

551

Appendix A. Supplementary data

553 Supplementary material related to this article can be found in the online version.

554

References

556 Abril, G., Nogueira, M., Etcheber, H., Cabeçadas, G., Lemaire, E., Brogueira, M.J., 2002. Behaviour of

557   Organic Carbon in Nine Contrasting European Estuaries. Est. Coast. Shelf Sci. 54, 241-262.

558 Aly, W., Williams, I.D., Hudson, M.D., 2013. Metal contamination in water, sediment and biota from a

559   semi-enclosed coastal area. Environ. Monit. Assess. 185, 3879-3895.

560 Aminot, A., Kérouel, R., 2004. Dissolved organic carbon, nitrogen and phosphorus in the N-E Atlantic

561   and the N-W Mediterranean with particular reference to non-refractory fractions and

562   degradation. Deep-Sea Res. Part I Oceanogr. Res. Pap. 51, 1975-1999.

563 Arleny, I., Tabouret, H., Rodriguez-Gonzalez, P., Bareille, G., Donard, O.F.X., Amouroux, D., 2007.

564   Methylmercury bioconcentration in muscle tissue of the European eel (Anguilla anguilla) from

565   the Adour estuary (Bay of Biscay, France). Mar. Pollut. Bull. 54, 1031-1036.

566 Azad, A.M., Frantzen, S., Bank M.S, Johnsen, I.A., Tessier, E., Amouroux, D., Madsen, L., Maage,

567   A., 2019. Spatial distribution of mercury in seawater, sediment, and seafood from the

568   Hardangerfjord ecosystem, Norway. Sci. Total Environ. 667, 622-637.

569 Azaroff, A., Tessier, E., Deborde, J., Guyoneaud, R., Monperrus, M., 2019. Mercury and methylmercury

570   concentrations, sources and distribution in submarine canyon sediments (Capbreton, SW

571   France): Implications for the net methylmercury production. Sci. Total Environ. 673, 511-521.

21

572 Balcom, P.H., Hammerschmidt, C.R., Fitzgerald, W.F., Lamborg, C.H., O'Connor, J.S., 2008. Seasonal
573 distributions and cycling of mercury and methylmercury in the waters of New York/New Jersey
574 Harbor Estuary. Mar. Chem. 109, 1-17.

575 Bloom, N.S., Moretto, L.M., Ugo, P., 2004. A comparison of the speciation and fate of mercury in two
576 contaminated coastal marine ecosystems: The Venice Lagoon (Italy) and Lavaca Bay (Texas).
577 Limnol. Oceanogr. 49, 367-375.

578 Borja, A., Amouroux, D., Anschutz, P., Gómez-Gesteira, M., Uyarra, M.C., Valdés, L., 2019. The Bay of
579 Biscay, In: World Seas: An Environmental Evaluation, Second Edition, Volume One: Europe,
580 The Americas and West Africa, Sheppard, C. (ed.), Elsevier, pp. 113-152.

581 Bouchet, S., Amouroux, D., Rodriguez-Gonzalez, P., Tessier, E., Monperrus, M., Thouzeau, G., Clavier,
582 J., Amice, E., Deborde, J., Bujan, S., Grall, J., Anschutz, P., 2013. MMHg production and export
583 from intertidal sediments to the water column of a tidal lagoon (Arcachon Bay, France).
584 Biogeochemistry 114, 341-358.

585 Bratkič, A., Ogrinc, N., Kotnik, J., Faganeli, J., Žagar, D., Yano, S., Tada, A., Horvat, M., 2013. Mercury
586 speciation driven by seasonal changes in a contaminated estuarine environment. Environ. Res.
587 125, 171-178.

588 Bravo, A.G., Kothawala, D.N., Attermeyer, K., Tessier, E., Bodmer, P., Amouroux, D., 2018. Cleaning
589 and sampling protocol for analysis of mercury and dissolved organic matter in freshwater
590 systems. MethodsX 5, 1017-1026.

591 Cavalheiro, J.; Sola, C.; Baldanza, J.; Tessier, E.; Lestremau, F.; Botta, F.; Preud'homme, H.;
592 Monperrus, M.; Amouroux, D., 2016. Assessment of Background Concentrations of
593 Organometallic Compounds (Methylmercury, Ethyllead and Butyl- and Phenyltin) in French
594 Aquatic Environments. Water Res. 94, 32-41.

595 Cavalheiro, J., Zuloaga, O., Prieto, A., Preudhomme, H., Amouroux, D., Monperrus, M., 2017.
596 Occurrence and Fate of Organic and Organometallic Pollutants in Municipal Wastewater
597 Treatment Plants and Their Impact on Receiving Waters (Adour Estuary, France). Arch.
598 Environ. Contam. Toxicol. 73, 619-630.

599 Crawley, M.J., 2007. The R book. Wiley, Chichester.

600 Driscoll, C.T., Mason, R.P., Chan, H.M., Jacob, D.J., Pirrone, N., 2013. Mercury as a Global Pollutant:
601 Sources, Pathways, and Effects. Environ. Sci. Technol. 47, 4967-4983.

602 ESBN, 2005. European Soil Bureau Network, Soil Atlas of Europe, European Commission, Office for

603   Official Publications of the European Communities, L-2995 Luxembourg, pp. 128.

604 Fabre, E., 1998. Aquatic hyphomycetes in three rivers of southwestern France. I. Spatial and temporal

605   changes in conidial concentration, species richness, and community diversity. Can. J. Bot. 76,

606   99-106.

607 García-Martín, E.E., Sanders, R., Evans, C.D., Kitidis, V., Lapworth, D.J., Rees, A.P., et al. 2021.

608   Contrasting Estuarine Processing of Dissolved Organic Matter Derived From Natural and

609   Human-Impacted Landscapes. Global Biogeochem. Cycles 35, e2021GB007023.

610 Gosnell, K., Balcom, P., Ortiz, V., DiMento, B., Schartup, A., Greene, R., Mason, R., 2016. Seasonal

611   Cycling and Transport of Mercury and Methylmercury in the Turbidity Maximum of the Delaware

612   Estuary. Aquat. Geochem. 22, 313-336.

613 Gredilla, A., Fdez-Ortiz de Vallejuelo, S., de Diego, A., Arana, G., Stoichev, T., Amigo, J.M.,

614   Wasserman, J.C., Botello, A.V., Sarkar, S.K., Schäfer, J., Moreno, C., de la Guardia, M.,

615   Madariaga, J.M., 2015. A chemical status predictor. A methodology based on World-Wide

616   sediment samples. J. Environ. Manage. 161, 21-29.

617 Horvat, M., Covelli, S., Faganeli, J., Logar, M., Mandić, V., Rajar, R., Širca, A., Žagar, D., 1999. Mercury

618   in contaminated coastal environments; a case study: the Gulf of Trieste. Sci. Total Environ.

619   237/238, 43-56.

620 Koroleff, F., 1969. Determination of ammonia as indophenol blue. International Council for the

621   Exploration of the sea (ICES), p8.

622 Laurier, F.J.G., Cossa, D., Gonzalez, J.L., Breviere, E., Sarazin, G. 2003. Mercury transformations and

623   exchanges in a high turbidity estuary: The role of organic matter and amorphous oxyhydroxides.

624   Geochim. Cosmochim. Acta, 67, 3329-3345.

625 Lee, S.-A., Kim, G. 2018. Sources, fluxes, and behaviors of fluorescent dissolved organic matter

626   (FDOM) in the Nakdong River Estuary, Korea. Biogeosciences 15, 1115-1122.

627 Leermakers, M., Galletti, S., De Galan, S., Brion, N., Baeyens, W., 2001. Mercury in the Southern North

628   Sea and Scheldt estuary. Mar. Chem. 75, 229-248.

629 Liu, M., Zhang, Q., Maavara, T., Liu, S., Wang, X., Raymond, P.A., 2021. Rivers as the largest source

630   of mercury to coastal oceans worldwide. Nat. Geosci. 14, 672-677.

631 Lorenzen, C., 1967. Determination of chlorophyll and pheo-pigments: spectrophotometric equations.

632   Limnol. Oceanogr. 12, 343-346.

633 Mullin, J.B., Riley, J.P., 1955. The colorimetric determination of silicate with special reference to sea

634   and natural waters. Anal. Chim. Acta 12, 162-176.

635 Murphy, J., Riley, J.P., 1962. A modified single solution method for determination of phosphate in natural

636   waters. Anal. Chim. Acta 27, 31-36.

637 Navarro, P., Amouroux, D., Thanh, N.D., Rochelle-Newall, E., Ouillon, S., Arfi, R., Van, T.C., Mari, X.,

638   Torréton, J.-P., 2012. Fate and tidal transport of butyltin and mercury compounds in the waters

639   of the tropical Bach Dang Estuary (Haiphong, Vietnam). Mar. Pollut. Bull. 64, 1789-1798.

640 Ortiz, V.L., Mason, R.P., Ward, J.E., 2015. An examination of the factors influencing mercury and

641   methylmercury particulate distributions, methylation and demethylation rates in laboratory-

642   generated marine snow. Mar. Chem. 177, 753-762.

643 Pato, P., Lopes, C., Válega, M., Lillebø, A.I., Dias, J.M., Pereira, E., Duarte, A.C., 2008. Mercury fluxes

644   between an impacted coastal lagoon and the Atlantic Ocean. Est. Coast. Shelf Sci. 76, 787-

645   796.

646 Pavoni, E., García-Ordiales, E., Covelli, S., Cienfuegos, P., Roqueñí, N., 2021. Legacy of Past Mining

647   Activity Affecting the Present Distribution of Dissolved and Particulate Mercury and

648   Methylmercury in an Estuarine Environment (Nalón River, Northern Spain). Appl. Sci. 11: 4396.

649 Point, D., 2004. Spéciation et biogéochimie des éléments traces métalliques dans l'estuaire de l'Adour.

650   PhD thesis, Université de Pau et des Pays de l'Adour, pp. 340.

651 Point, D., Bareille, G., Amouroux, D., Etcheber, H., Donard, O.F.X., 2007. Reactivity, interactions and

652   transport of trace elements, organic carbon and particulate material in a mountain range river

653   system (Adour River, France). J. Environ. Monit. 9, 157-167.

654 Point, D., Bareille, G., Stoichev, T., Amouroux, D., Donard, O.F.X., 2003. Trace metals inputs in the

655   Adour urban estuary: influence and impact of human pressure. J. Phys. IV, Volume II, Boutron,

656   C., Ferrari, C. (Eds.),107, 1071-1074.

657 R Core Team, 2017. R: A language and environment for statistical computing. Vienna, Austria: R

658   Foundation for Statistical Computing. Retrieved from http://www.R-proje ct.org/

659 Savoye, N., Aminot, A., Tréguer, P., Fontugne, M., Naulet, N., Kérouel, R., 2003. Dynamics of particulate

660 organic matter δ15N and δ13C during spring phytoplankton blooms in a macrotidal ecosystem

661 (Bay of Seine, France). Mar. Ecol. Prog. Ser. 255, 27-41.

662 Savoye, N., David, V., Morisseau, F., Etcheber, H., Abril, G., Billy, I., Charlier, K., Oggian, G., Derriennic,

663 H., Sautour, B., 2012. Origin and composition of particulate organic matter in a macrotidal turbid

664 estuary: The Gironde Estuary, France. Est. Coast. Shelf Sci. 108, 16-28.

665 SDAGE-PDM, 2014. Synthese de l'actualisation de l'état des lieux du SDAGE 2016-2021. Comité de

666 bassin Adour-Garonne (validée le 02 décembre 2013), Commission territoriale Adour. Le

667 Schema Directeur d'Amenagement et de Gestion des Eaux (SDAGE) et son Programme De

668 Mesures (PDM), pp 31.

669 SDES-OFB, 2020. Joassard, I., Bréjoux, E., Larrieu, C., Dequesne, J. (authors); Eau et milieux

670 aquatiques, les chiffres clés. Le Service des Données et Études Statistiques (SDES) en

671 partenariat avec l'Office Français de la Biodiversité (OFB), Ministère de la Transition

672 Écologique, pp.127.

673 Sharif, A., Monperrus, M., Tessier, E., Bouchet, S., Pinaly, H., Rodriguez-Gonzalez, P., Maron, P.,

674 Amouroux, D., 2014. Fate of mercury species in the coastal plume of the Adour River estuary

675 (Bay of Biscay, SW France). Sci. Total Environ. 496, 701-713.

676 Stoichev, T., Amouroux, D., Monperrus, M., Point, D., Tessier, E., Bareille, G., Donard, O.F.X., 2006.

677 Mercury in surface waters of a macrotidal urban estuary (River Adour, south-west France).

678 Chem. Ecol. 22,137-148.

679 Stoichev, T., Amouroux, D., Wasserman, J., Point, D., de Diego, A., Bareille, G., Donard, O.F.X., 2004.

680 Dynamics of mercury species in surface sediments from a macrotidal estuarine-coastal system

681 (Adour River, Bay of Biscay). Est. Coast. Shelf Sci. 59, 511-521.

682 Stoichev, T., Martin-Doimeadios, R.C.R., Amouroux, D., Molenat, N., Donard, O.F.X., 2002. Application

683 of cryofocusing hydride generation and atomic fluorescence detection for dissolved mercury

684 species determination in natural water samples. J. Environ. Monit. 4, 517-521.

685 Stoichev, T., Tessier, E., Almeida, C.M., Basto, M.C.P., Vasconcelos, V.M., Amouroux, D., 2018. Flux

686 model to estimate the transport of mercury species in a contaminated lagoon (Ria de Aveiro,

687 Portugal). Environ. Sci. Pollut. Res. 25, 17371-17382.

688 Stoichev, T., Tessier, E., Amouroux, D., Almeida, C.M., Basto, M.C.P., Vasconcelos, V.M., 2016.

689 Multiple regression analysis to assess the role of plankton on the distribution and speciation of

690 mercury in water of a contaminated lagoon. J. Haz. Mater. 318, 711-722.

691 Stoichev, T., Tessier, E., Coelho, J.P., Lobos Valenzuela, M.G., Pereira, M.E., Amouroux, D., 2019.

692 Multiple regression analysis to assess the spatial distribution and speciation of mercury in

693 surface sediments of a contaminated lagoon. J. Haz. Mater. 367, 715-724.

694 Stoichev, T., Marques, A., Almeida, C.M., 2021. Modeling the relationship between emerging and

695 persistent organic contaminants in water, sediment and oysters from a temperate lagoon. Mar.

696 Pollut. Bull. 164: 111994.

697 Stoichev, T., Tessier, E., Garraud, H., Amouroux, D., Donard, O.F.X., Tsalev, D.L., 2009. Mercury

698 speciation and partitioning along a municipal sewage treatment plant. J. Balkan Ecol., 12, 135-

699 145.

700 Strickland, J.D.H., Parsons, T.R., 1972. A practical handbook of seawater analysis. Fisheries Research

701 Board of Canada Bulletin 167, Fisheries Research Board of Canada, Ottawa.

702 Wang, S., Jia, Y., Wang, S., Wang, X., Wang, H., Zhao, Z., Liu, B., 2009. Total mercury and

703 monomethylmercury in water, sediments, and hydrophytes from the rivers, estuary, and bay

704 along the Bohai Sea coast, northeastern China. Appl. Geochem. 24, 1702-1711.

705

Figure captions

707

708 **Fig. 1.** Map of Adour estuary with sampling points. Sampling points separated according to

709 **type**: upstream (1, 2, 3, 4), estuary (A, B, C, D), STP (6), Urban/STP (7, 8, 9), and **place**:

710 Adour (1, 2, A, B, C, D), Trib/Adour (6, 8), Trib (7, 9), Nive (3, 4). The inset is map of France

711 with Adour Estuary highlighted.

712

713 **Fig. 2.** Schema of used statistical models concerning factors (Analysis of Variance, ANOVA),

714 continuous explanatory variables (Multiple Regression, MR) or both (Generalized Additive

715 Models, GAM and Analysis of Covariance, ANCOVA).

716

717 **Fig. 3.** Box-Whisker plot of biogeochemical variables in surface water from Adour Estuary

718 separated according to sample type levels (Fig. 1, upstream (1, 2, 3, 4), estuary (A, B, C, D),

719 STP (6), Urban/STP (7, 8, 9)). The box encompasses values between first (Q_1) and third (Q_3)

720 quartiles. The median is marked with a line and **×** represents the average value. The error bar

721 shows the range without outliers (for levels upstream, estuary and Urban/STP). A data is

722 considered outlier if exceeds the distance of 1.5 times (Q_3–Q_1) bellow Q_1 or above Q_2. Only

723 variables showing significant between type difference ($p<0.1$) are selected.

724

725 **Fig. 4.** Concentrations of IHg (**a**) total; (**b**) dissolved and of MeHg (**c**) total; (**d**) dissolved in

726 surface water from Adour estuary. Samples (Fig. 1) grouped into upstream (Adour: 1, 2; Nive:

727 3, 4), estuary (A, B, C, D), Urban/STP (7, 8, 9) and STP (6) categories.

728

729 **Fig. 5.** Model values for total concentrations of (**a**, **b**) IHg (Eq. 13, adjR^2=0.836), (**c**, **d**) MeHg

730 (Eq.14, adjR^2=0.798), (**e**, **f**) percentage of MeHg relative to total Hg (%MeHg) (Eq. 16,

731 adjR^2=0.756) in water (Adour Estuary) as a function of (**a**, **c**, **e**) changing SPM concentration

732 at fixed POC and (**b**, **d**, **f**) changing POC concentration at fixed SPM. Fixed values for POC

733 and SPM determined as group-based averages according to factor levels in the minimal

734 adequate models. The slope c_1 for the dependence between model values and experimental

735 values (**a**, **b**) 0.894 ± 0.067, (**c**, **d**) 0.809 ± 0.073 and (**e**, **f**) 0.694 ± 0.060.

736 $\ln[IHg] = a_0\big(time_{Sept(+)}; type_{Upstream(-)}\big) + |a_{11}|[SPM] - |a_{12}|/[POC]$

737 $\ln[MeHg] = a_0\big(type_{Urban/STP(-)}\big) + |a_{11}|[SPM] - |a_{12}|/[POC]$

738 $\ln[\%MeHg] = a_0\big(time_{Sept(-)}; type_{STPUrban/STP\,(-)}\big) - |a_{11}|[SPM] - |a_{12}|/[POC] + |a_{12,12}|/[POC]^2$

739

740 **Fig. 6.** Model values for concentrations of MeHg (**a**, **b**) total (Eq. 15, adjR^2=0.831) and

741 dissolved (Eq. 18, adjR^2=0.709) in water (Adour estuary) as a function of (**a**) changing IHg total

742 concentration at fixed POC; (**b**) changing POC at fixed IHg total concentration; (**c**) changing

743 IHg dissolved concentration at fixed SPM; (**d**) changing SPM at fixed IHg dissolved

744 concentration Fixed values of dependent variables determined as group-based averages

745 according to factor levels in the minimal adequate models. The slopes c_1 for the dependence

746 between model values and experimental values are (**a**, **b**) 0.806 ± 0.050, (**c**, **d**) 0.872 ± 0.062.

747 $\ln[MeHg] = a_0\big(type_{Urban/STP(-)}\big) - |a_{12}|/[POC] + |a_{18}|\ln[IHg]$

748 $\ln[MeHg_D] = a_0\big(type_{STP\,(+)}\big) - |a_{11}|[SPM] + |a_{11,11}|[SPM]^2 - |a_{11,11,11}|[SPM]^3 + |a_{19}|\ln[IHg_D]$

Table 1 Historical comparison of total mercury and methylmercury concentrations (<u>geometric mean</u> and *range*) in water from Adour Estuary. Data for previous studies filtered to salinity found here (0.1–16.9). Estimates of anthropogenic mercury emissions to the air (E) in France during the sampling years also presented.

Campaign	Salinity	Hg_{TOT} (ng L^{-1})[a]	MeHg (pg L^{-1})[a]	Emissions (E) (tons Hg year^{-1})[b]	References
Febr 1998 (n=5)	<u>3.7</u> *(0.3–11.6)*	<u>28.1</u> *(9.64–211.6)*	<u>536</u> *(<762–2086)*	14.12	Stoichev et al., 2006
July 1998 (n=6)	<u>3.4</u> *(0.2–15.9)*	<u>21.7</u> *(10.25–72.89)*	<u>381</u> *(<0.762)*	14.12	
Sept 1999 (n=18)	<u>4.3</u> *(0.2–17)*	<u>24.1</u> *(11.0–111.1)*	<u>690</u> *(228–1285)*	12.83	
Febr 2001 (n=9)	<u>0.23</u> *(0.1–4.9)*	<u>6.1</u> *(<0.54–194.8)*	<u>37</u> *(<0.020–1189)*	10.88	
April 2007 May 2010 (n=2)	<u>0.42</u> *(0.2–0.9)*	<u>2.03</u> *(1.52–2.70)*	<u>77</u> *(48–124)*	<u>5.05</u> *(4.78–5.34)*	Sharif et al., 2014
May 2017 (n=4)	<u>1.1</u> *(0.1–16.9)*	<u>0.95</u> *(0.60–1.49)*	<u>32</u> *(25–40)*	3.26	this study
Sept 2017 (n=4)	<u>0.69</u> *(0.1–10.8)*	<u>2.54</u> *(1.74–3.38)*	<u>43</u> *(34–52)*	3.26	
Jan 2018 (n=4)	<u>0.27</u> *(0.1–0.9)*	<u>2.12</u> *(1.75–2.46)*	<u>57</u> *(51–63)*	3.09	

[a]concentrations lower than limit of detection (LOD) replaced by 0.5*LOD to calculate geometric mean; [b]https://www.citepa.org/fr/2021-hg/. Deposited mercury in France (2019) is derived from emissions from France (43.9%) and from neighboring countries with similar environmental policies (46.1%), similar emission trends as in France (https://www.emep.int/) and should be proportional to E. There is no effect of Salinity on Hg_{TOT} geometric mean concentrations

$$\ln[Hg_{TOT}] = (-0.342 \pm 0.302) + (0.247 \pm 0.031)E$$

adjR^2=0.897, n=8
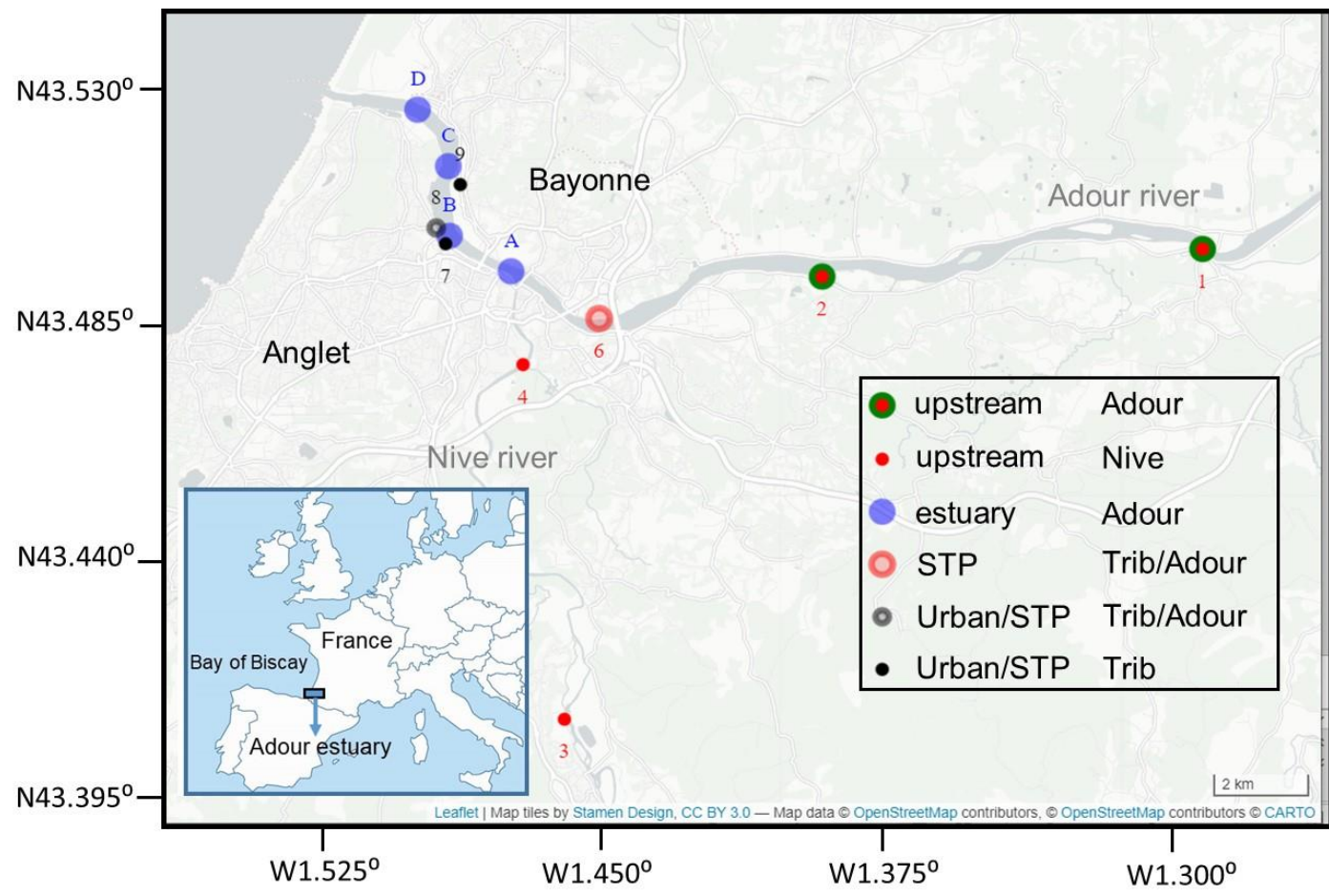
Figure 1
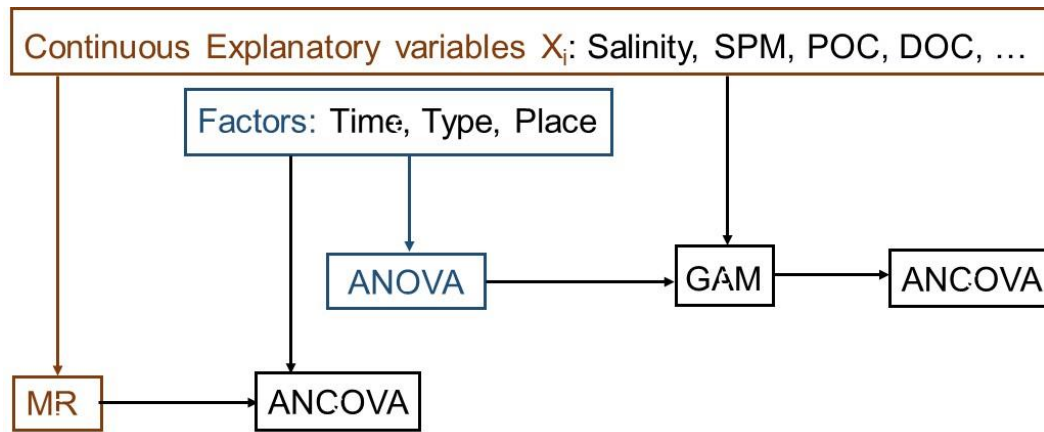
Figure 1.

Figure 2
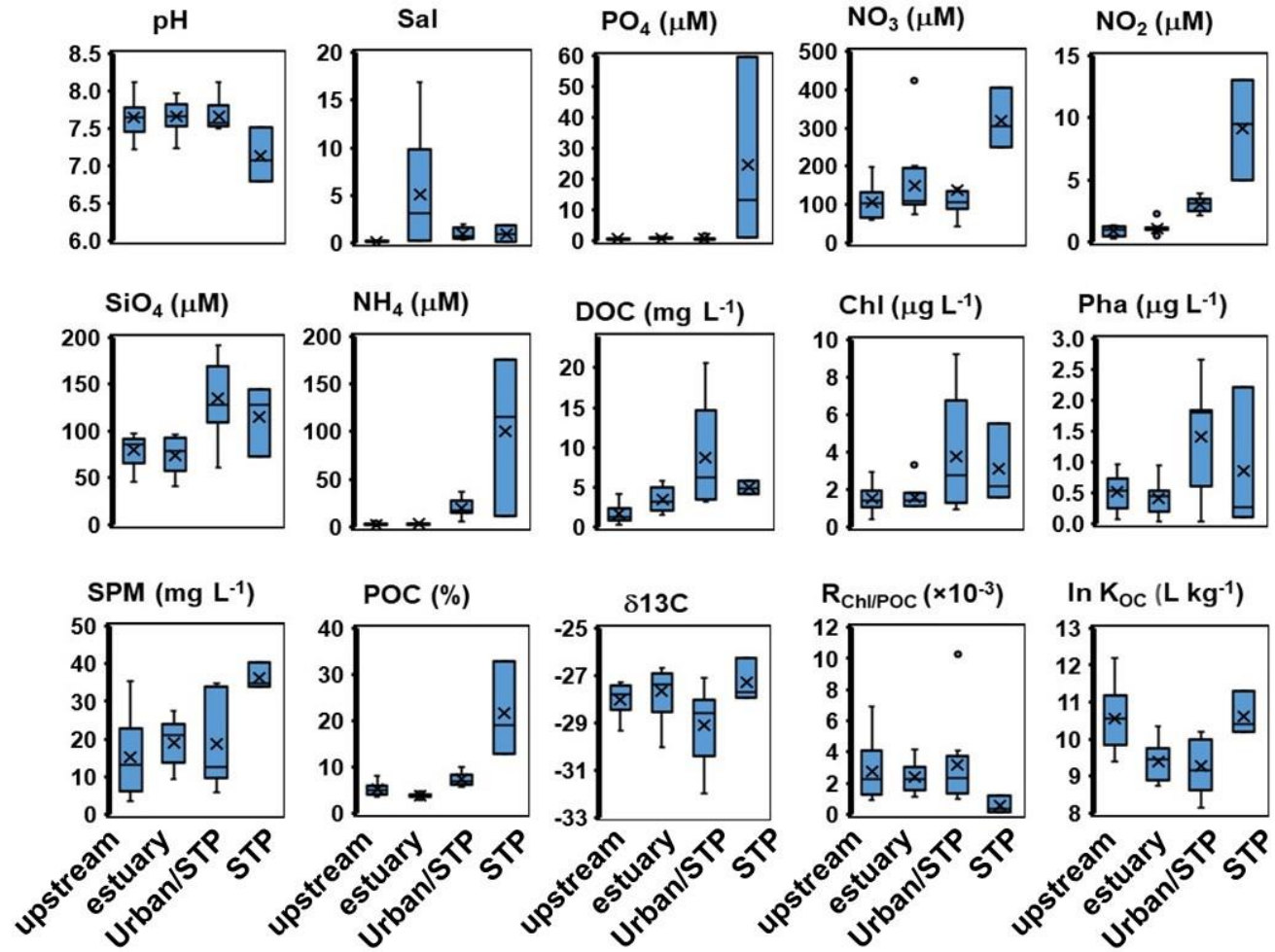
Figure 2.

Figure 3

Figure 3.

Figure 4.

Figure 5

Click here to access/download;Figure(s);Fig5.docx ±

Figure 5.

Figure 6   Click here to access/download;Figure(s);Fig6.docx ⬇
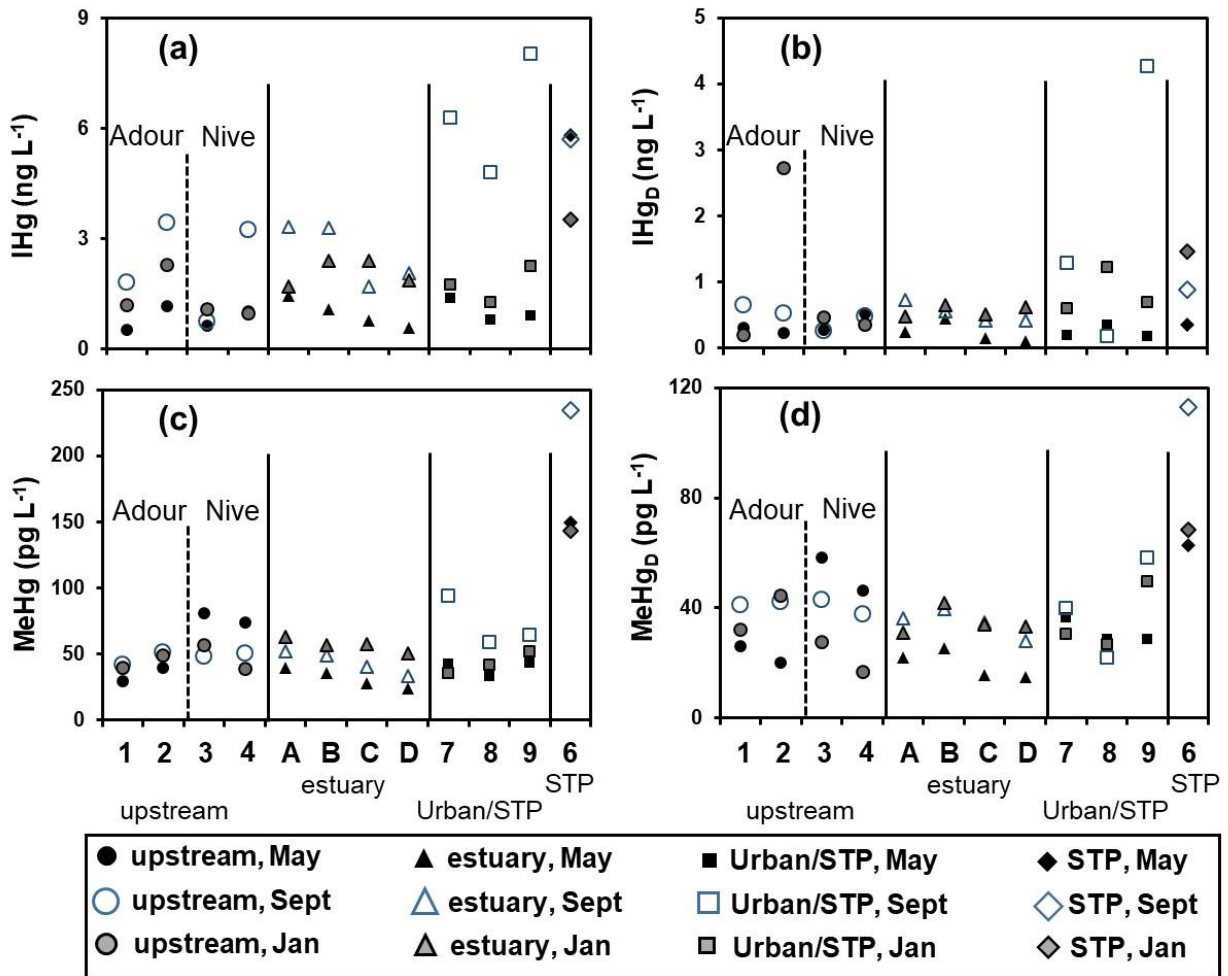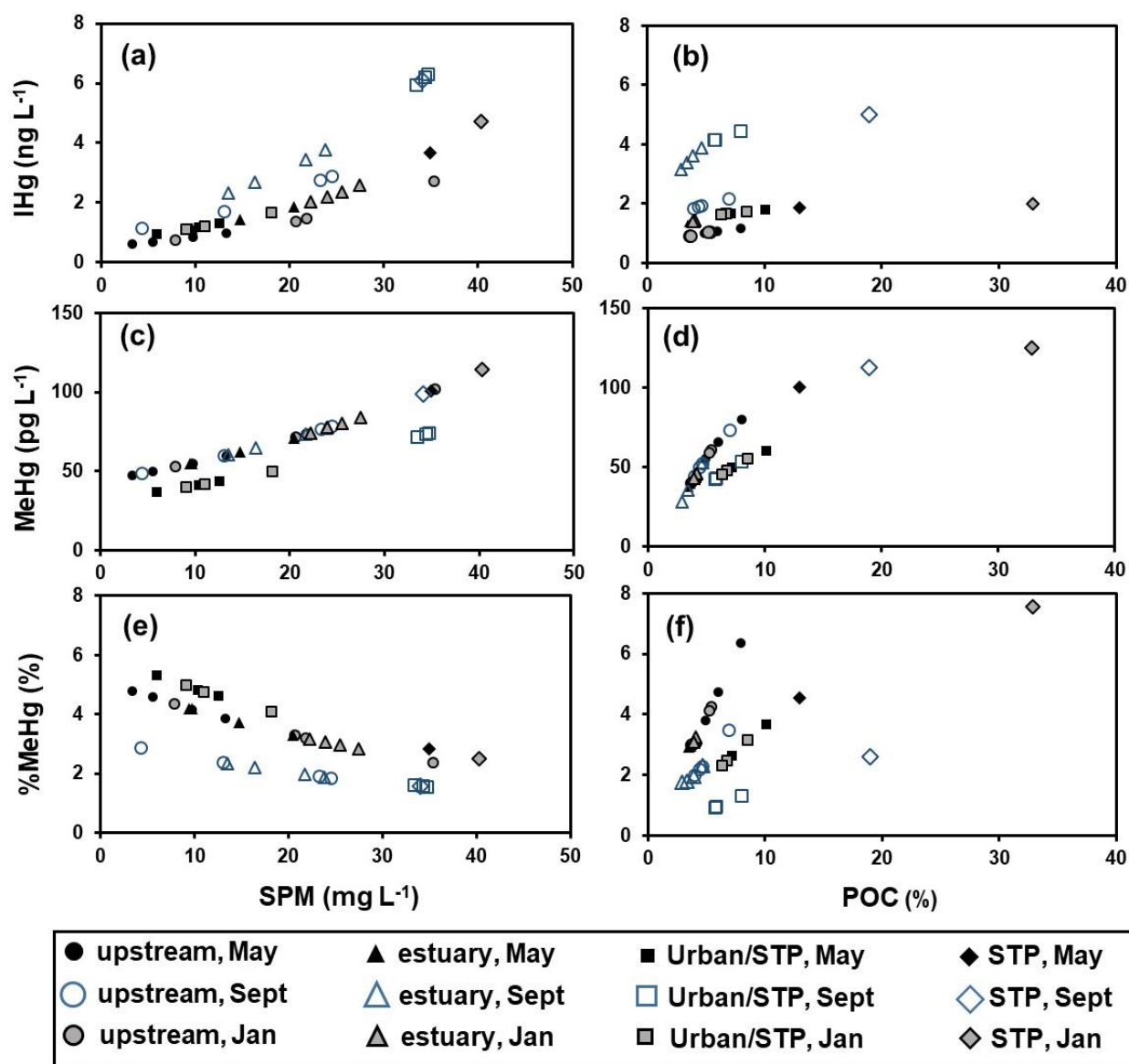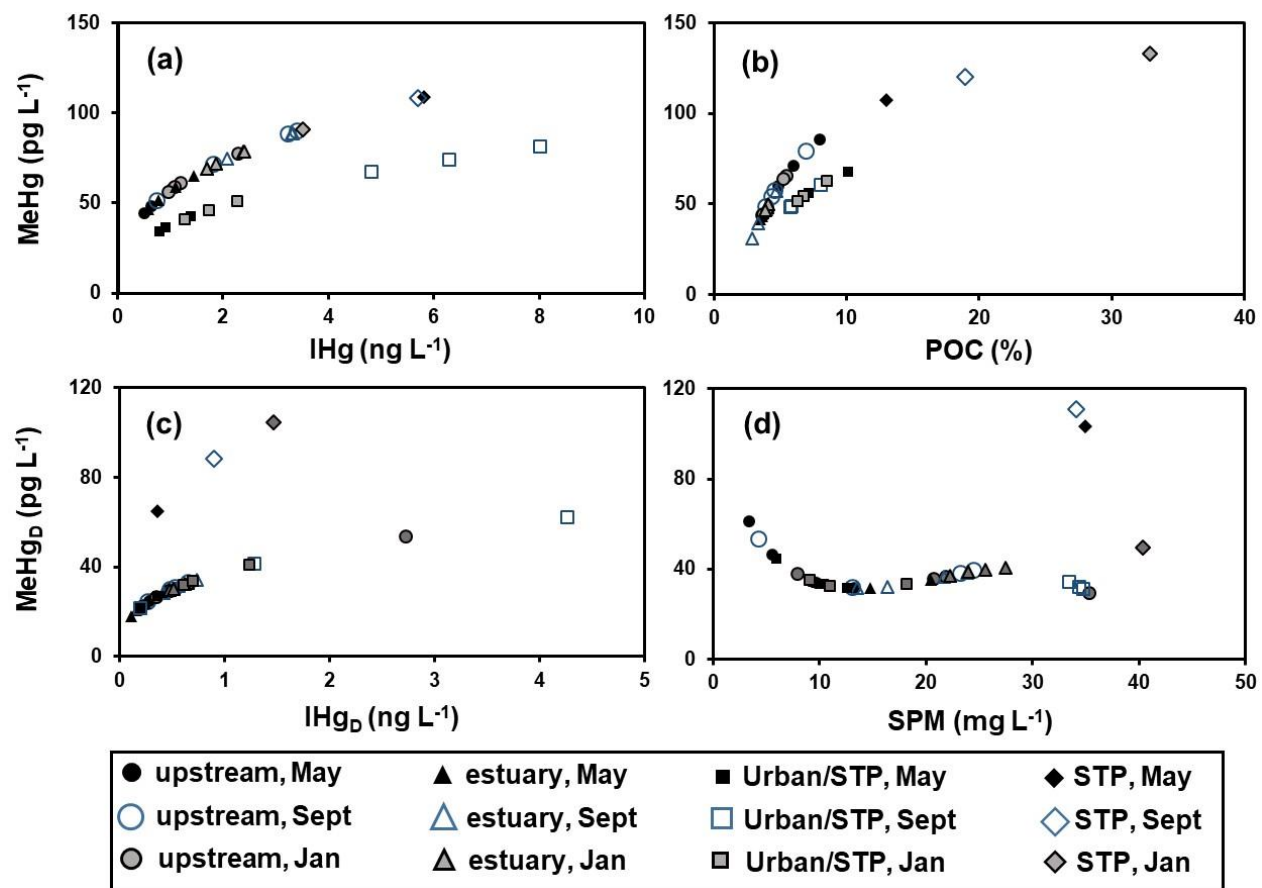
Figure 6.

SUPPLEMENTARY INFORMATION

(Tables)

Marine Pollution Bulletin

Assessing and predicting the changes for inorganic mercury and methylmercury concentrations in surface waters of a tidal estuary (Adour Estuary, SW France)

Teodor Stoichev*[a], Aubin Thibaut de Chanvalon[b], Sandrine Veloso[b],

Jonathan Deborde[b,c], Emmanuel Tessier[b], Laurent Lanceleur[b], David Amouroux*[b]

[a] Interdisciplinary Center of Marine and Environmental Research (CIIMAR/CIMAR), University of Porto, Terminal de Cruzeiros de Leixoes, Av. General Norton de Matos s/n, 4450-208 Matosinhos, Portugal,

E-mail: tstoichevbg@yahoo.com

[b] Universite de Pau et des Pays de l'Adour, E2S UPPA, CNRS, IPREM, Institut des Sciences Analytiques et de Physico-chimie pour l'Environnement et les matériaux, Pau, France,

E-mail: david.amouroux@univ-pau.fr

[c] Ifremer, LITTORAL, Laboratoire Environnement Ressources des Pertuis Charentais, F-17390 La Tremblade, France

Table SI-1 Average values (bold), geometric mean (underlined) and range (italic font) for continuous explanatory variables separated according to factor time with three levels (May (n=12), Sept (n=12), Jan (n=12)). Standard deviation presented if smaller than the average values. Significant difference (p<0.10) between groups studied with Wilcoxon rank sum test. Local background levels (LBL) in bulk water were calculated using 3σ and 4σ criteria (Gredilla et al. 2015) with samples from type upstream (Fig. 1: 1, 2, 3, 4) and estuary (Fig. 1: A, B, C, D).

	May	Sept	Jan	4σ LBL	3σ LBL
Salinity	**4.01**, 1.07	**1.86**, 0.69	**0.32** ± 0.22, 0.27	2.63	7.12
	(0.10 : 16.88)	*(0.12 : 10.80)*	*(0.13 : 0.87)*		
T (°C)	**15.67** ± 1.27, 15.63	**16.59** ± 1.69, 16.52	**9.33** ± 1.88, 9.19	13.38	17.08
	(13.87 : 17.83)	*(14.92 : 20.81)*	*(7.93 : 14.70)&#*		
O_2 (mg L^{-1})	**8.46** ± 1.22, 8.38	**7.97** ± 0.78, 7.93	**10.12** ± 1.04, 10.06	8.86	10.66
	(7.00 : 10.84)	*(6.85 : 9.85)*	*(7.62 : 11.37)&#*		
pH	**7.62** ± 0.32, 7.62	**7.65** ± 0.26, 7.65	**7.56** ± 0.25, 7.55	7.65	7.91
	(7.22 : 8.12)	*(7.07 : 7.98)*	*(6.80 : 7.74)*		
PO_4 (μM)	**0.66** ± 0.23, 0.62	**1.77**, 0.77	**5.46**, 0.70	0.65	1.00
	(0.32 : 1.13)	*(0.12 : 13.30)*	*(0.16 : 59.5)*		
NO_3 (μM)	**110.3** ± 53.2, 100.1	**122.5** ± 91.6, 106.5	**204.7** ± 118.4, 176.2	127.2	195.4
	(42.5 : 249)	*(65.0 : 405)*	*(68.3 : 424)&#*		
NO_2 (μM)	**1.94** ± 1.32, 1.62	**2.41**, 1.30	**2.17**, 1.47	0.99	1.23
	(0.88 : 4.93)	*(0.28 : 13.06)*	*(0.31 : 9.52)*		
NH_4 (μM)	**9.44**, 5.80	**16.18**, 5.74	**20.03**, 5.21	2.78	3.91
	(2.27 : 36.5)	*(1.91 : 116)*	*(1.14 : 175)*		

SiO$_4$ (μM)	**82.3** ± 46.9, <u>73.6</u> (41.5 : 191.6)	**100.9** ± 40.7, <u>93.5</u> (44.3 : 173)&	**100.6** ± 15.3, <u>99.6</u> (83.2 : 128.1)&	76.8	95.5
TN (mg L^{-1})	**2.45**, <u>1.38</u> (0.71 : 16.79)	**2.66**, <u>1.34</u> (0.63 : 19.74)	**5.04**, <u>2.38</u> (0.72 : 38.10)&#	1.33	2.47
DOC (mg L^{-1})	**6.75** ± 6.26, <u>4.30</u> (0.30 : 20.55)	**2.74** ± 1.73, <u>2.32</u> (0.96 : 6.18)&	**3.30** ± 2.73, <u>2.55</u> (0.63 : 11.23)&	2.53	4.94
Chl (μg L^{-1})	**2.89** ± 2.26, <u>2.34</u> (1.11 : 8.86)	**2.53** ± 2.33, <u>1.99</u> (1.08 : 9.23)	**1.29** ± 0.44, <u>1.20</u> (0.40 : 1.94)&#	1.55	2.13
Pha (μg L^{-1})	**0.73**, <u>0.36</u> (0.04 : 2.22)	**0.82** ± 0.81, <u>0.45</u> (0.04 : 2.66)	**0.66** ± 0.45, <u>0.55</u> (0.24 : 1.80)	0.47	0.87
SPM (mg L^{-1})	**12.50** ± 8.40, <u>10.49</u> (3.36 : 34.93)	**23.09** ± 9.92, <u>20.34</u> (4.35 : 34.72)&	**21.95** ± 9.84, <u>19.70</u> (7.88 : 40.30)&	17.15	25.20
POC (%)	**6.34** ± 2.90, <u>5.82</u> (3.51 : 12.97)	**6.13** ± 4.31, <u>5.33</u> (2.89 : 18.97)	**7.39**, <u>5.71</u> (3.67 : 32.89)	4.50	5.84
POC$_V$ (mg L^{-1})	**0.878**, <u>0.611</u> (0.268 : 4.532)	**1.579**, <u>1.084</u> (0.303 : 6.461)&	**1.962**, <u>1.126</u> (0.415 : 13.254)&	0.716	1.111
δ13C	**−29.05** ± 1.59 (−32.00 : −26.23)	**−27.60** ± 0.53 (−28.59 : −26.84)&	**−27.69** ± 0.69 (−28.98 : −26.66)&	−27.85	−26.91
δ15N	**5.26** ± 1.34, <u>5.09</u> (2.81 : 7.82)	**4.78** ± 0.61, <u>4.74</u> (3.43 : 5.62)	**1.53** (−5.73 : 4.32)&#	4.26	5.67
R$_{Chl/POC}$ (10^{-3})	**4.32** ± 2.31, <u>3.84</u> (1.22 : 10.31)	**2.11** ± 0.93, <u>1.84</u> (0.33 : 3.56)&	**1.25** ± 0.51, <u>1.07</u> (0.12 : 2.02)&	2.57	4.23
ActChl	**0.83** ± 0.12, <u>0.82</u>	**0.78** ± 0.14, <u>0.76</u>	**0.67** ± 0.17, <u>0.65</u>	0.77	0.95

	(0.63 : 1.00)	*(0.53 : 1.00)*	*(0.38 : 0.86)&*		
ln(K_{OC}) (L kg^{-1})	**9.51** ± 1.16, 9.45	**10.04** ± 0.53, 10.03	**10.02** ± 0.86, 9.98	9.98	11.18
	(8.15 : 12.20)	*(9.14 : 11.10)&*	*(8.63 : 11.33)*		
N/P	**192.7** ± 68.4, 182.8	**211.4**, 150.9	**417.5** ± 282.5, 271.4	236.1	409.5
	(125.2 : 338.1)	*(40.2 : 851.4)*	*(8.2 : 903.1)&#*		
Si/N	**0.73** ± 0.41, 0.65	**0.88** ± 0.37, 0.80	**0.60** ± 0.33, 0.52	0.69	1.17
	(0.27 : 1.75)	*(0.27 : 1.67)*	*(0.22 : 1.22)#*		

& Significant difference for levels "Sept" and "Jan" relative to level "May"

Significant difference for level "Jan" relative to level "Sept"

Table SI-2 Average values (bold), geometric mean (underlined) and range (italic font) for continuous explanatory variables separated according to factor type with four levels (upstream (n=12), estuary (n=12), Urban/STP (n=9), STP (n=3)). Standard deviation presented if smaller than the average values. Significant difference (p<0.10) between groups studied with Wilcoxon rank sum test. The local background levels (LBL) for bulk water are considered the ranges between 4s LBL and 3s LBL values (Table SI-1). The proportion (P, %) of samples with values of the dependent variables equal to the LBL (marked with superscript (0) in front of P value), higher than LBL (marked with superscript (+) in front of P value) and lower than LBL (marked with superscript (–) in front of P value) are also presented. The binomial errors are given as subscript after P if at least two times smaller than the respective proportions. If P equaled 0 or 100%, the binomial errors are 0.

	upstream	estuary	Urban/STP	STP
Salinity	**0.16** ± 0.03, <u>0.16</u>	**5.09**, <u>1.81</u>	**0.94** ± 0.63, <u>0.76</u>	**0.93** ± 0.86, <u>0.53</u>
–	*(0.12 : 0.21)*	*(0.21 : 16.88)*&	*(0.38 : 1.95)*&	*(0.10 : 1.82)*
P (%)	$^{(-)}100$; $^{(0)}0$; $^{(+)}0$	$^{(-)}50.0_{14.4}$; $^{(0)}16.7$; $^{(+)}33.3_{13.6}$	$^{(-)}100$; $^{(0)}0$; $^{(+)}0$	$^{(-)}100$; $^{(0)}0$; $^{(+)}0$
T	**13.49** ± 3.41, <u>13.04</u>	**13.27** ± 3.86, <u>12.68</u>	**14.02** ± 3.71, <u>13.53</u>	**17.28** ± 3.16, <u>17.09</u>
(°C)	*(8.45 : 17.30)*	*(8.16 : 17.90)*	*(7.93 : 17.83)*	*(14.70 : 20.81)*
P (%)	$^{(-)}33.3_{13.6}$; $^{(0)}58.3_{14.2}$; $^{(+)}8.3$	$^{(-)}33.3_{13.6}$; $^{(0)}50.0_{14.4}$; $^{(+)}16.7$	$^{(-)}33.3_{15.7}$; $^{(0)}33.3_{15.7}$; $^{(+)}33.3_{15.7}$	$^{(-)}0$; $^{(0)}66.7_{27.2}$; $^{(+)}33.3$
O$_2$	**9.09** ± 1.56, <u>8.97</u>	**8.63** ± 1.37, <u>8.53</u>	**8.98** ± 1.32, <u>8.89</u>	**8.37** ± 0.98, <u>8.33</u>
(mg L^{-1})	*(7.00 : 11.37)*	*(7.02 : 10.44)*	*(6.85 : 10.84)*	*(7.62 : 9.48)*
P (%)	$^{(-)}50.0_{14.4}$; $^{(0)}25.0_{12.5}$; $^{(+)}25.0_{12.5}$	$^{(-)}66.7_{13.6}$; $^{(0)}33.3_{13.6}$; $^{(+)}0$	$^{(-)}44.4_{16.6}$; $^{(0)}33.3_{15.7}$; $^{(+)}22.2$	$^{(-)}66.7_{27.2}$; $^{(0)}33.3$; $^{(+)}0$
pH	**7.64** ± 0.25, <u>7.64</u>	**7.66** ± 0.22, <u>7.66</u>	**7.67** ± 0.22, <u>7.67</u>	**7.13** ± 0.36, <u>7.12</u>
–	*(7.22 : 8.12)*	*(7.24 : 7.98)*	*(7.50 : 8.12)*	*(6.80 : 7.51)*&#$
P (%)	$^{(-)}50.0_{14.4}$; $^{(0)}33.3_{13.6}$; $^{(+)}16.7$	$^{(-)}50.0_{14.4}$; $^{(0)}41.7_{14.2}$; $^{(+)}8.3$	$^{(-)}66.7_{15.7}$; $^{(0)}11.1$; $^{(+)}22.2$	$^{(-)}100$
PO$_4$	**0.53** ± 0.22, <u>0.49</u>	**0.77** ± 0.28, <u>0.73</u>	**0.56** ± 0.44, <u>0.43</u>	**24.65**, <u>9.64</u>
(μM)	*(0.31 : 1.04)*	*(0.44 : 1.36)*&	*(0.12 : 1.55)*	*(1.13 : 59.5)*&#$

P (%)	$^{(-)}75.0_{12.5}$; $^{(0)}16.7$; $^{(+)}8.3$	$^{(-)}41.7_{14.2}$; $^{(0)}41.7_{14.2}$; $^{(+)}16.7$	$^{(-)}77.8_{13.9}$; $^{(0)}11.1$; $^{(+)}11.1$	$^{(-)}0$; $^{(0)}0$; $^{(+)}100$
NO$_3$ (µM)	**104.7** ± 42.8, <u>97.3</u> *(59.5 : 199)*	**149.8** ± 97.1, <u>131.1</u> *(75.2 : 424)*	**137.6** ± 107.9, <u>114.6</u> *(42.5 : 415)*	**319.5** ± 79.4, <u>313.1</u> *(249 : 405)&#$*
P (%)	$^{(-)}75.0_{12.5}$; $^{(0)}16.7$; $^{(+)}8.3$	$^{(-)}66.7_{13.6}$; $^{(0)}8.3$; $^{(+)}25.0_{12.5}$	$^{(-)}66.7_{15.7}$; $^{(0)}22.2$; $^{(+)}11.1$	$^{(-)}0$; $^{(0)}0$; $^{(+)}100$
NO$_2$ (µM)	**0.88** ± 0.38, <u>0.78</u> *(0.28 : 1.34)*	**1.09** ± 0.41, <u>1.03</u> *(0.47 : 2.24)*	**3.01** ± 0.59, <u>2.96</u> *(2.12 : 3.89)&#*	**9.17** ± 4.08, <u>8.50</u> *(4.93 : 13.06)&#$*
P (%)	$^{(-)}50.0_{14.4}$; $^{(0)}33.3_{13.6}$; $^{(+)}16.7$	$^{(-)}33.3_{13.6}$; $^{(0)}50.0_{14.4}$; $^{(+)}16.7$	$^{(-)}0$; $^{(0)}0$; $^{(+)}100$	$^{(-)}0$; $^{(0)}0$; $^{(+)}100$
NH$_4$ (µM)	**2.56** ± 0.79, <u>2.45</u> *(1.14 : 4.42)*	**3.00** ± 0.73, <u>2.92</u> *(2.22 : 4.49)*	**19.83** ± 9.55, <u>17.74</u> *(6.17 : 36.5)&#*	**100.9** ± 82.9, <u>61.7</u> *(11.6 : 175)&#*
P (%)	$^{(-)}75.0_{12.5}$; $^{(0)}16.7$; $^{(+)}8.3$	$^{(-)}50.0_{14.4}$; $^{(0)}33.3_{13.6}$; $^{(+)}16.7$	$^{(-)}0$; $^{(0)}0$; $^{(+)}100$	$^{(-)}0$; $^{(0)}0$; $^{(+)}100$
SiO$_4$ (µM)	**79.3** ± 17.0, <u>77.4</u> *(45.8 : 97.5)*	**74.2** ± 19.5, <u>71.5</u> *(41.5 : 96.8)*	**135.3** ± 41.1, <u>128.8</u> *(60.5 : 192)&#*	**115.1** ± 37.5, <u>110.4</u> *(72.8 : 144)*
P (%)	$^{(-)}33.3_{13.6}$; $^{(0)}58.3_{14.2}$; $^{(+)}8.3$	$^{(-)}50.0_{14.4}$; $^{(0)}33.3_{13.6}$; $^{(+)}16.7$	$^{(-)}11.1$; $^{(0)}0$; $^{(+)}88.9_{10.5}$	$^{(-)}33.3$; $^{(0)}0$; $^{(+)}66.7_{27.2}$
TN (mg L^{-1})	**1.16** ± 0.55, <u>1.06</u> *(0.63 : 2.47)*	**1.50** ± 0.78, <u>1.33</u> *(0.73 : 2.80)*	**5.73**, <u>2.26</u> *(0.96 : 38.10)&*	**12.71** ± 9.73, <u>8.10</u> *(1.60 : 19.74)&#*
P (%)	$^{(-)}66.7_{13.6}$; $^{(0)}25.0_{12.5}$; $^{(+)}8.3$	$^{(-)}66.7_{13.6}$; $^{(0)}16.7$; $^{(+)}16.7$	$^{(-)}44.4_{16.6}$; $^{(0)}33.3_{15.7}$; $^{(+)}22.2$	$^{(-)}0$; $^{(0)}33.3$; $^{(+)}66.7_{27.2}$
DOC (mg L^{-1})	**1.63** ± 1.06, <u>1.31</u> *(0.30 : 4.08)*	**3.43** ± 1.52, <u>3.12</u> *(1.49 : 5.82)&*	**8.68** ± 6.63, <u>6.75</u> *(3.20 : 20.6)&#*	**4.92** ± 0.86, <u>4.87</u> *(4.09 : 5.81)&*
P (%)	$^{(-)}91.7_{8.0}$; $^{(0)}8.3$; $^{(+)}0$	$^{(-)}33.3_{13.6}$; $^{(0)}41.7_{14.2}$; $^{(+)}25.0_{12.5}$	$^{(-)}0$; $^{(0)}44.4_{16.6}$; $^{(+)}55.6_{16.6}$	$^{(-)}0$; $^{(0)}66.7_{27.2}$; $^{(+)}33.3$
Chl (µg L^{-1})	**1.53** ± 0.68, <u>1.37</u> *(0.40 : 2.95)*	**1.58** ± 0.62, <u>1.50</u> *(1.11 : 3.32)*	**3.78** ± 3.20, <u>2.76</u> *(0.92 : 9.23)&#*	**3.10** ± 2.13, <u>2.67</u> *(1.60 : 5.54)#*

P (%)	$^{(-)}58.3_{14.2}$; $^{(0)}25.0_{12.5}$; $^{(+)}16.7$	$^{(-)}58.3_{14.2}$; $^{(0)}33.3_{13.6}$; $^{(+)}8.3$	$^{(-)}33.3_{15.7}$; $^{(0)}11.1$; $^{(+)}55.6_{16.6}$	$^{(-)}0$; $^{(0)}33.3$; $^{(+)}66.7_{27.2}$
Pha	**0.51** ± 0.28, <u>0.41</u>	**0.42** ± 0.28, <u>0.30</u>	**1.41** ± 0.84, <u>0.91</u>	**0.86**, <u>0.40</u>
(μg L^{-1})	*(0.08 : 0.97)*	*(0.04 : 0.94)*	*(0.04 : 2.66)&#*	*(0.11 : 2.22)*
P (%)	$^{(-)}33.3_{13.6}$; $^{(0)}50.0_{14.4}$; $^{(+)}16.7$	$^{(-)}58.3_{14.2}$; $^{(0)}33.3_{13.6}$; $^{(+)}8.3$	$^{(-)}22.2$; $^{(0)}0$; $^{(+)}77.8_{13.9}$	$^{(-)}66.7_{27.2}$; $^{(0)}0$; $^{(+)}33.3$
SPM	**15.24** ± 9.89, <u>12.10</u>	**19.07** ± 6.14, <u>18.00</u>	**18.83** ± 11.95, <u>15.62</u>	**36.43** ± 3.38, <u>36.33</u>
(mg L^{-1})	*(3.36 : 35.35)*	*(9.43 : 27.5)*	*(5.94 : 34.72)*	*(34.07 : 40.30)&#$*
P (%)	$^{(-)}58.3_{14.2}$; $^{(0)}33.3_{13.6}$; $^{(+)}8.3$	$^{(-)}41.7_{14.2}$; $^{(0)}41.7_{14.2}$; $^{(+)}16.7$	$^{(-)}55.6_{16.6}$; $^{(0)}11.1$; $^{(+)}33.3_{15.7}$	$^{(-)}0$; $^{(0)}0$; $^{(+)}100$
POC	**5.19** ± 1.30, <u>5.06</u>	**3.81** ± 0.44, <u>3.79</u>	**7.26** ± 1.40, <u>7.15</u>	**21.6** ± 10.2, <u>20.1</u>
(%)	*(3.67 : 7.97)*	*(2.89 : 4.69)&*	*(5.78 : 10.09)&#*	*(13.0 : 32.9)&#$*
P (%)	$^{(-)}33.3_{13.6}$; $^{(0)}41.7_{14.2}$; $^{(+)}25.0_{12.5}$	$^{(-)}91.7_{8.0}$; $^{(0)}8.3$; $^{(+)}0$	$^{(-)}0$; $^{(0)}11.1$; $^{(+)}88.9_{10.5}$	$^{(-)}0$; $^{(0)}0$; $^{(+)}100$
POC$_v$	**0.696** ± 0.353, <u>0.612</u>	**0.737** ± 0.282, <u>0.683</u>	**1.287** ± 0.764, <u>1.117</u>	**8.082** ± 4.581, <u>7.294</u>
(mg L^{-1})	*(0.268 : 1.316)*	*(0.340 : 1.116)*	*(0.600 : 2.756)&*	*(4.532 : 13.254)&#$*
P (%)	$^{(-)}58.3_{14.2}$; $^{(0)}25.0_{12.5}$; $^{(+)}16.7$	$^{(-)}50.0_{14.4}$; $^{(0)}41.7_{14.2}$; $^{(+)}8.3$	$^{(-)}11.1$; $^{(0)}44.4_{16.6}$; $^{(+)}44.4_{16.6}$	$^{(-)}0$; $^{(0)}0$; $^{(+)}100$
δ13C	**−28.03** ± 0.68	**−27.67** ± 1.02	**−29.08** ± 1.61	**−27.28** ± 0.92
–	*(−29.31 : −27.26)*	*(−30.02 : −26.66)*	*(−32.00 : −27.09)#*	*(−27.94 : −26.23)$*
P (%)	$^{(-)}41.7_{14.2}$; $^{(0)}58.3_{14.2}$; P+: 0	$^{(-)}25.0_{12.5}$; $^{(0)}50.0_{14.4}$; $^{(+)}25.0_{12.5}$	$^{(-)}88.9_{10.5}$; $^{(0)}11.1$; $^{(+)}0$	$^{(-)}33.3$; $^{(0)}33.3$; $^{(+)}33.3$
δ15N	**4.10** ± 1.23, <u>3.91</u>	**4.42** ± 1.09, <u>4.28</u>	**2.28**	**5.37** ± 2.58, <u>4.89</u>
–	*(2.16 : 5.82)*	*(2.08 : 6.25)*	*(−5.73 : 6.43)*	*(2.67 : 7.82)*
P (%)	$^{(-)}50.0_{14.4}$; $^{(0)}33.3_{13.6}$; $^{(+)}16.7$	$^{(-)}33.3_{13.6}$; $^{(0)}58.3_{14.2}$; $^{(+)}8.3$	$^{(-)}44.4_{16.6}$; $^{(0)}33.3_{15.7}$; $^{(+)}22.2$	$^{(-)}33.3$; $^{(0)}0$; $^{(+)}66.7_{27.2}$
R$_{Chl/POC}$	**2.75** ± 1.84, <u>2.24</u>	**2.38** ± 1.02, <u>2.19</u>	**3.21** ± 2.87, <u>2.47</u>	**0.56**, <u>0.37</u>
(10^{-3})	*(0.91 : 6.90)*	*(1.14 : 4.13)*	*(0.97 : 10.31)*	*(0.12 : 1.22)&#$*

	upstream	estuary	Urban/STP	STP
P (%)	$^{(-)}$58.3$_{14.2}$; $^{(0)}$16.7; $^{(+)}$25.0$_{12.5}$	$^{(-)}$58.3$_{14.2}$; $^{(0)}$41.7$_{14.2}$; $^{(+)}$0	$^{(-)}$55.6$_{16.6}$; $^{(0)}$33.3$_{15.7}$; $^{(+)}$11.1	$^{(-)}$100; $^{(0)}$0; $^{(+)}$0
ActChl	**0.73** ± 0.16, <u>0.71</u>	**0.80** ± 0.14, <u>0.79</u>	**0.71** ± 0.18, <u>0.68</u>	**0.84** ± 0.12, <u>0.84</u>
–	(0.43 : 0.95)	(0.57 : 1.00)	(0.38 : 1.00)	(0.71 : 0.95)
P (%)	$^{(-)}$58.3$_{14.2}$; $^{(0)}$33.3$_{13.6}$; $^{(+)}$8.3	$^{(-)}$33.3$_{13.6}$; $^{(0)}$50.0$_{14.4}$; $^{(+)}$16.7	$^{(-)}$55.6$_{16.6}$; $^{(0)}$33.3$_{15.7}$; $^{(+)}$11.1	$^{(-)}$33.3; $^{(0)}$66.7$_{27.2}$; $^{(+)}$0
ln(K$_{OC}$)	**10.56** ± 0.82, <u>10.53</u>	**9.41** ± 0.48, <u>9.39</u>	**9.27** ± 0.72, <u>9.24</u>	**10.63** ± 0.59, <u>10.62</u>
(L kg^{-1})	(9.39 : 12.20)	(8.74 : 10.36)&	(8.15 : 10.19)&	(10.19 : 11.29)#$
P (%)	$^{(-)}$25.0$_{12.5}$; $^{(0)}$50.0$_{14.4}$; $^{(+)}$25.0$_{12.5}$	$^{(-)}$91.7$_{8.0}$; $^{(0)}$8.3; $^{(+)}$0	$^{(-)}$77.8$_{13.9}$; $^{(0)}$22.2; $^{(+)}$0	$^{(-)}$0; $^{(0)}$66.7$_{27.2}$; $^{(+)}$33.3
N/P	**222.7** ± 108.9, <u>204.7</u>	**249.5** ± 222.6, <u>185.5</u>	**434.4** ± 311.2, <u>328.7</u>	**94.4**, <u>42.6</u>
–	(119.1 : 474.3)	(77.2 : 817.8)	(78.3 : 903.1)	(8.2 : 234.9)$
P (%)	$^{(-)}$75.0$_{12.5}$; $^{(0)}$8.3; $^{(+)}$16.7	$^{(-)}$66.7$_{13.6}$; $^{(0)}$16.7; $^{(+)}$16.7	$^{(-)}$33.3$_{15.7}$; $^{(0)}$33.3$_{15.7}$; $^{(+)}$33.3$_{15.7}$	$^{(-)}$100; $^{(0)}$0; $^{(+)}$0
Si/N	**0.82** ± 0.31, <u>0.77</u>	**0.56** ± 0.17, <u>0.53</u>	**1.02** ± 0.46, <u>0.91</u>	**0.27** ± 0.01, <u>0.27</u>
–	(0.42 : 1.25)	(0.22 : 0.84)&	(0.26 : 1.75)#	(0.26 : 0.27)&#$
P (%)	$^{(-)}$33.3$_{13.6}$; $^{(0)}$41.7$_{14.2}$; $^{(+)}$25.0$_{12.5}$	$^{(-)}$75.0$_{12.5}$; $^{(0)}$25.0$_{12.5}$; $^{(+)}$0	$^{(-)}$11.1; $^{(0)}$66.7$_{15.7}$; $^{(+)}$22.2	$^{(-)}$100; $^{(0)}$0; $^{(+)}$0

& Significant difference for levels "estuary", "Urban/STP" and "STP" relative to level "upstream"

Significant difference for levels "Urban/STP" and "STP" relative to level "estuary"

$ Significant difference for level "STP" relative to level "Urban/STP"

Factor **type** (levels) with corresponding sampling points (Fig. 1): upstream (1, 2, 3, 4), estuary (A, B, C, D) , Urban/STP (7, 8, 9), STP (6)

Table SI-3 Average values (bold), geometric mean (underlined) and range (italic font) for continuous explanatory variables separated according to factor place with three levels (Adour (n=18), Trib_Trib/Adour (n=12), Nive (n=6)). Additional column added for Adour upstream samples in order to compare with Nive samples. Standard deviation presented if smaller than the average values. Significant difference (p<0.10) between groups studied with Wilcoxon rank sum test. The local background levels (LBL) for bulk water are considered the ranges between 4s LBL and 3s LBL values (Table SI-1). The proportion (P, %) of samples with values of the dependent variables equal to the LBL (marked with superscript (0) in front of P value), higher than LBL (marked with superscript (+) in front of P value) and lower than LBL (marked with superscript (–) in front of P value) are also presented. The binomial errors are given as subscript after P if at least two times smaller than the respective proportions. If P equaled 0 or 100%, the binomial errors are 0.

	Adour	Trib_Trib/Adour	Nive	Adour (upstream)
Salinity	**3.45**, <u>0.83</u>	**0.94** ± 0.65, <u>0.70</u>	**0.14** ± 0.03, <u>0.14</u>	**0.18** ± 0.03, <u>0.17</u>
–	*(0.12 : 16.88)*	*(0.10 : 1.95)*	*(0.12 : 0.20)*&#	*(0.12 : 0.21)*$
P (%)	$^{(-)}66.7_{11.1}$; $^{(0)}11.1$; $^{(+)}22.2_{9.8}$	$^{(-)}100$; $^{(0)}0$; $^{(+)}0$	$^{(-)}100$; $^{(0)}0$; $^{(+)}0$	$^{(-)}100$; $^{(0)}0$; $^{(+)}0$
T	**13.32** ± 3.73, <u>12.76</u>	**14.84** ± 3.74, <u>14.34</u>	**13.54** ± 3.33, <u>13.16</u>	**13.43** ± 3.80, <u>12.91</u>
(°C)	*(8.16 : 17.90)*	*(7.93 : 20.81)*	*(9.17 : 17.30)*	*(8.45 : 16.50)*
P (%)	$^{(-)}33.3_{11.1}$; $^{(0)}55.6_{11.7}$; $^{(+)}11.1$	$^{(-)}25.0_{12.5}$; $^{(0)}41.7_{14.2}$; $^{(+)}33.3_{13.6}$	$^{(-)}33.3$; $^{(0)}50.0_{20.4}$; $^{(+)}16.7$	$^{(-)}33.3$; $^{(0)}66.7_{19.2}$; $^{(+)}0$
O$_2$	**8.70** ± 1.34, <u>8.60</u>	**8.83** ± 1.23, <u>8.75</u>	**9.34** ± 1.80, <u>9.19</u>	**8.84** ± 1.40, <u>8.75</u>
(mg L^{-1})	*(7.02 : 10.76)*	*(6.85 : 10.84)*	*(7.00 : 11.37)*	*(7.42 : 10.76)*
P (%)	$^{(-)}61.1_{11.5}$; $^{(0)}33.3_{11.1}$; $^{(+)}5.6$	$^{(-)}50.0_{14.4}$; $^{(0)}33.3_{13.6}$; $^{(+)}16.7$	$^{(-)}50.0_{20.4}$; $^{(0)}16.7$; $^{(+)}33.3$	$^{(-)}50.0_{20.4}$; $^{(0)}33.3$; $^{(+)}16.7$
pH	**7.63** ± 0.21, <u>7.63</u>	**7.53** ± 0.34, <u>7.53</u>	**7.70** ± 0.29, <u>7.70</u>	**7.58** ± 0.22, <u>7.58</u>
–	*(7.22 : 7.98)*	*(6.80 : 8.12)*	*(7.31 : 8.12)*	*(7.22 : 7.80)*
P (%)	$^{(-)}50.0_{11.8}$; $^{(0)}44.4_{11.7}$; $^{(+)}5.6$	$^{(-)}75.0_{12.5}$; $^{(0)}8.3$; $^{(+)}16.7$	$^{(-)}50.0_{20.4}$; $^{(0)}16.7$; $^{(+)}33.3$	$^{(-)}50.0_{20.4}$; $^{(0)}50.0_{20.4}$; $^{(+)}0$
PO$_4$	**0.73** ± 0.27, <u>0.68</u>	**6.58**, <u>0.94</u>	**0.41** ± 0.05, <u>0.40</u>	**0.65** ± 0.26, <u>0.60</u>

(μM)	*(0.31 : 1.36)*	*(0.12 : 59.52)*	*(0.35 : 0.48)&*	*(0.31 : 1.04)$*
P (%)	$^{(-)}44.4_{11.7}$; $^{(0)}38.9_{11.5}$; $^{(+)}16.7$	$^{(-)}58.3_{14.2}$; $^{(0)}8.3$; $^{(+)}33.3_{13.6}$	$^{(-)}100$; $^{(0)}0$; $^{(+)}0$	$^{(-)}50.0_{20.4}$; $^{(0)}33.3$; $^{(+)}16.7$
NO$_3$	**146.6** ± 80.0, <u>133.3</u>	**183.1** ± 128.0, <u>147.4</u>	**69.3** ± 9.5, <u>68.8</u>	**140.1** ± 30.4, <u>137.7</u>
(μM)	*(75.2 : 424)*	*(42.5 : 415)*	*(59.5 : 87.3)&#*	*(119.2 : 199.1)$*
P (%)	$^{(-)}61.1_{11.5}$; $^{(0)}16.7$; $^{(+)}22.2_{9.8}$	$^{(-)}50.0_{14.4}$; $^{(0)}16.7$; $^{(+)}33.3_{13.6}$	$^{(-)}100$; $^{(0)}0$; $^{(+)}0$	$^{(-)}50.0_{20.4}$; $^{(0)}33.3$; $^{(+)}16.7$
NO$_2$	**1.10** ± 0.36, <u>1.05</u>	**4.55** ± 3.32, <u>3.85</u>	**0.65** ± 0.36, <u>0.56</u>	**1.11** ± 0.25, <u>1.08</u>
(μM)	*(0.47 : 2.24)*	*(2.12 : 13.06)&*	*(0.28 : 1.11)&#*	*(0.65 : 1.34)$*
P (%)	$^{(-)}27.8_{10.6}$; $^{(0)}50.0_{11.8}$; $^{(+)}22.2_{9.8}$	$^{(-)}0$; $^{(0)}0$; $^{(+)}100$	$^{(-)}83.3_{15.2}$; $^{(0)}16.7$; $^{(+)}0$	$^{(-)}16.7$; $^{(0)}50.0_{20.4}$; $^{(+)}33.3$
NH$_4$	**2.87** ± 0.66, <u>2.80</u>	**40.09**, <u>24.23</u>	**2.53** ± 1.09, <u>2.33</u>	**2.60** ± 0.41, <u>2.57</u>
(μM)	*(2.06 : 4.49)*	*(6.17 : 175)&*	*(1.14 : 4.42)#*	*(2.06 : 3.22)*
P (%)	$^{(-)}55.6_{11.7}$; $^{(0)}33.3_{11.1}$; $^{(+)}11.1$	$^{(-)}0$; $^{(0)}0$; $^{(+)}100$	$^{(-)}83.3_{15.2}$; $^{(0)}0$; $^{(+)}16.7$	$^{(-)}66.7_{19.2}$; $^{(0)}33.3$; $^{(+)}0$
SiO$_4$	**76.6** ± 19.1, <u>74.0</u>	**130.3** ± 39.6, <u>123.9</u>	**77.4** ± 16.1, <u>75.6</u>	**81.3** ± 19.1, <u>79.1</u>
(μM)	*(41.5 : 97.5)*	*(60.5 : 192)&*	*(45.8 : 88.0)#*	*(51.9 : 97.5)*
P (%)	$^{(-)}44.4_{11.7}$; $^{(0)}38.9_{11.5}$; $^{(+)}16.7$	$^{(-)}16.7$; $^{(0)}0$; $^{(+)}83.3_{10.8}$	$^{(-)}33.3$; $^{(0)}66.7_{19.2}$; $^{(+)}0$	$^{(-)}33.3$; $^{(0)}50.0_{20.4}$; $^{(+)}16.7$
TN	**1.54** ± 0.68, <u>1.41</u>	**7.48**, <u>3.11</u>	**0.72** ± 0.05, <u>0.72</u>	**1.61** ± 0.44, <u>1.57</u>
(mg L^{-1})	*(0.73 : 2.80)*	*(0.96 : 38.10)&*	*(0.63 : 0.77)&#*	*(1.29 : 2.47)$*
P (%)	$^{(-)}55.6_{11.7}$; $^{(0)}27.8_{10.6}$; $^{(+)}16.7$	$^{(-)}33.3_{13.6}$; $^{(0)}33.3_{13.6}$; $^{(+)}33.3_{13.6}$	$^{(-)}100$; $^{(0)}0$; $^{(+)}0$	$^{(-)}33.3$; $^{(0)}50.0_{20.4}$; $^{(+)}16.7$
DOC	**3.03** ± 1.46, <u>2.71</u>	**7.74** ± 5.91, <u>6.22</u>	**1.03** ± 0.76, <u>0.84</u>	**2.22** ± 1.03, <u>2.05</u>
(mg L^{-1})	*(1.10 : 5.82)*	*(3.20 : 20.55)&*	*(0.30 : 2.49)&#*	*(1.10 : 4.08)$*
P (%)	$^{(-)}50.0_{11.8}$; $^{(0)}33.3_{11.1}$; $^{(+)}16.7$	$^{(-)}0$; $^{(0)}50.0_{14.4}$; $^{(+)}50.0_{14.4}$	$^{(-)}100$; $^{(0)}0$; $^{(+)}0$	$^{(-)}83.3_{15.2}$; $^{(0)}16.7$; $^{(+)}0$
Chl	**1.69** ± 0.63, <u>1.60</u>	**3.61** ± 2.89, <u>2.74</u>	**1.13** ± 0.47, <u>1.03</u>	**1.92** ± 0.66, <u>1.83</u>

(μg L^{-1})	*(1.01 : 3.32)*	*(0.92 : 9.23)&*	*(0.40 : 1.85)&#*	*(1.01 : 2.95)$*
P (%)	$^{(-)}$50.0$_{11.8}$; $^{(0)}$33.3$_{11.1}$; $^{(+)}$16.7	$^{(-)}$25.0$_{12.5}$; $^{(0)}$16.7; $^{(+)}$58.3$_{14.2}$	$^{(-)}$83.3$_{15.2}$; $^{(0)}$16.7; $^{(+)}$0	$^{(-)}$33.3; $^{(0)}$33.3; $^{(+)}$33.3
Pha	**0.43** ± 0.28, <u>0.31</u>	**1.28** ± 0.91, <u>0.74</u>	**0.58** ± 0.27, <u>0.51</u>	**0.45** ± 0.30, <u>0.33</u>
(μg L^{-1})	*(0.04 : 0.94)*	*(0.04 : 2.66)&*	*(0.18 : 0.97)*	*(0.08 : 0.89)*
P (%)	$^{(-)}$55.6$_{11.7}$; $^{(0)}$33.3$_{11.1}$; $^{(+)}$11.1	$^{(-)}$33.3$_{13.6}$; $^{(0)}$0; $^{(+)}$66.7$_{13.6}$	$^{(-)}$16.7; $^{(0)}$66.7$_{19.2}$; $^{(+)}$16.7	$^{(-)}$50.0$_{20.4}$; $^{(0)}$33.3; $^{(+)}$16.7
SPM	**19.19** ± 7.12, <u>17.90</u>	**23.23** ± 13.01, <u>19.29</u>	**11.04** ± 9.14, <u>8.28</u>	**19.43** ± 9.44, <u>17.67</u>
(mg L^{-1})	*(9.43 : 35.35)*	*(5.94 : 40.30)*	*(3.36 : 24.48)&#*	*(9.76 : 35.35)*
P (%)	$^{(-)}$44.4$_{11.7}$; $^{(0)}$38.9$_{11.5}$; $^{(+)}$16.7	$^{(-)}$41.7$_{14.2}$; $^{(0)}$8.3; $^{(+)}$50.0$_{14.4}$	$^{(-)}$66.7$_{19.2}$; $^{(0)}$33.3; $^{(+)}$0	$^{(-)}$50.0$_{20.4}$; $^{(0)}$33.3; $^{(+)}$16.7
POC	**4.00** ± 0.58, <u>3.96</u>	**10.85** ± 7.91, <u>9.26</u>	**6.01** ± 1.28, <u>5.90</u>	**4.38** ± 0.68, <u>4.33</u>
(%)	*(2.89 : 5.32)*	*(5.78 : 32.89)&*	*(4.42 : 7.97)&#*	*(3.67 : 5.32)$*
P (%)	$^{(-)}$77.8$_{9.8}$; $^{(0)}$22.2$_{9.8}$; $^{(+)}$0	$^{(-)}$0; $^{(0)}$8.3; $^{(+)}$91.7$_{8.0}$	$^{(-)}$16.7; $^{(0)}$33.3; $^{(+)}$50.0$_{20.4}$	$^{(-)}$50.0$_{20.4}$; $^{(0)}$50.0$_{20.4}$; $^{(+)}$0
POC$_v$	**0.759** ± 0.278, <u>0.709</u>	**2.986**, <u>1.786</u>	**0.587** ± 0.403, <u>0.489</u>	**0.804** ± 0.290, <u>0.766</u>
(mg L^{-1})	*(0.340 : 1.316)*	*(0.600 : 13.254)&*	*(0.268 : 1.124)#*	*(0.519 : 1.316)*
P (%)	$^{(-)}$50.0$_{11.8}$; $^{(0)}$38.9$_{11.5}$; $^{(+)}$11.1	$^{(-)}$8.3; $^{(0)}$33.3$_{13.6}$; $^{(+)}$58.3$_{14.2}$	$^{(-)}$66.7$_{19.2}$; $^{(0)}$16.7; $^{(+)}$16.7	$^{(-)}$50.0$_{20.4}$; $^{(0)}$33.3; $^{(+)}$16.7
δ13C	**−27.83** ± 0.97	**−28.63** ± 1.64	**−27.92** ± 0.53	**−28.15** ± 0.84
–	*(−30.02 : −26.66)*	*(−32.00 : −26.23)*	*(−28.43 : −27.27)*	*(−29.31 : −27.26)*
P (%)	$^{(-)}$27.8$_{10.6}$; $^{(0)}$55.6$_{11.7}$; $^{(+)}$16.7	$^{(-)}$75.0$_{12.5}$; $^{(0)}$16.7; $^{(+)}$8.3	$^{(-)}$50.0$_{20.4}$; $^{(0)}$50.0$_{20.4}$; $^{(+)}$0	$^{(-)}$33.3; $^{(0)}$66.7$_{19.2}$; $^{(+)}$0
δ15N	**4.46** ± 1.06, <u>4.32</u>	**3.05**	**3.66** ± 1.30, <u>3.45</u>	**4.53** ± 1.09, <u>4.42</u>
–	*(2.08 : 6.25)*	*(−5.73 : 7.82)*	*(2.16 : 5.48)*	*(3.33 : 5.82)*
P (%)	$^{(-)}$38.9$_{11.5}$; $^{(0)}$44.4$_{11.7}$; $^{(+)}$16.7	$^{(-)}$41.7$_{14.2}$; $^{(0)}$25.0$_{12.5}$; $^{(+)}$33.3$_{13.6}$	$^{(-)}$50.0$_{20.4}$; $^{(0)}$50.0$_{20.4}$; $^{(+)}$0	$^{(-)}$50.0$_{20.4}$; $^{(0)}$16.7; $^{(+)}$33.3
R$_{Chl/POC}$	**2.48** ± 1.13, <u>2.25</u>	**2.54**, <u>1.53</u>	**2.81** ± 2.33, <u>2.11</u>	**2.68** ± 1.41, <u>2.39</u>

(10^{-3})	*(1.14 : 4.55)*	*(0.12 : 10.31)*	*(0.91 : 6.90)*	*(1.26 : 4.55)*
P (%)	$^{(-)}$61.1$_{11.5}$; $^{(0)}$27.8$_{10.6}$; $^{(+)}$11.1	$^{(-)}$66.7$_{13.6}$; $^{(0)}$25.0$_{12.5}$; $^{(+)}$8.3	$^{(-)}$50.0$_{20.4}$; $^{(0)}$33.3; $^{(+)}$16.7	$^{(-)}$66.7$_{19.2}$; $^{(0)}$0; $^{(+)}$33.3
ActChl	**0.81** ± 0.13, 0.80	**0.74** ± 0.17, 0.72	**0.65** ± 0.17, 0.63	**0.81** ± 0.11, 0.80
–	*(0.57 : 1.00)*	*(0.38 : 1.00)*	*(0.43 : 0.86)&*	*(0.71 : 0.95)*
P (%)	$^{(-)}$38.9$_{11.5}$; $^{(0)}$44.4$_{11.7}$; $^{(+)}$16.7	$^{(-)}$50.0$_{14.4}$; $^{(0)}$41.7$_{14.2}$; $^{(+)}$8.3	$^{(-)}$66.7$_{19.2}$; $^{(0)}$33.3; $^{(+)}$0	$^{(-)}$50.0$_{20.4}$; $^{(0)}$33.3; $^{(+)}$16.7
ln(K$_{OC}$)	**9.59** ± 0.54, 9.58	**9.61** ± 0.91, 9.57	**11.16** ± 0.62, 11.15	**9.96** ± 0.48, 9.95
(L kg^{-1})	*(8.74 : 10.79)*	*(8.15 : 11.29)*	*(10.37 : 12.20)&#*	*(9.39 : 10.79)$*
P (%)	$^{(-)}$77.8$_{9.8}$; $^{(0)}$22.2$_{9.8}$; $^{(+)}$0	$^{(-)}$58.3$_{14.2}$; $^{(0)}$33.3$_{13.6}$; $^{(+)}$8.3	$^{(-)}$0; $^{(0)}$50.0$_{20.4}$; $^{(+)}$50.0$_{20.4}$	$^{(-)}$50.0$_{20.4}$; $^{(0)}$50.0$_{20.4}$; $^{(+)}$0
N/P	**255.1** ± 195.8, 200.8	**349.4** ± 311.2, 197.3	**179.2** ± 21.6, 178.1	**266.3** ± 145.2, 235.4
–	*(77.2 : 817.8)*	*(8.2 : 903.1)*	*(152.1 : 205.5)*	*(119.1 : 474.3)*
P (%)	$^{(-)}$61.1$_{11.5}$; $^{(0)}$16.7; $^{(+)}$22.2$_{9.8}$	$^{(-)}$50.0$_{14.4}$; $^{(0)}$25.0$_{12.5}$; $^{(+)}$25.0$_{12.5}$	$^{(-)}$100; $^{(0)}$0; $^{(+)}$0	$^{(-)}$50.0$_{20.4}$; $^{(0)}$16.7; $^{(+)}$33.3
Si/N	**0.56** ± 0.16, 0.54	**0.83** ± 0.52, 0.67	**1.07** ± 0.21, 1.05	**0.57** ± 0.14, 0.56
–	*(0.22 : 0.84)*	*(0.26 : 1.75)*	*(0.71 : 1.25)&*	*(0.42 : 0.73)$*
P (%)	$^{(-)}$72.2$_{10.6}$; $^{(0)}$27.8$_{10.6}$; $^{(+)}$0	$^{(-)}$33.3$_{13.6}$; $^{(0)}$50.0$_{14.4}$; $^{(+)}$16.7	$^{(-)}$0; $^{(0)}$50.0$_{20.4}$; $^{(+)}$50.0$_{20.4}$	$^{(-)}$66.7$_{19.2}$; $^{(0)}$33.3; $^{(+)}$0

& Significant difference for levels "Trib_Trib/Adour" and "Nive" relative to level "Adour"

Significant difference for level "Nive" relative to level "Trib_Trib/Adour"

$ Significant difference for "Adour (upstream)" relative to level "Nive"

Factor **place** (levels) with corresponding sampling points (Fig. 1): Adour (1, 2, A, B, C, D), Trib_Trib/Adour (6, 7, 8, 9), Nive (3, 4); Adour upstream (1, 2)

Table SI-4 Average values (bold), geometric mean (underlined) and range (italic) for total and dissolved IHg and MeHg concentrations, percentage of MeHg relative to total Hg and dissolved fractions (F_D, %) separated according to factor time with three levels (May (n=12), Sept (n=12), Jan (n=12)). Standard deviation presented if smaller than the average values. Significant difference (p<0.10) between groups studied with t test on transformed dependent variables (Eqs. 4a, 4b) and with Wilcox test on F_D. Local background levels (LBL) were calculated using 3σ and 4σ criteria (Gredilla et al. 2015) with samples from type upstream (Fig. 1: 1, 2, 3, 4) and estuary (Fig. 1: A, B, C, D).

	May	Sept	Jan	4σ LBL	3σ LBL
IHg (ng L^{-1})	**1.34**, <u>1.04</u>	**3.71** ± 2.14, <u>3.11</u>	**1.89** ± 0.73, <u>1.76</u>	1.70	3.28
	(0.51 : 5.82)	*(0.75 : 8.02)&*	*(0.96 : 3.52)&#*		
IHg$_D$ (ng L^{-1})	**0.29** ± 0.12, <u>0.26</u>	**0.89**, <u>0.62</u>	**0.84** ± 0.69, <u>0.66</u>	0.42	0.65
	(0.11 : 0.53)	*(0.19 : 4.26)&*	*(0.20 : 2.73)&*		
F_D (IHg)	**30** ± 18, <u>25</u>	**23** ± 13, <u>20</u>	**43** ± 27, <u>37</u>	–	–
	(6.2 : 61)	*(4.0 : 53)*	*(17 : 100)#*		
MeHg (ng L^{-1})	**0.0519** ± 0.0352, <u>0.0448</u>	**0.0684** ± 0.0545, <u>0.0584</u>	**0.0573** ± 0.0285, <u>0.0532</u>	0.0473	0.0615
	(0.0245 : 0.1493)	*(0.0336 : 0.2346)*	*(0.0356 : 0.1434)*		
MeHg$_D$ (ng L^{-1})	**0.0322** ± 0.0159, <u>0.0291</u>	**0.0446** ± 0.0232, <u>0.0410</u>	**0.0365** ± 0.0133, <u>0.0345</u>	0.0331	0.0441
	(0.0149 : 0.0628)	*(0.0219 : 0.1128)&*	*(0.0170 : 0.0685)*		
F_D (MeHg)	**66** ± 15, <u>65</u>	**73** ± 20, <u>70</u>	**67** ± 18, <u>65</u>	–	–
	(42 : 88)	*(37 : 98)*	*(44 : 96)*		
%MeHg (%)	**4.53** ± 2.45, <u>4.11</u>	**2.14** ± 1.45, <u>1.84</u>	**3.05** ± 0.93, <u>2.93</u>	3.49	5.37
	(2.50 : 11.31)	*(0.80 : 6.00)&*	*(2.00 : 5.00)&#*		
%MeHg$_D$ (%)	**10.57** ± 3.89, <u>9.94</u>	**7.08** ± 3.41, <u>6.14</u>	**5.57** ± 2.98, <u>4.91</u>	7.64	13.11
	(5.35 : 17.24)	*(1.35 : 13.66)&*	*(1.60 : 13.63)&*		

& Significant difference for levels "Sept" and "Jan" relative to level "May"; # Significant difference for level "Jan" relative to level "Sept"

Table SI-5 Average values (bold), geometric mean (underlined) and range (italic font) for total and dissolved IHg and MeHg concentrations, percentage of MeHg relative to total Hg and dissolved fractions (F_D, %) separated according to factor type with four levels (upstream (n=12), estuary (n=12), Urban/STP (n=9), STP (n=3)). Standard deviation presented if smaller than the average values. Significant difference (p<0.10) between groups studied with t test on transformed dependent variables (Eqs. 4a, 4b) and with Wilcox test on F_D. The local background levels (LBL) are between 4s LBL and 3s LBL values (Table SI-4). The proportion (P, %) of samples with values of the dependent variables equal to the LBL (marked with superscript (0) in front of P value), higher than LBL (marked with superscript (+) in front of P value) and lower than LBL (marked with superscript (–) in front of P value) are also presented. The binomial errors are given as subscript after P if at least two times smaller than the respective proportions. If P equaled 0 or 100%, the binomial errors are 0.

	upstream	estuary	Urban/STP	STP
IHg	**1.51** ± 0.98, <u>1.27</u>	**1.88** ± 0.88, <u>1.68</u>	**3.05** ± 2.66, <u>2.20</u>	**5.01** ± 1.30, <u>4.89</u>
(ng L^{-1})	*(0.51 : 3.42)*	*(0.58 : 3.32)*	*(0.79 : 8.02)*	*(3.52 : 5.82)&#$*
P (%)	$^{(-)}66.7_{13.6}$; $^{(0)}25.0_{12.5}$; $^{(+)}8.3$	$^{(-)}50.0_{14.4}$; $^{(0)}33.3_{13.6}$; $^{(+)}16.7$	$^{(-)}44.4_{16.6}$; $^{(0)}22.2$; $^{(+)}33.3_{15.7}$	$^{(-)}0$; $^{(0)}0$; $^{(+)}100$
IHg$_D$	**0.59**, <u>0.43</u>	**0.45** ± 0.19, <u>0.40</u>	**1.00**, <u>0.58</u>	**0.91** ± 0.55, <u>0.78</u>
(ng L^{-1})	*(0.20 : 2.73)*	*(0.11 : 0.74)*	*(0.18 : 4.26)*	*(0.36 : 1.47)*
P (%)	$^{(-)}50.0_{14.4}$; $^{(0)}33.3_{13.6}$; $^{(+)}16.7$	$^{(-)}41.7_{14.2}$; $^{(0)}41.7_{14.2}$; $^{(+)}16.7$	$^{(-)}44.4_{16.6}$; $^{(0)}11.1$; $^{(+)}44.4_{16.6}$	$^{(-)}33.3$; $^{(0)}0$; $^{(+)}66.7_{27.2}$
F$_D$ (IHg)	**40** ± 24, <u>34</u>	**24** ± 7, <u>24</u>	**36** ± 28, <u>26</u>	**21** ± 18, <u>16</u>
	(15 : 100)	*(17 : 41)*	*(4.0 : 98)*	*(6.2 : 42)*
MeHg	**0.0502** ± 0.0148, <u>0.0484</u>	**0.0444** ± 0.0125, <u>0.0427</u>	**0.0520** ± 0.0190, <u>0.0494</u>	**0.1758** ± 0.0510, <u>0.1713</u>
(ng L^{-1})	*(0.0297 : 0.0809)*	*(0.0245 : 0.0633)*	*(0.0337 : 0.0946)*	*(0.1434 : 0.2346)&#$*
P (%)	$^{(-)}41.7_{14.2}$; $^{(0)}41.7_{14.2}$; $^{(+)}16.7$	$^{(-)}50.0_{14.4}$; $^{(0)}41.7_{14.2}$; $^{(+)}8.3$	$^{(-)}55.6_{16.6}$; $^{(0)}22.2$; $^{(+)}22.2$	$^{(-)}0$; $^{(0)}0$; $^{(+)}100$
MeHg$_D$	**0.0364** ± 0.0120, <u>0.0344</u>	**0.0298** ± 0.0087, <u>0.0284</u>	**0.0358** ± 0.0118, <u>0.0342</u>	**0.0814** ± 0.0274, <u>0.0786</u>
(ng L^{-1})	*(0.0170 : 0.0584)*	*(0.0149 : 0.0418)*	*(0.0219 : 0.0582)*	*(0.0628 : 0.1128)&#$*

	upstream	estuary	Urban/STP	STP
P (%)	$^{(-)}41.7_{14.2}$; $^{(0)}33.3_{13.6}$; $^{(+)}25.0_{12.5}$	$^{(-)}50.0_{14.4}$; $^{(0)}50.0_{14.4}$; $^{(+)}0$	$^{(-)}55.6_{16.6}$; $^{(0)}22.2$; $^{(+)}22.2$	$^{(-)}0$; $^{(0)}0$; $^{(+)}100$
F_D (MeHg)	**73** ± 18, <u>71</u>	**68** ± 12, <u>67</u>	**73** ± 21, <u>69</u>	**46** ± 3, <u>46</u>
	(44 : 98)	*(49 : 86)*	*(37 : 96)*	*(42 : 48)*&#
%MeHg	**4.36** ± 2.80, <u>3.65</u>	**2.61** ± 0.85, <u>2.48</u>	**2.51** ± 1.30, <u>2.19</u>	**3.46** ± 0.83, <u>3.38</u>
(%)	*(1.48 : 11.31)*	*(1.47 : 4.07)*&	*(0.80 : 4.61)*&	*(2.50 : 3.95)*
P (%)	$^{(-)}50.0_{14.4}$; $^{(0)}16.7$; $^{(+)}33.3_{13.6}$	$^{(-)}75.0_{12.5}$; $^{(0)}25.0_{12.5}$; $^{(+)}0$	$^{(-)}77.8_{13.9}$; $^{(0)}22.2$; $^{(+)}0$	$^{(-)}33.3$; $^{(0)}66.7_{27.2}$; $^{(+)}0$
%MeHg$_D$	**8.38** ± 4.38, <u>7.23</u>	**6.91** ± 2.00, <u>6.68</u>	**7.19** ± 5.05, <u>5.47</u>	**10.18** ± 5.29, <u>9.06</u>
(%)	*(1.60 : 17.24)*	*(4.68 : 11.90)*	*(1.35 : 15.46)*	*(4.46 : 14.90)*
P (%)	$^{(-)}50.0_{14.4}$; $^{(0)}25.0_{12.5}$; $^{(+)}25.0_{12.5}$	$^{(-)}66.7_{13.6}$; $^{(0)}33.3_{13.6}$; $^{(+)}0$	$^{(-)}66.7_{15.7}$; $^{(0)}11.1$; $^{(+)}22.2$	$^{(-)}33.3$; $^{(0)}33.3$; $^{(+)}33.3$

& Significant difference for levels "estuary", "Urban/STP" and "STP" relative to level "upstream"

Significant difference for levels "Urban/STP" and "STP" relative to level "estuary"

$ Significant difference for level "STP" relative to level "Urban/STP"

Factor **type** (levels) with corresponding sampling points (Fig. 1): upstream (1, 2, 3, 4), estuary (A, B, C, D) , Urban/STP (7, 8, 9), STP (6)

Table SI-6 Average values (bold), geometric mean (underlined) and range (italic font) for total and dissolved IHg and MeHg concentrations, percentage of MeHg relative to total Hg and dissolved fractions (F_D, %) separated according to factor place with three levels (Adour (n=18), Trib_Trib/Adour (n=12), Nive (n=6)). Additional column added for Adour upstream samples in order to compare with Nive samples. Standard deviation presented if smaller than the average values. Significant difference (p<0.10) between groups studied with t test on transformed dependent variables (Eqs. 4a, 4b) and with Wilcox test on F_D. The local background levels (LBL) are between 4s LBL and 3s LBL values (Table SI-4). The proportion (P, %) of samples with values of the dependent variables equal to the LBL (marked with superscript (0) in front of P value), higher than LBL (marked with superscript (+) in front of P value) and lower than LBL (marked with superscript (–) in front of P value) are also presented. The binomial errors are given as subscript after P if at least two times smaller than the respective proportions. If P equaled 0 or 100%, the binomial errors are 0.

	Adour	Trib_Trib/Adour	Nive	Adour (upstream)
IHg	**1.83** ± 0.90, <u>1.61</u>	**3.54** ± 2.49, <u>2.68</u>	**1.29** ± 0.98, <u>1.09</u>	**1.73** ± 1.03, <u>1.47</u>
(ng L^{-1})	*(0.51 : 3.42)*	*(0.79 : 8.02)&*	*(0.63 : 3.25)#*	*(0.51 : 3.42)*
P (%)	$^{(-)}50.0_{11.8}$; $^{(0)}33.3_{11.1}$; $^{(+)}16.7$	$^{(-)}33.3_{13.6}$; $^{(0)}16.7$; $^{(+)}50.0_{14.4}$	$^{(-)}83.3_{15.2}$; $^{(0)}16.7$; $^{(+)}0$	$^{(-)}50.0_{20.4}$; $^{(0)}33.3$; $^{(+)}16.7$
IHg$_D$	**0.56**, <u>0.43</u>	**0.98**, <u>0.62</u>	**0.40** ± 0.11, <u>0.38</u>	**0.78**, <u>0.49</u>
(ng L^{-1})	*(0.11 : 2.73)*	*(0.18 : 4.26)*	*(0.27 : 0.53)*	*(0.20 : 2.73)*
P (%)	$^{(-)}44.4_{11.7}$; $^{(0)}33.3_{11.1}$; $^{(+)}22.2_{9.8}$	$^{(-)}41.7_{14.2}$; $^{(0)}8.3$; $^{(+)}50.0_{14.4}$	$^{(-)}50.0_{20.4}$; $^{(0)}50.0_{20.4}$; $^{(+)}0$	$^{(-)}50.0_{20.4}$; $^{(0)}16.7$; $^{(+)}33.3$
F$_D$ (IHg)	**30** ± 21, <u>26</u>	**32** ± 26, <u>23</u>	**38** ± 13, <u>35</u>	**42** ± 33, <u>32</u>
	(16 : 100)	*(4.0 : 98)*	*(15 : 52)*	*(16 : 100)*
MeHg	**0.0436** ± 0.0109, <u>0.0423</u>	**0.0829** ± 0.0622, <u>0.0674</u>	**0.0584** ± 0.0161, <u>0.0566</u>	**0.0421** ± 0.0078, <u>0.0414</u>
(ng L^{-1})	*(0.0245 : 0.0633)*	*(0.0337 : 0.2346)&*	*(0.0389 : 0.0809)&*	*(0.0297 : 0.0514)$*
P (%)	$^{(-)}55.6_{11.7}$; $^{(0)}38.9_{11.5}$; $^{(+)}5.6$	$^{(-)}41.7_{14.2}$; $^{(0)}16.7$; $^{(+)}41.7_{14.2}$	$^{(-)}16.7$; $^{(0)}50.0_{20.4}$; $^{(+)}33.3$	$^{(-)}66.7_{19.2}$; $^{(0)}33.3$; $^{(+)}0$

MeHg$_D$	**0.0313** ± 0.0091, <u>0.0299</u>	**0.0472** ± 0.0257, <u>0.0421</u>	**0.0384** ± 0.0146, <u>0.0357</u>	**0.0344** ± 0.0098, <u>0.0331</u>
(ng L^{-1})	(0.0149 : 0.0445)	(0.0219 : 0.1128)&	(0.0170 : 0.0584)	(0.0202 : 0.0445)
P (%)	$^{(-)}$50.0$_{11.8}$; $^{(0)}$44.4$_{11.7}$; $^{(+)}$5.6	$^{(-)}$41.7$_{14.2}$; $^{(0)}$16.7; $^{(+)}$41.7$_{14.2}$	$^{(-)}$33.3; $^{(0)}$33.3; $^{(+)}$33.3	$^{(-)}$50.0$_{20.4}$; $^{(0)}$33.3; $^{(+)}$16.7
F$_D$ (MeHg)	**72** ± 15, <u>71</u>	**66** ± 22, <u>62</u>	**65** ± 17, <u>63</u>	**81** ± 16, <u>80</u>
	(49 : 98)	(37 : 96)	(44 : 89)	(51 : 98)$
%MeHg	**2.73** ± 1.04, <u>2.56</u>	**2.75** ± 1.24, <u>2.44</u>	**5.74** ± 3.27, <u>4.89</u>	**2.98** ± 1.41, <u>2.73</u>
(%)	(1.47 : 5.47)	(0.80 : 4.61)	(1.54 : 11.31)&#	(1.48 : 5.47)
P (%)	$^{(-)}$77.8$_{9.8}$; $^{(0)}$16.7; $^{(+)}$5.6	$^{(-)}$66.7$_{13.6}$; $^{(0)}$33.3$_{13.6}$; $^{(+)}$0	$^{(-)}$16.7; $^{(0)}$33.3; $^{(+)}$50.0$_{20.4}$	$^{(-)}$83.3$_{15.2}$; $^{(0)}$0; $^{(+)}$16.7
%MeHg$_D$	**7.06** ± 2.66, <u>6.53</u>	**7.94** ± 5.05, <u>6.21</u>	**9.39** ± 4.98, <u>8.40</u>	**7.37** ± 3.88, <u>6.23</u>
(%)	(1.60 : 13.63)	(1.35 : 15.46)	(4.59 : 17.24)	(1.60 : 13.63)
P (%)	$^{(-)}$61.1$_{11.5}$; $^{(0)}$33.3$_{11.1}$; $^{(+)}$5.6	$^{(-)}$58.3$_{14.2}$; $^{(0)}$16.7; $^{(+)}$25.0$_{12.5}$	$^{(-)}$50.0$_{20.4}$; $^{(0)}$16.7; $^{(+)}$33.3	$^{(-)}$50.0$_{20.4}$; $^{(0)}$33.3; $^{(+)}$16.7

& Significant difference for levels "Trib_Trib/Adour" and "Nive" relative to level "Adour";

Significant difference for level "Nive" relative to level "Trib_Trib/Adour"

$ Significant difference for "Adour (upstream)" relative to level "Nive"

Factor **place** (levels) with corresponding sampling points (Fig. 1): Adour (1, 2, A, B, C, D), Trib_TribAdour (6, 7, 8, 9), Nive (3, 4); Adour upstream (1, 2)

Data for particulate and dissolved concentrations of IHg and MeHg in Adour upstream and Nive samples for period 2001-2002 (Point 2004) were compared with the bulk concentration data in the current study. At low river discharge (RD) during 2001-2002, SPM for Adour upstream was 5 to 11 mg L^{-1} (assumed 8 mg L^{-1} to estimate bulk concentrations) and for Nive it was between 1 and 3 mg L^{-1} (assumed 2 mg L^{-1}). Averages and standard deviations were available for particulate and dissolved concentrations in Adour upstream samples. Only concentration ranges were available for Nive samples and the mid-ranges of particulate and dissolved concentrations were assumed in order to estimate bulk concentrations at low RD (2001-2002). The current bulk concentration data were selected from May 2017 to have similar (but still slightly higher) SPM (Adour upstream 11.50±2.47 mg L^{-1}; Nive 4.44±1.53 mg L^{-1}).

	Adour upstream (2001-2002)	**Adour upstream (May 2017, n=2)**	**Nive (2001-2002)**	**Nive (May 2017, n=2)**
IHg (ng L^{-1})	3.50 ± 1.70	**0.837** ± 0.458	3.00	**0.834** ± 0.282
MeHg (ng L^{-1})	0.231	**0.0348** ± 0.0072	0.351	**0.0775** ± 0.0048

The concentrations of IHg and MeHg in 2001-2002 are 4-7 times higher (despite slightly lower SPM concentrations) than in May 2017.

Table SI-7 Effect of factor levels (ANOVA) on total and dissolved concentrations of IHg and MeHg in water samples from the Adour estuary.

Model	adjR^2
$\ln[IHg] = f\left(time_{May(-),Sept(+)}; type_{Urban/STP\ (+),STP(++)}\right)$	0.596
$\ln[IHg] = f\left(time_{May(-),Sept(+)}; place_{Nive\ (-),Trib\_Trib/Adour(+)}\right)$	0.549
$\ln[IHg_D] = f\left(time_{May(-)}; type_{STPUrban/STP\ (+)}\right)$	0.338
$\ln[IHg_D] = f\left(time_{May(-)}; place_{Trib\_Trib/Adour(+)}\right)$	0.338
$\ln[MeHg] = f\left(place_{Nive\ (+),Trib/Adour(++)}\right)$	0.265
$\ln[MeHg_D] = f\left(time_{May(-)}; type_{STP(+)}\right)$	0.408
$\ln[MeHg_D] = f\left(time_{May(-)}; place_{Trib/Adour(+)}\right)$	0.116
$\ln[\%MeHg] = f\left(time_{Sept(-),May(+)}; place_{Trib(-),Nive\ (+)}\right)$	0.595
$\sqrt{\%MeHg_D} = f\left(time_{May(+)}\right)$	0.237

The sign behind the factor level shows the effect that level has (relative to levels not shown) on the dependent variables.

Factors (bold) and their levels for corresponding sampling points: **time**: May 2017, Sept 2017, Jan 2018 (all points); **type**: upstream (1, 2, 3, 4), estuary (A, B, C, D) , Urban/STP (7, 8, 9), STP (6); **place**: Adour (1, 2, A, B, C, D), Trib/Adour (6, 8), Trib (7, 9), Nive (3, 4)

Significant interactions were only observed for total IHg between **type** and **time**. In that case, the combined mean square of the single effects was an order of magnitude higher than the mean square of the interaction term. For the sake of simplicity, the effects of factors on the dependent variables were always considered additive.

Table SI-8 Generalized additive models (GAM) for total and dissolved concentrations of IHg and MeHg in water from Adour estuary with root mean square deviation for transformed dependent variable ($RMSD_T$), estimated degrees of freedom (edf) as well as the slope (c_1) and intercept (c_0) for the dependence between model values and experimental values. Models with $c_1 < 0.25$ were not considered.

$RMSD_T$	GAM model	edf_1	edf_2	$c_1 \times 10^{-3}$	$c_0 \times 10^{-3}$
0.308[a]	$\ln[IHg] = a_0\left(time_{Sept(+)}; type_{STP(+)}\right) + s(pH)$	5.04	–	706 ± 64	532 ± 188
0.280[a]	$\ln[IHg] = a_0\left(time_{Sept(+)}; type_{STP(+)}\right) + s(1/\sqrt{Sal})$	7.20	–	755 ± 50	444 ± 146
0.343[a]	$\ln[IHg] = a_0\left(time_{May(-),Sept(+)}; type_{STP(+)}\right) + s(\ln[NO_2])$	4.10	–	646 ± 61	651 ± 177
0.328[a]	$\ln[IHg] = a_0\left(time_{May(-)}; type_{STP(+)}\right) + s(\ln[Chl])$	4.74	–	730 ± 48	471 ± 140
0.282[a]	$\ln[IHg] = a_0\left(time_{Sept(+)}; type_{Urban/STP(+)}\right) + |a_{11}|[SPM]$	1.00	–	881 ± 65	210 ± 191
0.401[a]	$\ln[IHg] = a_0\left(time_{May(-),Sept(+)}; type_{Urban/STP(+),STP(++)}\right) + |a_{12}|/[POC]$	1.00	–	614 ± 91	719 ± 266
0.370[a]	$\ln[IHg] = a_0\left(time_{Sept(+)}; place_{Nive(-),Trib\_Trib/Adour(+)}\right) + s(\delta 13C)$	4.50	–	643 ± 62	645 ± 181
0.342[a]	$\ln[IHg] = a_0\left(time_{May(-)}; place_{Trib\_Trib/Adour(+)}\right) + s(\delta 15N)$	5.79	–	718 ± 48	486 ± 140
0.401[a]	$\ln[IHg] = a_0\left(time_{Sept(+)}; place_{Nive(-),Trib\_Trib/Adour(+)}\right) - |a_{15}|\sqrt{R_{Chl/POC}}$	1.00	–	586 ± 80	767 ± 233
0.349[a]	$\ln[IHg] = a_0\left(time_{May(-),Sept(+)}; type_{Urban/STP(+),STP(++)}\right) + s(\ln K_{OC})$	3.34	–	679 ± 94	596 ± 275
0.222[b]	$\ln[IHg] = a_0\left(time_{Sept(+)}; type_{STP(+)}\right) + s(1/\sqrt{Sal}) + s(pH)$	3.72	4.50	813 ± 53	338 ± 156
0.284[b]	$\ln[IHg] = a_0\left(time_{Sept(+)}; type_{STP(+)}\right) + s(1/\sqrt{Sal}) + s(1/\sqrt{[PO_4]})$	3.61	3.48	835 ± 60	272 ± 176
0.271[b]	$\ln[IHg] = a_0\left(time_{Sept(+)}\right) + s(1/\sqrt{Sal}) + s(\ln[NO_2])$	8.07	2.02	767 ± 39	412 ± 114
0.240[b]	$\ln[IHg] = a_0\left(time_{May(-),Sept(+)}; type_{STP(+)}\right) + s(1/\sqrt{Sal}) + |a_9|\ln[Chl]$	7.39	1.00	823 ± 48	320 ± 142
0.180[b]	$\ln[IHg] = a_0\left(time_{Sept(+)}\right) + s(1/\sqrt{Sal}) + |a_{11}|[SPM]$	7.47	1.00	939 ± 35	102 ± 103

$0.299^{(b)}$	$\ln[IHg] = a_0\left(time_{May(-)}\right) + s(1/\sqrt{Sal}) + s(\delta15N)$	3.25	6.95	658 ± 56	625 ± 164
$0.277^{(b)}$	$\ln[IHg] = a_0\left(time_{May(+),Sept(++)}\right) + s(1/\sqrt{Sal}) + s\left(\sqrt{R_{Chl/POC}}\right)$	6.26	1.91	721 ± 47	505 ± 137
$0.282^{(b)}$	$\ln[IHg] = a_0\left(time_{Sept(+)}; type_{STP(+)}\right) + s(1/\sqrt{Sal}) - |a_{17}| \ln K_{OC}$	6.16	1.00	779 ± 53	396 ± 155
$0.209^{(c)}$	$\ln[IHg] = a_0\left(time_{May(-),Sept(+)}; type_{STP(+)}\right) + |a_{11}|[SPM] + s(\ln[NO_2])$	1.00	5.44	906 ± 39	165 ± 115
$0.289^{(c)}$	$\ln[IHg] = a_0\left(time_{Sept(+)}\right) + |a_{11}|[SPM] + |a_7| \ln[SiO_4]$	1.00	1.00	827 ± 63	316 ± 185
$0.255^{(c)}$	$\ln[IHg] = a_0\left(time_{May(-),Sept(+)}\right) + |a_{11}|[SPM] + s(\ln[DOC])$	1.00	3.47	857 ± 62	259 ± 180
$0.211^{(c)}$	$\ln[IHg] = a_0\left(time_{Sept(+)}; type_{Urban/STP(+)}\right) + |a_{11}|[SPM] + s(1/[POC])$	1.00	6.74	919 ± 47	140 ± 137
$0.251^{(c)}$	$\ln[IHg] = a_0\left(time_{Sept(+)}\right) + |a_{11}|[SPM] + s(\delta15N)$	1.00	4.52	802 ± 44	364 ± 127
$0.226^{(c)}$	$\ln[IHg] = a_0\left(time_{Sept(+)}; type_{Urban/STP(+),STP(++)}\right) + |a_{11}|[SPM] + s\left(\sqrt{R_{Chl/POC}}\right)$	1.00	3.53	920 ± 44	134 ± 129
$0.504^{(a)}$	$\ln[IHg_D] = a_0\left(time_{May(-)}\right) + s(1/\sqrt{[PO_4]})$	4.16	–	515 ± 58	221 ± 59
$0.528^{(b)}$	$\ln[IHg_D] = a_0 + s(1/\sqrt{Sal}) + s(1/\sqrt{[PO_4]})$	2.44	2.40	332 ± 46	314 ± 47
$0.506^{(b)}$	$\ln[IHg_D] = a_0 + s(1/\sqrt{Sal}) + s(SPM)$	3.11	1.53	309 ± 47	342 ± 48
$0.558^{(c)}$	$\ln[IHg_D] = a_0 + |a_{11}|[SPM] + s(1/\sqrt{[PO_4]})$	1.00	2.06	458 ± 46	243 ± 48
$0.240^{(a)}$	$\ln[MeHg] = a_0\left(type_{STP(+)}\right) + s(1/\sqrt{Sal})$	2.19	–	777 ± 71	11.4 ± 5.0
$0.247^{(a)}$	$\ln[MeHg] = a_0\left(time_{May(-)}; type_{STP(+)}\right) + |a_9| \ln[Chl]$	1.00	–	811 ± 60	9.4 ± 4.3
$0.273^{(a)}$	$\ln[MeHg] = a_0\left(type_{STP(+)}\right) + |a_{10}| \ln[Pha]$	1.00	–	757 ± 80	12.4 ± 5.7
$0.179^{(a)}$	$\ln[MeHg] = a_0\left(type_{STP(+)}\right) + s([SPM])$	5.57	–	861 ± 53	7.0 ± 3.7
$0.245^{(a)}$	$\ln[MeHg] = a_0\left(time_{May(-)}; type_{STP(+)}\right) - |a_{12}|/[POC]$	1.00	–	819 ± 68	9.1 ± 4.8
$0.242^{(a)}$	$\ln[MeHg] = a_0\left(type_{STP(+)}\right) + s(\delta13C)$	3.42	–	804 ± 62	9.7 ± 4.4

0.276[a]	$\ln[MeHg] = a_0(type_{STP(+)}) + \lvert a_{17}\rvert \ln K_{OC}$	1.00	–	769 ± 71	11.6 ± 5.1
0.193[b]	$\ln[MeHg] = a_0 + s(1/\sqrt{Sal}) + s(1/\sqrt{[PO_4]})$	5.25	7.54	797 ± 45	10.1 ± 3.2
0.223[b]	$\ln[MeHg] = a_0(type_{STP(+)}) + s(1/\sqrt{Sal}) + \lvert a_5\rvert/\sqrt{[NO_3]}$	2.39	1.00	786 ± 71	11.0 ± 5.1
0.208[b]	$\ln[MeHg] = a_0 + s(1/\sqrt{Sal}) + s(\ln[NO_2])$	4.58	3.64	827 ± 44	8.3 ± 3.2
0.225[b]	$\ln[MeHg] = a_0(time_{May(-)}; type_{STP(+)}) + s(1/\sqrt{Sal}) + \lvert a_9\rvert \ln[Chl]$	1.43	1.00	797 ± 68	10.5 ± 4.9
0.131[b]	$\ln[MeHg] = a_0(type_{STP(+)}) + s(1/\sqrt{Sal}) + s([SPM])$	2.58	6.32	907 ± 36	4.6 ± 2.6
0.187[b]	$\ln[MeHg] = a_0 + s(1/\sqrt{Sal}) + s(\sqrt{R_{Chl/POC}})$	5.24	8.09	805 ± 40	9.6 ± 2.8
0.167[c]	$\ln[MeHg] = a_0(type_{STP(+)}) + s([SPM]) + \lvert a_6\rvert \ln[NO_2]$	5.85	1.00	882 ± 45	5.9 ± 3.2
0.120[c]	$\ln[MeHg] = a_0(time_{May(-)}; type_{STP(+)}) + s([SPM]) + s(\ln[DOC])$	6.99	4.80	915 ± 35	4.3 ± 2.5
0.164[c]	$\ln[MeHg] = a_0(time_{May(-)}; type_{STP(+)}) + s([SPM]) + \lvert a_9\rvert \ln[Chl]$	5.29	1.00	882 ± 45	5.9 ± 3.2
0.138[c]	$\ln[MeHg] = a_0(time_{May(-)}; type_{STP(+)}) + s([SPM]) + s(\ln[Pha])$	4.88	3.86	886 ± 41	5.7 ± 3.0
0.141[c]	$\ln[MeHg] = a_0(type_{STP(+)}) + s([SPM]) - \lvert a_{12}\rvert/[POC]$	6.14	1.00	885 ± 44	5.9 ± 3.1
0.167[c]	$\ln[MeHg] = a_0(type_{STP(+)}) + s([SPM]) + \lvert a_{17}\rvert \ln K_{OC}$	5.71	1.00	868 ± 49	6.7 ± 3.5
0.289[a]	$\ln[MeHg_D] = a_0(type_{STP(+)}) + s(1/\sqrt{Sal})$	2.14	–	576 ± 83	14.4 ± 3.5
0.340[a]	$\ln[MeHg_D] = a_0(time_{May(-)}) + s(T)$	2.44	–	368 ± 67	21.6 ± 2.8
0.326[a]	$\ln[MeHg_D] = a_0(time_{May(-)}) + s(\ln[NO_2])$	2.29	–	480 ± 69	17.5 ± 2.9
0.297[a]	$\ln[MeHg_D] = a_0(time_{May(-)}; type_{STP(+)}) + \lvert a_9\rvert \ln[Chl]$	1.00	–	610 ± 80	13.2 ± 3.4
0.233[a]	$\ln[MeHg_D] = a_0(time_{May(-)}; type_{STP(+)}) + s([SPM])$	5.67	–	730 ± 64	9.1 ± 2.7
0.293[a]	$\ln[MeHg_D] = a_0(time_{May(-)}; type_{STP(+)}) - \lvert a_{12}\rvert/[POC]$	1.00	–	630 ± 85	12.6 ± 3.5

21

$0.291^{(a)}$	$\ln[MeHg_D] = a_0\big(time_{May(-)}; type_{STP(+)}\big) + |a_{15}|\sqrt{R_{Chl/POC}}$	1.00	–	647 ± 79	11.9 ± 3.3
$0.269^{(b)}$	$\ln[MeHg_D] = a_0\big(time_{May(-)}\big) + s(1/\sqrt{Sal}) + |a_3|T$	5.77	1.00	405 ± 71	20.7 ± 3.0
$0.250^{(b)}$	$\ln[MeHg_D] = a_0\big(type_{STP(+)}\big) + s(1/\sqrt{Sal}) + s(T)$	2.30	1.96	720 ± 68	9.3 ± 2.8
$0.216^{(b)}$	$\ln[MeHg_D] = a_0 + s(1/\sqrt{Sal}) + s(1/\sqrt{[PO_4]})$	5.76	4.78	727 ± 65	9.2 ± 2.7
$0.270^{(b)}$	$\ln[MeHg_D] = a_0\big(type_{STP(+)}\big) + s(1/\sqrt{Sal}) + |a_5|/\sqrt{[NO_3]}$	2.39	1.00	610 ± 83	13.3 ± 3.5
$0.221^{(b)}$	$\ln[MeHg_D] = a_0\big(place_{Trib/Adour(-)}\big) + s(1/\sqrt{Sal}) + s(\ln[NO_2])$	5.24	3.37	747 ± 57	8.4 ± 2.4
$0.260^{(b)}$	$\ln[MeHg_D] = a_0\big(time_{May(-)}; type_{STP(+)}\big) + s(1/\sqrt{Sal}) + s(\ln[Chl])$	1.16	2.32	625 ± 80	12.8 ± 3.3
$0.287^{(b)}$	$\ln[MeHg_D] = a_0 + s(1/\sqrt{Sal}) + s(1/[POC])$	2.01	2.52	471 ± 76	18.1 ± 3.2
$0.309^{(b)}$	$\ln[MeHg_D] = a_0 + s(1/\sqrt{Sal}) - |a_{15}|\sqrt{R_{Chl/POC}}$	5.93	1.00	317 ± 67	24.0 ± 2.8
$0.276^{(b)}$	$\ln[MeHg_D] = a_0\big(time_{May(-)}\big) + s(1/\sqrt{Sal}) + |a_{16}|\,ActChl$	6.15	1.00	385 ± 68	21.3 ± 2.8
$0.312^{(b)}$	$\ln[MeHg_D] = a_0 + s(1/\sqrt{Sal}) + |a_{17}|\ln K_{OC}$	5.64	1.00	276 ± 64	25.1 ± 2.7
$0.224^{(c)}$	$\ln[MeHg_D] = a_0 + s([SPM]) + s(1/\sqrt{[PO_4]})$	5.75	3.24	744 ± 56	8.5 ± 2.4
$0.244^{(c)}$	$\ln[MeHg_D] = a_0 + s([SPM]) + s(\ln[NO_2])$	5.95	2.00	627 ± 61	12.6 ± 2.5
$0.206^{(c)}$	$\ln[MeHg_D] = a_0\big(time_{May(-)}; type_{STP(+)}\big) + s([SPM]) + s(\ln[Chl])$	5.09	1.98	770 ± 63	7.7 ± 2.6
$0.219^{(c)}$	$\ln[MeHg_D] = a_0\big(time_{May(-)}; type_{STP(+)}\big) + s([SPM]) - |a_{12}|/[POC]$	5.84	1.00	745 ± 63	8.6 ± 2.7
$0.211^{(c)}$	$\ln[MeHg_D] = a_0\big(time_{May(-)}; type_{STP(+)}\big) + s([SPM]) - |a_{13}|\delta13C$	6.15	1.00	808 ± 59	6.3 ± 2.5
$0.230^{(c)}$	$\ln[MeHg_D] = a_0\big(type_{STP(+)}\big) + s([SPM]) - |a_{14}|\delta15N$	6.14	1.00	716 ± 66	9.6 ± 2.8
$0.211^{(a)}$	$\ln[\%MeHg] = a_0\big(time_{Sept(-)}; place_{Nive(+)}\big) + s(pH)$	5.00	–	740 ± 64	747 ± 240
$0.240^{(a)}$	$\ln[\%MeHg] = a_0\big(time_{Sept(-)}; type_{UpstreamSTP(+)}\big) + s(1/\sqrt{Sal})$	7.89	–	666 ± 73	962 ± 273

$0.271^{(a)}$	$\ln[\%MeHg] = a_0\left(time_{Sept(-),May(+)}; place_{Nive(+)}\right) + s(1/\sqrt{[PO_4]})$	2.87	–	614 ± 69	1107 ± 261
$0.276^{(a)}$	$\ln[\%MeHg] = a_0\left(time_{Sept(-),May(+)}; type_{UpstreamSTP(+)}\right) + s(1/\sqrt{[NO_3]})$	5.26	–	715 ± 62	786 ± 234
$0.236^{(a)}$	$\ln[\%MeHg] = a_0\left(time_{Sept(-),May(+)}; place_{Nive(+)}\right) + s(\ln[NO_2])$	6.37	–	662 ± 63	972 ± 238
$0.252^{(a)}$	$\ln[\%MeHg] = a_0\left(time_{Sept(-),May(+)}; type_{UpstreamSTP(+)}\right) + s(\ln[NO_2])$	6.42	–	554 ± 66	1293 ± 249
$0.286^{(a)}$	$\ln[\%MeHg] = a_0\left(time_{Sept(-),May(+)}; type_{UpstreamSTP(+)}\right) + s(\ln[Chl])$	4.44	–	511 ± 75	1416 ± 282
$0.278^{(a)}$	$\ln[\%MeHg] = a_0\left(time_{Sept(-)}; place_{Trib(-),Nive(+)}\right) + s([SPM])$	2.17	–	651 ± 69	990 ± 259
$0.291^{(a)}$	$\ln[\%MeHg] = a_0\left(time_{Sept(-)}; type_{UpstreamSTP(+)}\right) + s([SPM])$	1.96	–	579 ± 69	1206 ± 259
$0.291^{(a)}$	$\ln[\%MeHg] = a_0\left(time_{Sept(-),May(+)}; place_{Trib(-),Nive(+)}\right) + s(1/[POC])$	1.21	–	634 ± 71	1045 ± 268
$0.209^{(a)}$	$\ln[\%MeHg] = a_0\left(time_{Sept(-)}; place_{Trib(-),Nive(+)}\right) + s(\sqrt{R_{Chl/POC}})$	6.45	–	839 ± 54	447 ± 204
$0.270^{(a)}$	$\ln[\%MeHg] = a_0\left(time_{Sept(-)}; type_{UpstreamSTP(+)}\right) + s(\sqrt{R_{Chl/POC}})$	5.83	–	687 ± 63	875 ± 238
$0.201^{(b)}$	$\ln[\%MeHg] = a_0\left(time_{Sept(-)}\right) + s(1/\sqrt{Sal}) + s(pH)$	7.44	3.21	714 ± 72	830 ± 272
$0.225^{(b)}$	$\ln[\%MeHg] = a_0\left(time_{Sept(-)}\right) + s(1/\sqrt{Sal}) - |a_4|/\sqrt{[PO_4]}$	8.49	1.00	696 ± 75	879 ± 282
$0.193^{(b)}$	$\ln[\%MeHg] = a_0\left(time_{Sept(-),May(+)}; type_{UpstreamSTP(+)}\right) + s(1/\sqrt{Sal}) + s(\ln[Chl])$	7.60	2.79	729 ± 58	776 ± 217
$0.171^{(b)}$	$\ln[\%MeHg] = a_0\left(time_{Sept(-)}; place_{Nive(+)}\right) + s(1/\sqrt{Sal}) + s(\ln[Pha])$	8.38	3.61	835 ± 48	464 ± 180
$0.230^{(b)}$	$\ln[\%MeHg] = a_0\left(time_{Sept(-)}\right) + s(1/\sqrt{Sal}) + s([SPM])$	7.23	2.02	716 ± 59	800 ± 223
$0.209^{(b)}$	$\ln[\%MeHg] = a_0\left(time_{Sept(-)}\right) + s(1/\sqrt{Sal}) - |a_{12}|/[POC]$	7.79	1.00	710 ± 58	834 ± 219
$0.199^{(b)}$	$\ln[\%MeHg] = a_0\left(time_{Sept(-)}\right) + s(1/\sqrt{Sal}) + s(\sqrt{R_{Chl/POC}})$	7.16	5.80	797 ± 55	566 ± 208
$0.218^{(b)}$	$\ln[\%MeHg] = a_0\left(time_{Sept(-)}\right) + s(1/\sqrt{Sal}) + |a_{17}|\ln K_{OC}$	8.29	1.00	701 ± 73	872 ± 276

0.210[c]	$\ln[\%MeHg] = a_0\left(time_{Sept(-),May(+)}; place_{Nive(+)}\right) + s([SPM]) + s(1/\sqrt{[PO_4]})$	1.04	3.98	684 ± 62	916 ± 232
0.208[c]	$\ln[\%MeHg] = a_0\left(time_{Sept(-)}; type_{UpstreamSTP(+)}\right) + s([SPM]) + s(1/\sqrt{[PO_4]})$	2.20	4.07	657 ± 60	994 ± 227
0.209[c]	$\ln[\%MeHg] = a_0\left(time_{Sept(-),May(+)}; place_{Nive(+)}\right) + s([SPM]) + s(\ln[NO_2])$	1.28	3.60	671 ± 56	952 ± 212
0.190[c]	$\ln[\%MeHg] = a_0\left(time_{Sept(-),May(+)}; type_{UpstreamSTP(+)}\right) - |a_{11}|[SPM] + s(\ln[NO_2])$	1.00	6.12	667 ± 53	971 ± 200
0.243[c]	$\ln[\%MeHg] = a_0\left(time_{Sept(-)}; place_{Trib(-),Nive(+)}\right) - |a_{11}|[SPM] + s(1/[POC])$	1.00	1.89	676 ± 64	933 ± 240
0.278[c]	$\ln[\%MeHg] = a_0\left(time_{Sept(-)}; type_{UpstreamSTP(+)}\right) - |a_{11}|[SPM] + s(1/[POC])$	1.00	1.86	563 ± 67	1261 ± 254
0.292[c]	$\ln[\%MeHg] = a_0\left(time_{Sept(-)}\right) + s([SPM]) + |a_{14}|\delta15N$	4.20	1.00	659 ± 65	953 ± 247
0.186[c]	$\ln[\%MeHg] = a_0\left(time_{Sept(-)}\right) + s([SPM]) + s(\sqrt{R_{Chl/POC}})$	7.74	3.32	919 ± 59	196 ± 222
0.204[c]	$\ln[\%MeHg] = a_0\left(time_{Sept(-)}; type_{UpstreamSTP(+)}\right) + s([SPM]) + s(\sqrt{R_{Chl/POC}})$	3.43	3.59	811 ± 52	525 ± 195
0.297[c]	$\ln[\%MeHg] = a_0\left(time_{Sept(-),May(+)}\right) + s([SPM]) + |a_{17}|\ln K_{OC}$	1.16	1.00	607 ± 92	1140 ± 348
0.488[a]	$\sqrt{[\%MeHg_D]} = a_0\left(time_{May(+)}\right) + s(1/\sqrt{Sal})$	4.95	–	499 ± 80	3601 ± 696
0.464[a]	$\sqrt{[\%MeHg_D]} = a_0\left(place_{Trib(+)}\right) + s(1/\sqrt{Sal})$	5.24	–	546 ± 78	3252 ± 673
0.565[a]	$\sqrt{[\%MeHg_D]} = a_0\left(time_{May(+)}; type_{STP(+)}\right) + |a_5|/\sqrt{[NO_3]}$	1.00	–	390 ± 82	4405 ± 711
0.458[a]	$\sqrt{[\%MeHg_D]} = a_0\left(time_{May(+)}; type_{STP(+)}\right) + s([SPM])$	3.84	–	546 ± 79	3269 ± 689
0.587[a]	$\sqrt{[\%MeHg_D]} = a_0\left(type_{STP(+)}\right) + |a_{15}|\sqrt{R_{Chl/POC}}$	1.00	–	361 ± 81	4602 ± 702
0.403[b]	$\sqrt{[\%MeHg_D]} = a_0\left(type_{STPUrban/STP(+)}\right) + s(1/\sqrt{Sal}) + s([SPM])$	4.79	3.53	627 ± 71	2656 ± 616
0.483[b]	$\sqrt{[\%MeHg_D]} = a_0 + s(1/\sqrt{Sal}) + |a_{15}|\sqrt{R_{Chl/POC}}$	4.93	1.00	517 ± 78	3469 ± 674
0.493[c]	$\sqrt{[\%MeHg_D]} = a_0\left(time_{May(+)}\right) + s([SPM]) - |a_4|/\sqrt{[PO_4]}$	3.61	1.00	462 ± 81	3876 ± 698

$0.377^{(c)}$	$\sqrt{[\%MeHg_D]} = a_0\left(type_{STP(+)}\right) + s([SPM]) + s(1/\sqrt{[NO_3]})$	4.66	4.10	655 ± 72	2474 ± 620
$0.356^{(c)}$	$\sqrt{[\%MeHg_D]} = a_0\left(time_{May(+)}; type_{STP(+)}\right) + s([SPM]) + s(1/\sqrt{[NO_3]})$	4.65	4.19	696 ± 71	2170 ± 618
$0.482^{(c)}$	$\sqrt{[\%MeHg_D]} = a_0\left(type_{STP(+)}\right) + s([SPM]) + |a_8|\ln[DOC]$	3.84	1.00	503 ± 76	3569 ± 661
$0.462^{(c)}$	$\sqrt{[\%MeHg_D]} = a_0\left(type_{STP(+)}\right) + s([SPM]) + |a_9|\ln[Chl]$	3.60	1.00	546 ± 75	3260 ± 653
$0.470^{(c)}$	$\sqrt{[\%MeHg_D]} = a_0\left(time_{May(+)}\right) + s([SPM]) + s(1/[POC])$	3.76	3.36	523 ± 77	3411 ± 667
$0.531^{(c)}$	$\sqrt{[\%MeHg_D]} = a_0\left(time_{May(+)}\right) - |a_{11}|[SPM] + s(\delta 13C)$	1.00	2.11	416 ± 82	4215 ± 708
$0.440^{(c)}$	$\sqrt{[\%MeHg_D]} = a_0\left(type_{STP(+)}\right) + s([SPM]) + s(\delta 15N)$	3.64	2.21	554 ± 78	3213 ± 676
$0.434^{(c)}$	$\sqrt{[\%MeHg_D]} = a_0\left(type_{STP(+)}\right) + s([SPM]) + |a_{15}|\sqrt{R_{Chl/POC}}$	3.63	1.00	610 ± 77	2790 ± 669
$0.475^{(c)}$	$\sqrt{[\%MeHg_D]} = a_0\left(type_{STP(+)}\right) + s([SPM]) - |a_{17}|\ln K_{OC}$	3.85	1.00	521 ± 76	3439 ± 658

(a) Models developed from one continuous explanatory variable (Eq. 6) (b) Models developed from two continuous explanatory variables (one of them Sal) (Eq. 7); (c) Models developed from two continuous explanatory variables (one of them SPM) (Eq. 8). Total and dissolved concentrations of IHg and MeHg expressed in ng L^{-1}. The sign in front of the absolute values of the parametric coefficients shows the direction of the effect of respective continuous explanatory variables on the dependent variable. The intercept a_0 may be positive or negative and depends on factor levels. The sign behind the factor level shows the effect that level has (relative to levels not shown) on a_0. Starting factor levels determined according to ANOVA in Table SI-7.

Factors (bold) and their levels for corresponding sampling points (Fig. 1): **time**: May 2017, Sept 2017, Jan 2018 (all points); **type**: upstream (1, 2, 3, 4), estuary (A, B, C, D), Urban/STP (7, 8, 9), STP (6); **place**: Adour (1, 2, A, B, C, D), Trib/Adour (6, 8), Trib (7, 9), Nive (3, 4).

Indexes in a_i for different continuous variables X_i: 1: pH, 2: Sal, 3: T, 4: PO$_4$, 5: NO$_3$, 6: NO$_2$, 7: SiO$_4$, 8: DOC, 9: Chl, 10: Pha, 11: SPM, 12: POC, 13: δ13C, 14: δ15N, 15: $R_{Chl/POC}$, 16: ActChl, 17: K_{OC}

Table SI-9 Multiple regression (MR) models (Eq. 11) for total and dissolved concentrations of IHg and MeHg in water from Adour estuary with root mean square deviation for transformed dependent variable (RMSD$_T$) as well as the slope (c_1) and intercept (c_0) for the dependence between model values and experimental values.

RMSD$_T$	Minimal adequate model	c_1 x10^{-3}	c_0 x10^{-3}
0.326	$\ln[IHg] = a_0 + |a_3|T + |a_{11}|[SPM] - |a_{14}|\delta 15N$	776 ± 94	434 ± 276
0.568	$\ln[IHg_D] = a_0 + |a_{11}|[SPM] - |a_{14}|\delta 15N$	205 ± 53	402 ± 55
0.213	$\ln[MeHg] = |a_{11}|[SPM] - |a_{12}|/[POC] + |a_{13}|\delta 13C$	636 ± 61	19 ± 4
0.286	$\ln[MeHg_D] = a_0 + |a_2|/\sqrt{Sal} + |a_3|T + |a_{11}|[SPM] - |a_{14}|\delta 15N$	454 ± 75	19 ± 3
0.354	$\ln[\%MeHg] = a_0 - |a_3|T - |a_{11}|[SPM] - |a_{12}|/[POC] + |a_{14}|\delta 15N$	476 ± 73	1495 ± 276
0.607	$\sqrt{[\%MeHg_D]} = a_0 - |a_{11}|[SPM] + |a_{14}|\delta 15N$	250 ± 73	5437 ± 64

The sign in front of the absolute values of the coefficients shows the direction of the effect of respective continuous explanatory variables has on the dependent variable. The intercept a_0 may be positive or negative. Total and dissolved concentrations of IHg and MeHg expressed in ng L^{-1}.

Indexes in a_i for different continuous variables X$_i$: 1: pH, 2: Sal, 3: T, 4: PO$_4$, 5: NO$_3$, 6: NO$_2$, 7: SiO$_4$, 8: DOC, 9: Chl, 10: Pha, 11: SPM, 12: POC, 13: δ13C, 14: δ15N, 15: R$_{Chl/POC}$, 16: ActChl, 17: K$_{OC}$

Table SI-10 Linear models (ANCOVA) for the dependent variable Y_T with root mean square deviation for transformed dependent variable ($RMSD_T$) as well as the slope (c_1) and intercept (c_0) for the dependence between model values and experimental values. For the best models, $RMSD_T$ is marked in bold. Models with $c_1 < 0.50$ were not considered.

$RMSD_T$	Minimal adequate model	c_1 x10^{-3}	c_0 x10^{-3}
0.279[a]	$\ln[IHg] = a_0\big(time_{May\,(+),Sept(++)}\big) + |a_{11}|[SPM] - |a_{14}|\delta15N$	810±60	355±175
0.274[a,b]	$\ln[IHg] = a_0\big(time_{Sept(+)}; type_{STPUrban/STP(+)}\big) + |a_{11}|[SPM]$	905±62	166±181
0.414[b]	$\ln[IHg] = a_0\big(time_{May(-),Sept(+)}; type_{STP(+)}\big) + |a_1|pH - |a_{1,1}|(pH)^2$	600±100	744±293
0.389[b]	$\ln[IHg] = a_0\big(time_{May(-),Sept(+)}; type_{Upstream(-),STP(+)}\big) + |a_2|/\sqrt{Sal}$	611±71	719±209
0.342[b]	$\ln[IHg] = a_0\big(time_{Sept(+)}; type_{Upstream(-),STP(+)}\big) + |a_2|/\sqrt{Sal} - |a_{2,2}|/Sal$	721±74	516±216
0.354[b]	$\ln[IHg] = a_0\big(time_{May(-),Sept(+)}; type_{STP(+)}\big) + |a_9|\ln[Chl]$	728±72	490±210
0.401[b]	$\ln[IHg] = a_0\big(time_{May(-),Sept(+)}; type_{Urban/STP(+),STP(++)}\big) + |a_{12}|/[POC]$	614±91	719±266
0.365[b]	$\ln[IHg] = a_0\big(time_{May(-),Sept(+)}; type_{Urban/STP(+),STP(++)}\big) + |a_{12}|/[POC] - |a_{12,12}|/[POC]^2$	708±81	530±237
0.409[b]	$\ln[IHg] = a_0\big(time_{Sept(+)}; place_{Nive(-),Trib\_Trib/Adour(+)}\big) + |a_{13}|\delta13C$	616±71	700±207
0.439[b]	$\ln[IHg] = a_0\big(time_{May(-)}; type_{STPUrban/STP\,(+)}\big) + |a_{14}|\delta15N$	562±62	782±180
0.419[b]	$\ln[IHg] = a_0\big(time_{May(-),Sept(+)}; type_{STP(+)}\big) + |a_{17}|\ln K_{OC}$	567±108	818±316
0.283[c]	$\ln[IHg] = a_0\big(time_{Sept(+)}; type_{Upstream(-),STP(+)}\big) + (|a_1| - |a_{1,1}|pH)pH + (|a_2| - |a_{2,2,2}|/Sal)/\sqrt{Sal}$	809±97	366±283
0.279[d]	$\ln[IHg] = a_0\big(time_{Sept(+)}\big) + |a_6|\ln[NO_2] + |a_{11}|[SPM]$	885±72	213±212
0.289[d]	$\ln[IHg] = a_0\big(time_{Sept(+)}\big) + |a_7|\ln[SiO_4] + |a_{11}|[SPM]$	827±63	316±185
0.270[d]	$\ln[IHg] = a_0\big(time_{Sept(+)}; type_{Upstream(-)}\big) + |a_{11}|[SPM] - |a_{12}|/[POC]$	894±67	193±196
0.271[b]	$\ln[MeHg] = a_0\big(type_{STP\,(+)}\big) + |a_2|/\sqrt{Sal}$	760±81	12.2±5.8

0.239[b]	$\ln[MeHg] = a_0(type_{STP\,(+)}) + |a_2|/\sqrt{Sal} - |a_{2,2}|/Sal$	792±70	10.6±5.0
0.247[b]	$\ln[MeHg] = a_0(time_{May(-)};\ type_{STP\,(+)}) + |a_9|\ln[Chl]$	811±60	9.4±4.3
0.273[b]	$\ln[MeHg] = a_0(type_{STP\,(+)}) + |a_{10}|\ln[Pha]$	757±80	12.4±5.7
0.264[b]	$\ln[MeHg] = a_0(type_{STP\,(+)}) + |a_{11}|[SPM]$	776±70	11.3±5.0
0.202[b]	$\ln[MeHg] = a_0(type_{STP\,(+)}) - f(SPM)$	881±56	6.0±4.0
0.245[b]	$\ln[MeHg] = a_0(time_{May(-)};type_{STP\,(+)}) - |a_{12}|/[POC]$	819±68	9.1±4.8
0.255[b]	$\ln[MeHg] = a_0(type_{Urban/STP(+),STP(++)}) + |a_{13}|\delta 13C$	781±73	11.1±5.2
0.255[b]	$\ln[MeHg] = a_0(type_{STP\,(+)}) + |a_{17}|\ln K_{OC}$	769±71	11.6±5.1
0.214[c]	$\ln[MeHg] = a_0(time_{Sept(+)};type_{STP(+)}) + |a_2|/\sqrt{Sal} - |a_{2,2}|/Sal + |a_9|\ln[Chl]$	825±57	8.9±4.1
0.171[c]	$\ln[MeHg] = a_0(type_{STP\,(+)}) + |a_2|/\sqrt{Sal} - |a_{2,2}|/Sal - f(SPM)$	922±39	3.8±2.8
0.246[d]	$\ln[MeHg] = a_0(type_{Urban/STP(+),STP(++)}) - |a_8|\ln[DOC] + |a_{11}|[SPM]$	784±71	11.1±5.0
0.189[d]	$\ln[MeHg] = a_0(type_{Urban/STP(+),STP(++)}) - |a_8|\ln[DOC] - f(SPM)$	896±57	5.2±4.0
0.183[d]	$\ln[MeHg] = a_0(time_{May(-)};\ type_{STP\,(+)}) + |a_9|\ln[Chl] - f(SPM)$	919±49	4.0±3.5
0.198[d]	$\ln[MeHg] = a_0(type_{Urban/STP(-)}) + |a_{11}|[SPM] - |a_{12}|/[POC]$	809±73	10.1±5.2
0.181[d]	$\ln[MeHg] = a_0(type_{Urban/STP(+),STP\,(++)}) - f(SPM) + |a_{17}|\ln K_{OC}$	894±51	5.3±3.7
0.182[e]	$\ln[MeHg] = a_0(type_{Urban/STP(-)}) - |a_{12}|/[POC] + |a_{18}|\ln[IHg]$	806±50	10.2±3.6
0.262[a,c]	$\ln[MeHg_D] = a_0(time_{Sept(+)};type_{STP\,(+)}) + |a_2|/\sqrt{Sal} - |a_{2,2}|/Sal$	692±74	10.4±3.1
0.289[b]	$\ln[MeHg_D] = a_0(type_{STP\,(+)}) + |a_2|/\sqrt{Sal} - |a_{2,2}|/Sal$	604±85	13.5±3.5
0.282[b]	$\ln[MeHg_D] = a_0(time_{May(-)};type_{STP\,(+)}) + |a_9|\ln[Chl] - |a_{9,9}|(\ln[Chl])^2$	647±79	12.0±3.3
0.270[b]	$\ln[MeHg_D] = a_0(time_{May(-)};type_{STP\,(+)}) - f(SPM)$	715±71	9.5±3.0

0.293[b]	$\ln[MeHg_D] = a_0\left(time_{May(-)}; type_{STP\,(+)}\right) - |a_{12}|/[POC]$	630±85	12.6±3.5
0.291[b]	$\ln[MeHg_D] = a_0\left(time_{May(-)}; type_{STP\,(+)}\right) + |a_{15}|\sqrt{R_{Chl/POC}}$	647±79	11.9±3.3
0.268[c]	$\ln[MeHg_D] = a_0\left(type_{STP\,(+)}\right) + |a_2|/\sqrt{Sal} - |a_{2,2}|/Sal + |a_3|\,T$	672±76	11.1±3.2
0.301[c]	$\ln[MeHg_D] = a_0 + |a_2|/\sqrt{Sal} - |a_4|/\sqrt{[PO_4]} + |a_{4,4}|/[PO_4]$	540±84	15.8±3.5
0.272[c]	$\ln[MeHg_D] = a_0\left(type_{STP\,(+)}\right) + |a_2|/\sqrt{Sal} - |a_{2,2}|/Sal + |a_5|/\sqrt{[NO_3]}$	639±87	12.4±3.6
0.288[c]	$\ln[MeHg_D] = a_0 + |a_2|/\sqrt{Sal} - |a_{2,2}|/Sal - |a_{12}|/[POC] + |a_{12,12}|/[POC]^2$	526±93	16.4±3.9
0.266[d]	$\ln[MeHg_D] = a_0 - f(SPM) - |a_4|/\sqrt{[PO_4]} + |a_{4,4}|/[PO_4]$	771±67	7.5±2.8
0.260[f]	$\ln[MeHg_D] = a_0\left(type_{STP\,(+)}\right) + |a_2|/\sqrt{Sal} + |a_{19}|\ln[IHg_D]$	653±85	11.9±3.5
0.207[f]	$\ln[MeHg_D] = a_0\left(type_{STP\,(+)}\right) - f(SPM) + |a_{19}|\ln[IHg_D]$	872±62	4.2±2.6
0.251[a]	$\ln[\%MeHg] = a_0\left(time_{Sept(-)}; type_{Urban/STP\,(-)}\right) - |a_{11}|[SPM] - |a_{12}|/[POC]$	625±60	1083±227
0.242[a]	$\ln[\%MeHg] = a_0\left(time_{Sept(-)}; type_{STPUrban/STP\,(-)}\right) - |a_{11}|[SPM] - |a_{12}|/[POC] + |a_{12,12}|/[POC]^2$	694±60	878±227
0.286[b]	$\ln[\%MeHg] = a_0\left(time_{Sept(-),May(+)}; place_{Nive(+)}\right) - |a_1|pH + |a_{1,1}|(pH)^2$	664±85	970±322
0.291[b]	$\ln[\%MeHg] = a_0\left(time_{Sept(-),May(+)}; place_{Nive(+)}\right) - |a_4|/\sqrt{[PO_4]}$	600±74	1150±279
0.327[b]	$\ln[\%MeHg] = a_0\left(time_{Sept(-),May(+)}; type_{Upstream(+)}\right) - |a_5|/\sqrt{[NO_3]} + |a_{5,5}|/[NO_3]$	529±81	1352±306
0.278[b]	$\ln[\%MeHg] = a_0\left(time_{Sept(-)}; type_{Upstream(+),STP(++)}\right) - |a_{11}|[SPM]$	528±68	1371±258
0.269[b]	$\ln[\%MeHg] = a_0\left(time_{Sept(-)}; type_{Urban/STP(-),STP(+)}\right) - |a_{11}|[SPM] + |a_{11,11}|[SPM]^2$	601±68	1154±256
0.295[b]	$\ln[\%MeHg] = a_0\left(time_{Sept(-),May(+)}; type_{STPUrban/STP\,(-)}\right) - |a_{12}|/[POC]$	611±66	1106±248
0.328[b]	$\ln[\%MeHg] = a_0\left(time_{Sept(-)}; type_{Urban/STP(-),Upstream(+)}\right) - |a_{15}|\sqrt{R_{Chl/POC}} + |a_{15,15}|R_{Chl/POC}$	519±82	1382±308
0.275[d]	$\ln[\%MeHg] = a_0\left(time_{Sept(-)}; place_{Nive(+)}\right) - |a_4|/\sqrt{[PO_4]} - |a_{11}|[SPM]$	576±73	1266±275

$0.250^{(d)}$	$\ln[\%MeHg] = a_0(time_{Sept(-)}; place_{Nive(+)}) - |a_4|/\sqrt{[PO_4]} - |a_{11}|[SPM] + |a_{11,11}|[SPM]^2$	692±72	889±271
$\mathbf{0.242^{(d)}}$	$\ln[\%MeHg] = a_0(time_{Sept(-)}; type_{STPUrban/STP(-)}) - |a_{11}|[SPM] - |a_{12}|/[POC] + |a_{12,12}|/[POC]^2$	694±60	878±227
$0.251^{(d)}$	$\ln[\%MeHg] = a_0(time_{Sept(-)}; type_{Urban/STP(-)}) - |a_{11}|[SPM] - |a_{12}|/[POC]$	625±60	1083±227
$0.299^{(d)}$	$\ln[\%MeHg] = a_0(time_{Sept(-),May(+)}) - |a_{11}|[SPM] + |a_{17}| \ln K_{OC}$	602±93	1155±351
$\mathbf{0.460^{(a,b)}}$	$\sqrt{[\%MeHg_D]} = a_0(time_{May(+)}; type_{STP(+)}) - f(SPM)$	598±87	2899±757
$0.482^{(d)}$	$\sqrt{[\%MeHg_D]} = a_0(type_{STP(+)}) - f(SPM) + |a_8| \ln[DOC]$	566±86	3132±749
$0.471^{(d)}$	$\sqrt{[\%MeHg_D]} = a_0(time_{May(+)}) - f(SPM) - |a_{12}|/[POC] + |a_{12,12}|/[POC]^2$	591±87	2945±754
$\mathbf{0.477^{(d)}}$	$\sqrt{[\%MeHg_D]} = a_0(type_{STP(+)}) - f(SPM) - |a_{17}| \ln K_{OC}$	578±86	3043±745

(a) Models developed from several continuous explanatory variables without interaction terms (Table SI-9); (b) Models developed from one continuous explanatory variable (Table SI-8) (c) Models developed from two continuous explanatory variables (one of them Sal) with interaction terms (Table SI-8); (d) Models developed from two continuous explanatory variables (one of them SPM) with interaction terms (Table SI-8); (e) Model developed from two explanatory variables (one of them total IHg, Eq. 12); (f) Model developed from two explanatory variables (one of them dissolved IHg, Eq. 12).

$$f(SPM) = |a_{11}|[SPM] - |a_{11,11}|[SPM]^2 + |a_{11,11,11}|[SPM]^3$$

Total and dissolved concentrations of IHg and MeHg expressed in ng L^{-1}. The sign in front of the absolute values of the coefficients shows the direction of the effect of respective continuous explanatory variables and their interactions on the dependent variable. The intercept a_0 may be positive or negative and depends on factor levels. The sign behind the factor level shows the effect that level has (relative to levels not shown) on a_0. Factors: **time**: May 2017, Sept 2017, Jan 2018; **type**: upstream, estuary, Urban/STP, STP; **place**: Adour, Trib_Trib/Adour, Nive

Indexes in a_i for different continuous variables X_i: 1: pH, 2: Sal, 3: T, 4: PO$_4$, 5: NO$_3$, 6: NO$_2$, 7: SiO$_4$, 8: DOC, 9: Chl, 10: Pha, 11: SPM, 12: POC, 13: δ13C, 14: δ15N, 15: R$_{Chl/POC}$, 16: ActChl, 17: K$_{OC}$, 18: IHg, 19: IHg$_D$

Table SI-11 Correlation coefficients (p<0.05) between Hg species concentrations and transformed biogeochemical variables.

	$\ln[IHg]$	$\ln[MeHg]$	$\ln[IHg_D]$	$\ln[MeHg_D]$
pH		−0.390		
$1/\sqrt{[NO_3]}$			−0.343	
$\ln[NO_2]$	0.414	0.502		0.359
$\ln[SiO_4]$	0.440			
$\ln[Chl]$	0.381			
SPM	0.832	0.615	0.562	0.451
$1/[POC]$		−0.634		−0.523
$1/\sqrt{[POC_V]}$	−0.806	−0.638	−0.536	−0.482
$\delta 13C$	0.406	0.377		
$\sqrt{R_{Chl/POC}}$	−0.524	−0.419	−0.466	
$\ln K_{OC}$		0.382		

Significance legend:

p<0.05	*p<0.02*	*p<0.01*
p<0.001	**p<0.0001**	**p<0.00001**

31

SUPPLEMENTARY INFORMATION

(Minimal adequate ANCOVA)

Marine Pollution Bulletin

Assessing and predicting the changes for inorganic mercury and methylmercury concentrations in surface waters of a tidal estuary (Adour Estuary, SW France)

Teodor Stoichev*[a], Aubin Thibaut de Chanvalon[b], Sandrine Veloso[b],

Jonathan Deborde[b,c], Emmanuel Tessier[b], Laurent Lanceleur[b], David Amouroux*[b]

[a] Interdisciplinary Center of Marine and Environmental Research (CIIMAR/CIMAR), University of Porto, Terminal de Cruzeiros de Leixoes, Av. General Norton de Matos s/n, 4450-208 Matosinhos, Portugal,

E-mail: tstoichevbg@yahoo.com

[b] Universite de Pau et des Pays de l'Adour, E2S UPPA, CNRS, IPREM, Institut des Sciences Analytiques et de Physico-chimie pour l'Environnement et les matériaux, Pau, France,

E-mail: david.amouroux@univ-pau.fr

[c] Ifremer, LITTORAL, Laboratoire Environnement Ressources des Pertuis Charentais, F-17390 La Tremblade, France

All minimal adequate models in Table SI-10 were obtained after stepwise deletion of non-significant terms, starting from interactions, then quadratic or cubic effects followed by non-significant simple effects. Only models without interaction terms were included in Table SI-10. All models were compared using the linear dependence of model values Y_{MOD} against experimental ones Y_{EXP} with slope c_1 (should be close to 1) and intercept c_0 (should be close to 0) and minimal $RMSD_T$ values (Eq. 9). Concentrations of Hg species expressed in ng L^{-1};

The functions f_3 (having as higher order effects of one variable both quadratic and cubic terms) and f_2 (having as higher order effects of one variable only quadratic terms) were used for brief notation:

$$f_3(SPM) = |a_{11}|[SPM] - |a_{11,11}|[SPM]^2 + |a_{11,11,11}|[SPM]^3$$
$$f_2(Sal) = |a_2|/\sqrt{Sal} - |a_{2,2}|/Sal$$

$$f_2(POC) = |a_{12}|/[POC] - |a_{12,12}|/[POC]^2$$

Selected minimal adequate models with adjusted R^2 (adjR^2), regression coefficients for transformed explanatory variables (Eqs. 5) and their bootstrap range between percentiles P2.5 and P97.5 after row resampling are presented here. The sign of coefficient should not change between percentiles 2.5 and 97.5 after bootstrap with row resampling. Eventually, if better models were not available (e.g. %MeHg$_D$), and sign of some coefficient does change after bootstrap, the ratio between absolute values of the coefficient (percentile 2.5 and 97.5) should be at least on order of magnitude. In that case, the sign of the corresponding effect is as the sign of coefficient in the minimal adequate ANCOVA model but from one side is bound to 0. In all other cases, the coefficients instability after bootstrap lead to model elimination. For models with two continuous explanatory variables (Figs. 5, 6, Fig. SI-2) the average values of the explanatory variables, grouped according to significant factor levels are also presented. Equations for selected models marked in bold.

ANCOVA models could not be developed for IHg$_D$. Therefore, non-linear models relating dissolved concentrations with total concentrations of the same Hg species and SPM were tested. In these models, several functions relating particulate concentrations (C_p, µg g^{-1}) of IHg and MeHg with their total concentrations C_{TOT} were checked (constants d_1 and d_2 are to be determined from experimental data):

$$C_p = d_1[C_{TOT}]^{d_2}$$

$$C_p = d_1[C_{TOT}]/(d_2 + [C_{TOT}])$$

$$C_p = d_1(1 - \exp(-d_2[C_{TOT}]))$$

IHg

$$\ln[IHg] = a_0\big(time_{Sept(+)}; type_{Upstream(-)}\big) + |a_{11}|[SPM] - |a_{12}|/[POC]$$

adjR^2=0.836; <u>Regression coefficients:</u>

Effect		Estimate	P2.5	P97.5
a_0	Intercept	−0.124854	−0.590696	0.242281
	type upstream	−0.223214	−0.419995	−0.025610
	time Sept	0.579910	0.379587	0.792702
a_{11}	**SPM** ($\times 10^{-2}$)	4.6665	3.5938	5.9036
a_{12}	**POC** $_T$	−1.575496	−3.038280	−0.185141

<u>Average values:</u>

time / type	upstream	estuary_STP_Urban/STP	X_i
Sept	16.31	26.49	**SPM (mg L^{-1})**
MayJan	14.70	18.48	**SPM (mg L^{-1})**
Sept	5.01	6.69	**POC (%)**
MayJan	5.29	7.65	**POC (%)**

==

IHg$_D$

$$[IHg_D] = [IHg] - d_1[SPM](1 - exp(-d_2[IHg]))$$

$d_1 = 0.131 \pm 0.018$ $\qquad$ $d_2 = 0.631 \pm 0.197$

Relation between model and experimental values of IHg$_D$:

Slope: $c_1 = 0.733 \pm 0.114$ $\qquad$ Intercept: $c_0 = 0.119 \pm 0.106$

==

MeHg

$$\ln[MeHg] = a_0\big(type_{STP\,(+)}\big) + f_2(Sal) - f_3(SPM)$$

adjR^2=0.835; <u>Regression coefficients:</u>

Effect		Estimate	P2.5	P97.5
a_0	Intercept	−2.467	−3.2209	−1.9592
	type STP	1.363	1.238	1.883
a_2	**Sal** $_T$ (×10^{-1})	6.262	3.447	9.357
$a_{2,2}$	**[Sal** $_T$**]**^{2} (×10^{-1})	−1.848	−2.868	−0.884
a_{11}	**SPM** (×10^{-1})	−2.177	−3.303	−0.968
$a_{11,11}$	**[SPM]**^{2} (×10^{-2})	1.193	0.655	1.776
$a_{11,11,11}$	**[SPM]**^{3} (×10^{-4})	−1.821	−2.706	−1.137

<u>Average values:</u>

type $\quad$ / $\quad$ X$_i$	Sal	SPM (mg L^{-1})
STP	0.93	36.43
upstream_estuary_Urban/STP	2.17	17.61

$$\ln[MeHg] = a_0\big(type_{Urban/STP(-)}\big) + |a_{11}|[SPM] - |a_{12}|/[POC]$$

adjR^2=0.798; <u>Regression coefficients:</u>

Effect		Estimate	P2.5	P97.5
a_0	Intercept	−2.397455	−2.871380	−2.027424
	type Urban/STP	−0.393997	−0.572849	−0.186296
a_{11}	**SPM** (×10^{-2})	2.4013	1.6760	3.2966
a_{12}	**POC** $_T$	−4.713275	−6.138090	−3.191455

Average values:

type / X_i	SPM (mg L^{-1})	POC (%)
Urban/STP	18.73	7.26
upstream_estuary_STP	19.30	6.40

$$\ln[MeHg] = a_0\left(type_{Urban/STP(-)}\right) - |a_{12}|/[POC] + |a_{18}|\ln[IHg]$$

adjR^2=0.831; Regression coefficients:

Effect		Estimate	P2.5	P97.5
a_0	Intercept	–2.14703	–2.47095	–1.89364
	type Urban/STP	–0.49905	–0.66286	–0.31343
a_{12}	**POC** $_T$	–4.59964	–5.62891	–3.35462
a_{18}	**IHg** $_T$	0.36914	0.26967	0.45962

Average values:

type / X_i	IHg (ng L^{-1})	POC (%)
Urban/STP	3.05	7.26
upstream_estuary_STP	2.07	6.40

===

MeHg$_D$

$$\ln[MeHg_D] = a_0\left(time_{Sept(+)}; type_{STP\,(+)}\right) + f_2(Sal)$$

adjR^2=0.552; Regression coefficients:

Effect		Estimate	P2.5	P97.5
a_0	Intercept	–4.08305	–4.19107	–3.93250
	time Sept	0.26336	0.14840	0.34724
	type STP	0.97795	0.82104	1.11777
a_2	**Sal** $_T$	0.74596	0.43293	0.97359

$a_{2,2}$	$[Sal_T]^2$	−0.19322	−0.28140	−0.10052

$$\ln[MeHg_D] = a_0(type_{STP(+)}) + f_2(Sal) + |a_3|\,T$$

adjR^2=0.531; <u>Regression coefficients:</u>

Effect		Estimate	P2.5	P97.5
a_0	Intercept	−4.67732	−5.18666	−4.19409
	type STP	0.87621	0.51327	1.29881
a_2	**Sal** $_T$	1.02560	0.61482	1.45854
$a_{2,2}$	$[Sal_T]^2$	−0.26976	−0.39570	−0.13379
a_3	T ($\times 10^{-2}$)	3.604	0.331	5.939

<u>Average values:</u>

type / X_i			Sal	T (°C)
STP			0.93	17.28
upstream_estuary_Urban/STP			2.17	13.55

$$\ln[MeHg_D] = a_0(type_{STP(+)}) - f_3(SPM) + |a_{19}|\ln[IHg_D]$$

adjR^2=0.709; <u>Regression coefficients:</u>

Effect		Estimate	P2.5	P97.5
a_0	Intercept	−2.034	−2.843	−1.920
	type STP	1.112	0.982	1.455
a_2	**IHg**$_{D,\,T}$ ($\times 10^{-1}$)	3.397	2.400	3.969
a_{11}	**SPM** ($\times 10^{-1}$)	−2.220	−2.647	−1.020
$a_{11,11}$	$[SPM]^2$ ($\times 10^{-2}$)	1.201	0.611	1.490
$a_{11,11,11}$	$[SPM]^3$ ($\times 10^{-4}$)	−1.927	−2.458	−1.055

Average values:

type / X_i	IHg_D (ng L^{-1})	SPM (mg L^{-1})
STP	0.907	36.43
upstream_estuary_Urban/STP	0.651	17.61

$$[MeHg_D] = [MeHg] - d_1[SPM][MeHg]^{d_2}$$

$d_1 = 0.0132 \pm 0.0130$ $d_2 = 0.947 \pm 0.329$ (linear dependence from SPM and MeHg)

Relation between model and experimental values of MeHg_D:

Slope: $c_1 = 0.906 \pm 0.097$ Intercept: $c_0 = 0.0045 \pm 0.0040$

===

%MeHg

$$\ln[\%MeHg] = a_0\left(time_{Sept(-)}; type_{STPUrban/STP\,(-)}\right) - |a_{11}|[SPM] - f_2(POC)$$

adjR^2=0.756; Regression coefficients:

Effect		Estimate	P2.5	P97.5
a_0	Intercept	3.54395	2.55823	4.45521
	type STP_Urban/STP	–0.75437	–1.15449	–0.41952
	time Sept	–0.44986	–0.66902	–0.28588
a_{11}	**SPM** (×10^{-2})	–2.197	–3.218	–1.042
a_{12}	**POC** $_T$	–13.01827	–21.36554	–5.56752
$a_{12,12}$	**[POC** $_T$**]**^{2}	19.7801	2.4601	37.7481

Average values:

time / type	STP_Urban/STP	upstream_estuary	X_i
Sept	34.14	17.57	**SPM (mg L^{-1})**
MayJan	17.78	16.95	**SPM (mg L^{-1})**

Sept	9.66	4.36		**POC (%)**
MayJan	11.44	4.57		**POC (%)**

===

%MeHg$_D$

$$\sqrt{[\%MeHg_D]} = a_0\big(time_{May(+)}; type_{STP\,(+)}\big) - f_3(SPM)$$

adjR^2=0.511; <u>Regression coefficients:</u>

Effect		**Estimate**	**P2.5**	**P97.5**
a_0	Intercept	4.463	1.227	5.378
	time May	0.5350	0.3739	0.9921
	type STP	1.660	0.940	2.202
a_{11}	**SPM**	−0.3745	−0.5586	0.0700
$a_{11,11}$	**[SPM]^2** (×10^{-2})	2.075	0.324	3.078
$a_{11,11,11}$	**[SPM]^3** (×10^{-4})	−3.505	−5.213	−1.490

$$\sqrt{[\%MeHg_D]} = a_0\big(type_{STP(+)}\big) - f_3(SPM) - |a_{17}|\ln K_{OC}$$

adjR^2=0.474; <u>Regression coefficients:</u>

Effect		**Estimate**	**P2.5**	**P97.5**
a_0	Intercept	7.38524	5.29779	8.91027
	type STP	2.06011	1.23109	2.65746
a_{11}	**SPM**	−0.44975	−0.57598	−0.25248
$a_{11,11}$	**[SPM]^2** (×10^{-2})	2.3039	1.2398	3.0757
$a_{11,11,11}$	**[SPM]^3** (×10^{-4})	−3.752	−5.072	−2.197
a_{17}	**K$_{OC,\,T}$**	−0.21146	−0.34967	−0.03989

Average values:

type / X_i	SPM (mg L^{-1})	K_{OC} (L kg^{-1})
STP	36.43	46582
upstream_estuary_Urban/STP	17.61	27946

===

SUPPLEMENTARY INFORMATION

(Figures)

Marine Pollution Bulletin

Assessing and predicting the changes for inorganic mercury and methylmercury concentrations in surface waters of a tidal estuary (Adour Estuary, SW France)

Teodor Stoichev*[a], Aubin Thibaut de Chanvalon[b], Sandrine Veloso[b],

Jonathan Deborde[b,c], Emmanuel Tessier[b], Laurent Lanceleur[b], David Amouroux*[b]

[a] Interdiscliinary Center of Marine and Environmental Research (CIIMAR/CIMAR), University of Porto, Terminal de Cruzeiros de Leixoes, Av. General Norton de Matos s/n, 4450-208 Matosinhos, Portugal,

E-mail: tstoichevbg@yahoo.com

[b] Universite de Pau et des Pays de l'Adour, E2S UPPA, CNRS, IPREM, Institut des Sciences Analytiques et de Physico-chimie pour l'Environnement et les matériaux, Pau, France,

E-mail: david.amouroux@univ-pau.fr

[c] Ifremer, LITTORAL, Laboratoire Environnement Ressources des Pertuis Charentais, F-17390 La Tremblade, France
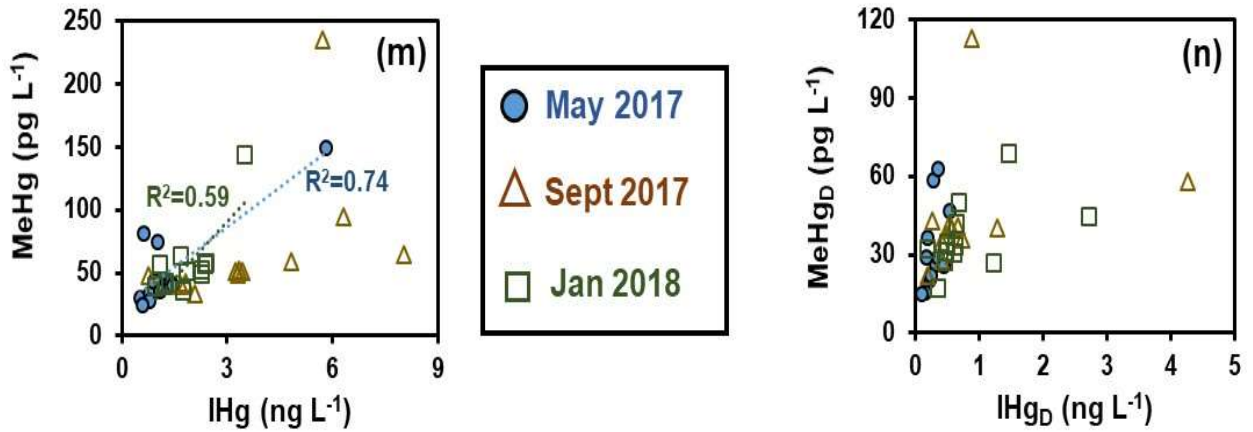
Fig. SI-1. Seasonal (May 2017, Sept 2017, Jan 2018) dependences of concentrations of (**a, b, c**) total IHg; (**d, e, f**) total MeHg; (**g, h, i**) dissolved IHg; (**j, k, l**) dissolved MeHg in surface water (Adour estuary) on concentrations of (**a, d, g, j**) particulate organic carbon (POC); (**b, e, h, k**) suspended particulate matter (SPM); (**c, f, i, l**) salinity. Seasonal dependences of concentrations of (**m**) total MeHg vs total IHg; (**n**) dissolved MeHg vs dissolved IHg. Coefficients of determination (R^2) for each sampling campaign (n=12, linear dependences) also shown if significant (p<0.01).
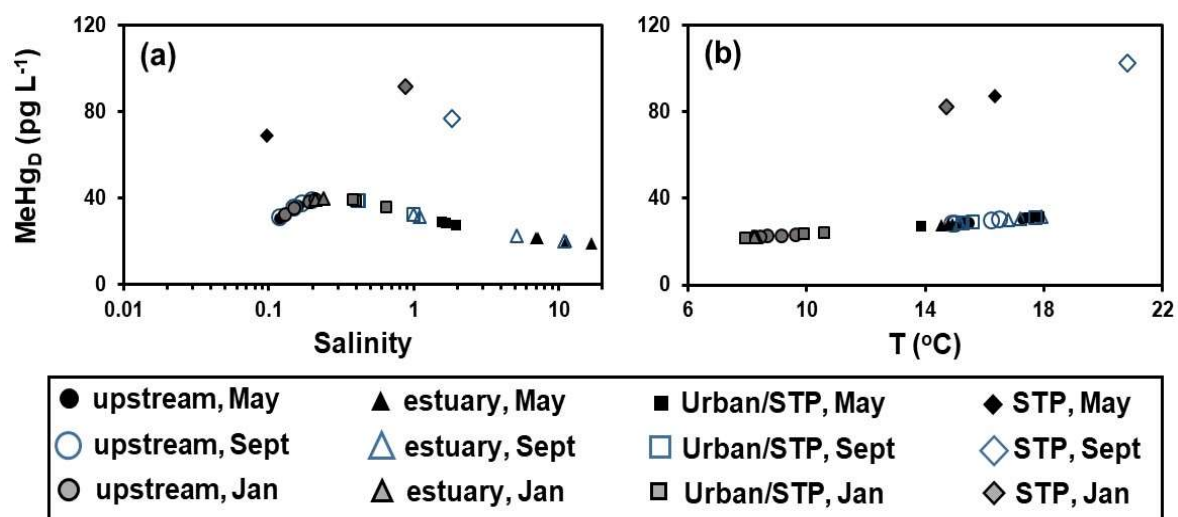
Fig. SI-2. Model values for (**a**, **b**) dissolved concentrations of MeHg (Eq. 17, adjR^2=0.531) in water (Adour estuary) as a function of (**a**) changing salinity at fixed T; (**b**) changing T at fixed salinity. Fixed values determined as group-based averages according to factor levels in the minimal adequate models. The slope c_1 for the dependence between model values and experimental values is 0.672 ± 0.076.

$$\ln[MeHg_D] = a_0\left(type_{STP\,(+)}\right) + |a_2|/\sqrt{Sal} - |a_{2,2}|/Sal + |a_3|\,T$$
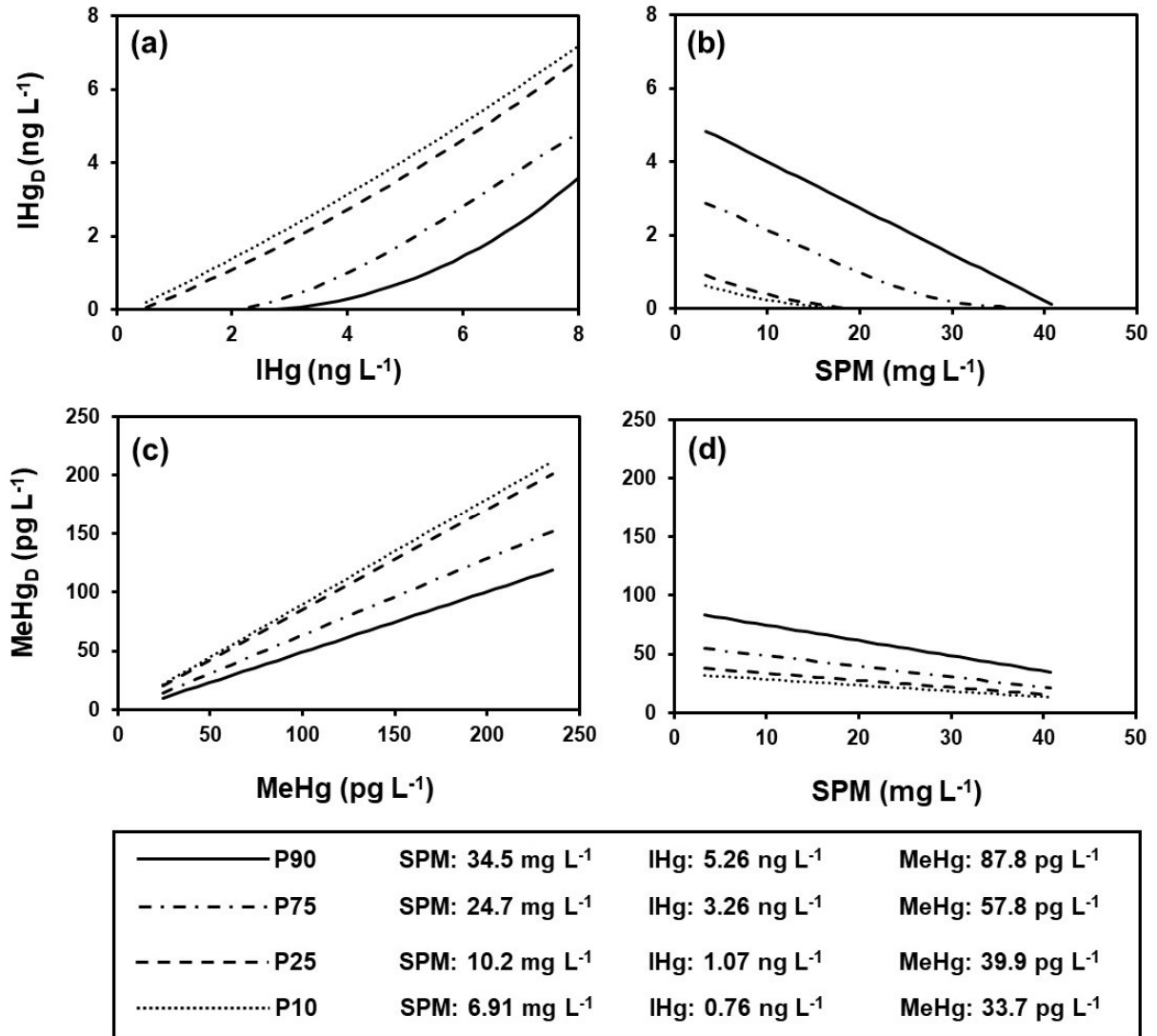
Fig. SI-3. Model values for dissolved concentrations (**a, b**) IHg_D and (**c, d**) $MeHg_D$ in water (Adour estuary) as a function of (**a**) changing total IHg at fixed SPM concentration; (**b**) changing SPM at fixed total IHg concentration; (**c**) changing total MeHg at fixed SPM concentration; (**d**) changing SPM at fixed total MeHg concentration. Fixed values are percentiles P10, P25, P75, P90 from SPM, IHg and MeHg concentrations. The slope c_1 for the dependence between model values and experimental values is (**a, b**) 0.733 ± 0.114 and (**c, d**) 0.906 ± 0.097.

$$[IHg_D] = [IHg] - d_1[SPM](1 - \exp(-d_2[IHg]))$$

$$[MeHg_D] = [MeHg] - d_1[SPM][MeHg]^{d_2}$$